

## A REVIEW ON HYDROGEN STORAGE TECHNOLOGIES

Ch. Christodoulou<sup>1</sup>, G. Karagiorgis<sup>1</sup>, A. Poullikkas<sup>2</sup>, N. Lymberopoulos<sup>3</sup>, E. Varkaraki<sup>3</sup>

<sup>1</sup> Frederick Institute of Technology (FIT) - Frederick Research Center (FRC), Nicosia, Cyprus

<sup>2</sup> Electricity Authority of Cyprus (EAC), Nicosia, Cyprus

<sup>3</sup> Centre for Renewable Energy Sources (CRES), Pikermi, Greece

**Abstract.** One way to store hydrogen is in the form of compressed gas, either above or below ground or on board vehicles. With a compressed gas system, the hydrogen is typically compressed and stored in gas cylinders or spherical containers. For storing hydrogen on board vehicles, compressed hydrogen is the simplest and presently the cheapest method, requiring only a compressor and a pressure vessel. Its main obstacle, however, is its low storage density, which is one-tenth that of gasoline. Higher storage pressures raise the cost, as well as safety issues. Researchers are working on aluminium-carbon and other composite tanks to increase the storage density (pressures up to 69 MPa) without creating additional safety problems.

As an alternative to compression, hydrogen can be liquefied for storage in stationary or onboard vehicle systems. Liquefaction takes place through a number of steps in which the hydrogen is compressed and cooled to form a dense liquid. The liquid hydrogen must then be stored at very low temperatures, below 252°C. A major drawback for stationary uses of liquid hydrogen is that storage costs are four to five times as high as those for compressed gas, even though transportation costs are much lower. With liquefied hydrogen storage on board vehicles, the main drawback is the high cost of liquefaction and the significant liquid “boil-off” that could occur in the small, insulated containers. Liquefying hydrogen gas also requires a large amount of electricity - as much as 30 percent of the hydrogen’s original fuel energy.

A novel means of hydrogen storage is the use of metal hydrides. These are compounds that chemically bond the hydrogen in the interatomic lattice of a metal. The hydrogen is absorbed into the lattice through cooling and released through heating, with the temperature and pressure of these reactions depending on the particular makeup of the hydride. The most well known metal hydrides are of the AB<sub>5</sub> (represented by LaNi<sub>5</sub>), AB<sub>2</sub> (represented by (Ti,Zr)(Mn,Ni,V)<sub>2</sub>) and AB (represented by TiFe) type. Hydrides are unusual in that they can draw in the hydrogen at or below atmospheric pressure, and release it at higher pressure when heated. Current drawbacks of metal hydrides are that they are heavy, have low hydrogen densities (<2wt%), require energy to refill and are comparatively costly.

Carbon-based systems are another strong hydrogen storage possibility in the early stage of development. Scientists are working to develop materials that can store significant amounts of hydrogen at room temperature - potentially a breakthrough that would enable the practical use of hydrogen-run vehicles. Two types are being explored. Single-walled carbon nanotubes, made up of molecule-sized pores, claim to achieve an uptake of 5-10 percent. Graphite nanofibers, stacks of nanocrystals that form a wall of similarly small pores is

claimed to achieve excellent hydrogen storage capacities. Chemical hydrides are also being considered for hydrogen storage on board vehicles. They have high hydrogen capacity, but their operating temperatures are very high or they are not refillable.

The most common way to deliver hydrogen today is with tanker trucks carrying liquid hydrogen, using double-walled insulated tanks to limit the amount of boil-off. Liquid hydrogen can also be transported in metal hydrides, which are loaded onto a truck or railcar. Upon reaching the customer's site, the hydride can be traded for an empty hydride container. Also under consideration are barges or other sea-bound vessels. Canada and Japan have developed ship designs for transatlantic hydrogen transport. However, once the hydrogen is on the ground, trucks may be less effective in distributing hydrogen to decentralized refuelling sites. Compressed gas can be transported using high-pressure cylinders, tube trailers, and pipelines. In the case of the first two, high-pressure compression is required. The most efficient option for delivering hydrogen gas will be through a network of underground pipelines. These pipelines are similar to those now used for natural gas pipelines, but are adjusted to handle the lower energy density and higher diffusion rate of the hydrogen relative to gas. Pipeline delivery of hydrogen gas already exists in industrial parts of the United States, Canada, and Europe. Germany has been operating a 210 km hydrogen pipeline since 1939. The world's longest hydrogen pipeline to date, running from northern France to Belgium, is 400 km long and is owned by Air Liquide. Over 720 km of hydrogen pipeline can be found in the United States, along the Gulf Coast and around the Great Lakes. One of the challenges in building hydrogen pipelines is overcoming the high initial expense of installation. One way to accomplish this is to have the cost shared among several suppliers and users, by installing a larger pipeline that can accommodate all of them.

Metal hydrides have very useful properties and more attention has to be put on the applications, especially in developing complete, reliable hydrogen storage systems. Such systems are expected to be useful mostly in stationary applications, in conjunction with remote solar and wind hydrogen production, and in short range mobile applications (motorcycles and city cars). Research activities for higher hydrogen capacity materials and lower materials cost will boost the use of metal hydrides in the future.

**Keywords:** Hydrogen, metal hydride, hydride, hydrogen storage, renewable

## 1. TYPES OF HYDROGEN STORAGE TECHNOLOGIES

### 1.1 Compressed gas

There is a lot of discussion going on now days about the different types of hydrogen storage. The type of storage method used is largely depending on the type of the application. One of the simplest forms of hydrogen storage is the compressed hydrogen [1-5]. The only equipment required is a compressor and a pressure vessel [6], the main problem with compressed gas storage is the low storage density which depends on the storage pressure. Higher storage pressure result in higher capital and operating costs [7]. Low-pressure spherical tanks can hold as much as 1,300 kg of hydrogen at 1.2-1.6 MPa [8]. High-pressure storage vessels have maximum

operating pressures of 20-30 MPa [9]. European countries tend to use low-pressure cylindrical tanks with a maximum operating pressure of 5 MPa and storage capacities of 115-400 kg of hydrogen [9].

The latest developments of the compressed hydrogen technology are applied to the aerospace and automotive industry. The major parameter that affects both these applications is the restriction to weight. Compressed hydrogen is considered to be a solution for hydrogen storage on a motor vehicle due to the relative simplicity of gaseous hydrogen, rapid refuelling capability, excellent dormancy characteristics, and low infrastructure impact [10].

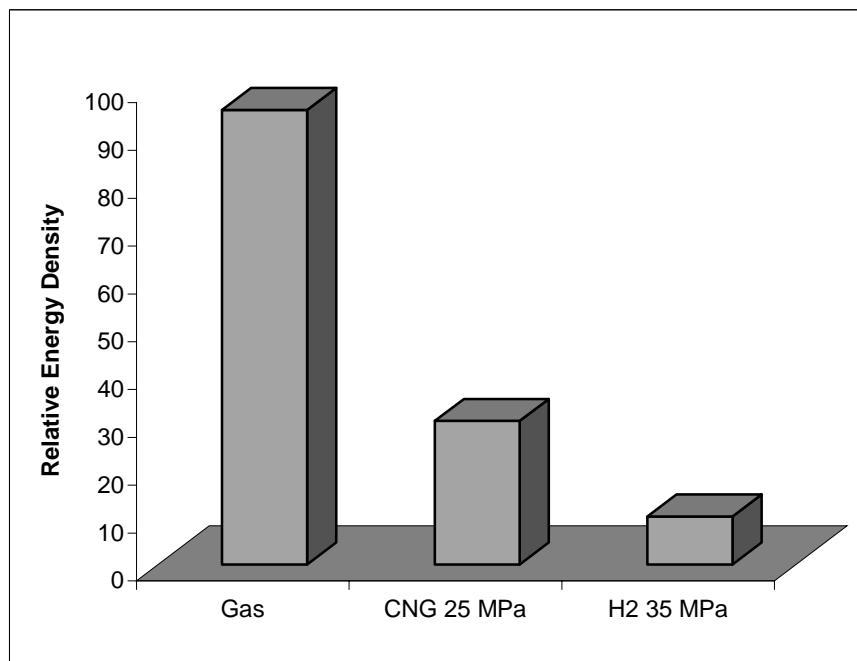
Despite these advantages, on-board high-pressure hydrogen storage must overcome several technical challenges in order to be viable in the long term. The energy density of hydrogen is significantly less than that of competing fuels as shown in Figure 1. Even with the high efficiencies projected for fuel cell vehicles, up to three times the current fuel efficiencies for internal combustion engines, a large volume of gaseous hydrogen storage will be required for acceptable vehicle range [5].

Thiokol propulsion [5] developed a composite wrapped tank prototype with ~12% hydrogen by weight at 34.5 MPa, 300 K, with a safety factor 2.25, which demonstrates the feasibility of using compressed hydrogen gas for vehicular operation.

The future use of hydrogen as a vehicular fuel will require a safe and cost-effective means of on-board storage. This physical storage may be accomplished in the form, or state, of compressed gas. To achieve a vehicle range comparable to a gasoline-powered vehicle will require storing gaseous hydrogen at pressures of 35 MPa and higher. High-strength composite materials will be necessary in order to minimize weight and maximize stored mass. The Natural Gas Vehicle (NGV) storage technology is serving as a springboard for on-board Hydrogen storage. In 1998, Lincoln Composites, a Division of Advanced Technical Products, began testing and delivery of the first all-composite high-pressure tanks for storage of hydrogen on fuel cell vehicles [11].

The aerospace industry has long used hydrogen as a fuel source, and LINCOLN COMPOSITES has designed and developed several aluminium-lined, carbon-overwrapped tanks for high-pressure storage. In 1998, however, LINCOLN COMPOSITES began evaluating the use of the all-composite tank technology for high-pressure storage of hydrogen, and delivered the first of several tanks for a hydrogen vehicle application.

Many of the challenges relating to the future of hydrogen as a vehicular fuel source are the same or similar to those as for natural gas. Hydrogen storage on an automobile is an even more complex problem than was the storage of natural gas. Natural gas is stored at 20 to 25 MPa. Since the energy density of hydrogen gas is so low, much higher pressures are being considered. To store enough hydrogen gas to provide an acceptable vehicular range will require pressures of approximately 35 MPa to 70 MPa. These high storage pressures depend on the use of high strength composite materials such as carbon fiber.



*Fig. 1: Comparison of fuel Energy Densities*

Most of the concern for hydrogen compatibility of pressure vessel materials is centered on hydrogen embrittlement issues. Hydrogen embrittlement is a problem for materials that develop a "homogeneous crystalline lattice" for strength. The effects of hydrogen on the material properties of a crystalline material are based on the interactions of the solute hydrogen (molecular or atom) or hydrogen-based chemical products at the grain boundaries of the molecular lattice. The hydrogen/hydrogen products affect the dislocation energies at the grain boundaries (micro level) which, in turn, affect ductility, reduction of area and tensile strengths (macro level) of the material.

**Carbon/Epoxy Laminate.** The question of hydrogen embrittlement is simply not appropriate for composite materials. Composite materials do not develop homogeneous structures. The mechanics of fiber-reinforced materials are based on a highly anisotropic material condition. Grain boundaries, edge dislocation energies, and other crystal phenomena simply do not exist in composite materials. Understanding the fundamental structure of filament wound composite helps to focus on what is important to the response of fiber-reinforced material in a hydrogen environment.

The molecular hydrogen, at worst case, can dissociate in the presence of water to form mild acid solutions. It can be shown easily that carbon fiber is inert to acid solutions. In the laboratory, determination of fiber content of a laminate is done by removing resin from the composite sample with extremely strong, heated acid solutions. These solutions digest the resin compounds to leave only the carbon fiber. In addition, testing of carbon-reinforced tanks in accordance with the NGV2 acid

environment test has demonstrated that the carbon fiber is unaffected.

**HDPE Liner.** The hydrogen compatibility of high-density polyethylene is well documented by many years of successful applications in hydrogen environments. These applications range from 30 years of natural gas pipeline service (significant percentage of hydrogen) to hydrogen gas service in the chemical industries.

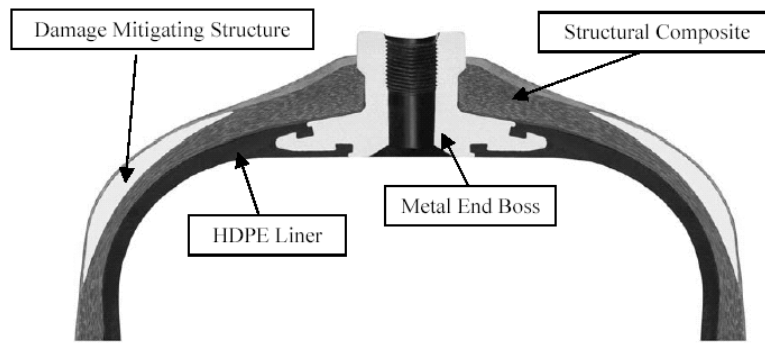
**Aluminum End Bosses.** The use of aluminum materials in hydrogen service is also well documented in numerous aerospace programs. NASA recognizes the use of aluminum in hydrogen systems in their safety manual [12]: aluminum is one of the few metals with only minimal susceptibility to hydrogen attack.

Aluminum shows little effect in hydrogen environments, because aluminum hydrides can not be formed during the production and service of aluminum. In addition, aluminum oxides can not be reduced by hydrogen, even at the melting point of aluminum. This exceptional chemical stability, coupled with a very low solubility of hydrogen within the aluminum material crystalline matrix prevents hydrogen interactions at the boundaries of the aluminum metal grains thus retaining the aluminum's intended material response. This has been confirmed in material testing done by Walter/Chandler [13] in which notched aluminum bars tested in 69 MPa hydrogen suffered no loss of strength or reduction of ductility.

The hydrogen fuel tanks developed by LINCOLN COMPOSITES are based on a composite that combines carbon and fiberglass reinforcements. The combination of carbon and fiberglass reinforcement provides a means of bringing together the best attributes of both materials. The high strength and low density of carbon fiber is used to reduce the weight and thickness that would be associated with a fiberglass-reinforced composite. The high cost and relative sensitivity of carbon fiber to impact damage is mitigated by the use of a tough, low cost fiberglass.

The hydrogen fuel tanks consists of a non-metallic liner which is wound with resin impregnated continuous fiber. The composite shell is comprised of carbon and glass fibers. Aluminum bosses that are integrally molded into the liner provide the interface to fittings/valves. Figure 2 depicts a cross-section of a typical LINCOLN COMPOSITES all-composite fuel tank.

The liner provides a permeation barrier, structural interfaces (bosses), and a stable mandrel for the filament winding process. The liner is not used to resist any of the shell membrane loads in the fuel tank. The primary function of the liner is to provide leak containment for the compressed gas. The liner's low modulus allows it to expand during pressurization, which permits transfer of all loads to the composite structure of the fuel tank.



*Fig. 2: Typical All- Composite Tank Cross-Section*

The outer shell of each tank is a continuous fiber epoxy composite produced by the filament winding process. The baseline construction for LINCOLN COMPOSITES' fuel containers has incorporated a hybrid construction with carbon and glass fibers in the same winding band. Carbon fiber was selected because of its high strength-to-weight ratio, excellent fatigue characteristics, insensitivity to environmental degradation, and performance reliability. While the fiberglass provides some strength, its primary function is to improve damage tolerance of the fuel tank. As the wall thickness of the fuel containers increases due to larger diameters or higher pressures, the damage tolerance of the wall accordingly increases, and the need for the fiberglass hybridization decreases. LINCOLN COMPOSITES has qualified some of its tanks using only carbon fiber in the structural reinforcement. The damage mitigating layers on the exterior of the tanks is constructed of glass fiber in an epoxy resin matrix. The overwrap consists of multiple helical layers interspersed with circumferential layers.



*Fig. 3: 3-Spindle Filament Winding*

The helical layers are wound using multi-circuit patterns. The stacking of the helical layers provides a uniform buildup at the boss, while giving a laminate construction highly tolerant to shock. The life of a composite structure that is subjected to static or cyclic loading is dependent upon the operating stress level.

**Design Comparisons.** Type 4 (all-composite) designs are well suited to hydrogen service, particularly at higher pressures, compared with other types of fuel tanks. Type 1 (all-metal) tanks are typically steel, and weigh about three times what a Type 4 tank would weigh. Although some stainless steel alloys are not affected (e.g. 316) or slightly affected (e.g. 304) by hydrogen embrittlement [13], most steels require additional material, which further adds to weight and cost. Type 2 and 3 (hoop wrap and full wrap/metal-lined) containers with steel liners would also be affected by hydrogen embrittlement.

Aluminium alloy 6061 is not subject to hydrogen embrittlement, but the higher pressures required of hydrogen fuel tanks may result in use limitations. The boss region of the liner must be more robust as pressure increases to handle the higher hoop and axial loads on the neck, as well as the shear loads on the flange. There must be sufficient material available to form these elements, which in turn might drive the cylinder portion to be thicker. A smaller port might be used, but there may still be limits of manufacturability when closing an end with small openings. In addition, the cycle life may be affected by the higher pressure due to changes in the three dimensional stress state. While the hoop and meridional strains in the liner are limited by the overwrap, the radial stress component is directly affected by internal pressure. Additional fiber might be required to limit strains in order to meet cycle life requirements.

There are no production vehicles currently available that use hydrogen as a fuel; however, automobile manufacturers are actively working to develop vehicles that use hydrogen. High production costs and low density have prevented hydrogen's use as a transportation fuel in all but test programs. It may be 10 to 20 years or more before hydrogen is a viable transportation fuel and then perhaps only in fuel-cell-powered vehicles.

## 1.2 Liquid hydrogen

A major concern in liquid hydrogen storage is minimizing hydrogen losses from liquid boil-off. Because liquid hydrogen is stored as a cryogenic liquid that is at its boiling point, any heat transfer to the liquid causes some hydrogen to evaporate. The source of this heat can be mixing or pumping energy, radiant heating, convection heating or conduction heating. Any evaporation will result in a net loss in system efficiency, because work went into liquefying the hydrogen, but there will be an even greater loss if the hydrogen is released to the atmosphere instead of being recovered. An important step in preventing boil-off is to use insulated cryogenic containers. Cryogenic containers, or dewars, are designed to minimize conductive, convective, and radiant heat transfer from the outer container wall to the liquid [1]. All cryogenic containers have a double-wall construction and the space between the walls is evacuated to nearly eliminate heat transfer from convection and conduction.

To prevent radiant heat transfer, multiple layers (30-100) of reflective, low-emittance heat shielding--usually aluminized plastic Mylar--are put between the inner and outer walls of the vessel. A cheaper alternative to Mylar film is perlite (colloidal silica) placed between the vessel walls [14]. Some large storage vessels have an additional outer wall with the space filled with liquid nitrogen. This reduces heat transfer by lowering the temperature difference driving the heat transfer [15].

Most liquid hydrogen tanks are spherical, because this shape has the lowest surface area for heat transfer per unit volume [14-18]. As the diameter of the tank increases, the volume increases faster than the surface area, so a large tank will have proportionally less heat transfer area than a small tank, reducing boil-off. Cylindrical tanks are sometimes used because they are easier and cheaper to construct than spherical tanks and their volume-to-surface area ratio is almost the same [14].

Liquid hydrogen storage vessels at customer sites typically have a capacity of 110-5,300 kg [15, 16, 19]. NASA has the largest spherical tank in the world with a capacity of 228,000 kg of liquid hydrogen [16, 19]. Hydrogen liquefaction plants normally have about 115,000 kg of storage onsite. Single tanks can be constructed to hold as much as 900,000 kg of hydrogen.

Even with careful insulation, some hydrogen will evaporate. This hydrogen gas can be vented, allowed to build up pressure in the vessel, or captured and returned to the liquefaction process. If the liquid hydrogen is stored in a pressure vessel, the gas can be left to build up gradually until it reaches the design pressure, then some of the gas must be vented [18].

Another option if the hydrogen is stored on the same site where it is liquefied is to pull the hydrogen gas out of the liquid hydrogen vessel and re-liquefy it. This way no hydrogen is lost, and because the hydrogen gas is still cold, it is easier to compress. In large transportation applications such as barges, the boil-off gas is being considered as transportation fuel--as the hydrogen gas boils off the liquid, it is recaptured and fed into the ship's boiler. If the hydrogen cannot be recovered, it can be vented. Venting the hydrogen to the atmosphere poses little safety risk because it will quickly diffuse into the air.

For mobile use hydrogen storage, tanks need above all to be light and small. In figure 4 different storage systems for LH<sub>2</sub> are compared on the basis of their storage of their storage densities in terms of the volume and weight of the respective storage vessels. Compared with the classical storage of compressed gas in metal cylinders, higher storage densities are reached, for example by composite vessels or with metal hydrides [17]. But only the storage of hydrogen as a liquid results in the highest storage densities, in both volumetric and gravimetric terms. [18]. On a weight basis, liquid hydrogen represents the highest energy density in a chemical fuel. It is mainly for this reason that liquid hydrogen has found such a widespread application as a principal fuel in the space programs. However, in view of the liquefaction temperature of about 20 K, there occurs a significant energy penalty for liquefaction process. It has been estimated that the process of liquefaction needs an energy level equivalent to approximately 30% of the combustion energy of the hydrogen that is liquefied [19].



A modern mobile LH<sub>2</sub> tank basically consists of (Fig 5):

1. The inner and outer vessel with a high-grade super-insulation between them.
2. Connections for filling, withdrawal and pressure relief valves.
3. The liquid level sensor and the pressurization device.

Liquid hydrogen is kept at a temperature level of about 20 K. The storage system needs perfect insulation, which is presently available as rigid, closed cell porous material. This is often considered a better mode of storage than compressed gas. However, there occurs a hydrogen loss of about 2% per day due to evaporation. Utilization of hydrogen in the liquid stage in various areas of applications is well known technology.

Insulated pressure vessels are cryogenic-capable pressure vessels that can be fueled with liquid hydrogen (LH<sub>2</sub>). These vessels offer the advantages of LH<sub>2</sub> tanks (low weight and volume), with reduced disadvantages (fuel flexibility, lower energy requirement for hydrogen liquefaction and reduced evaporative losses). S.M. Aceves et.al. [20-24] attempt to verify that commercially available pressure vessels can be safely used to store LH<sub>2</sub>. The use of commercially available pressure vessels significantly reduces the cost and complexity of the insulated pressure vessel development effort. In their work they describe a series of tests that have been done

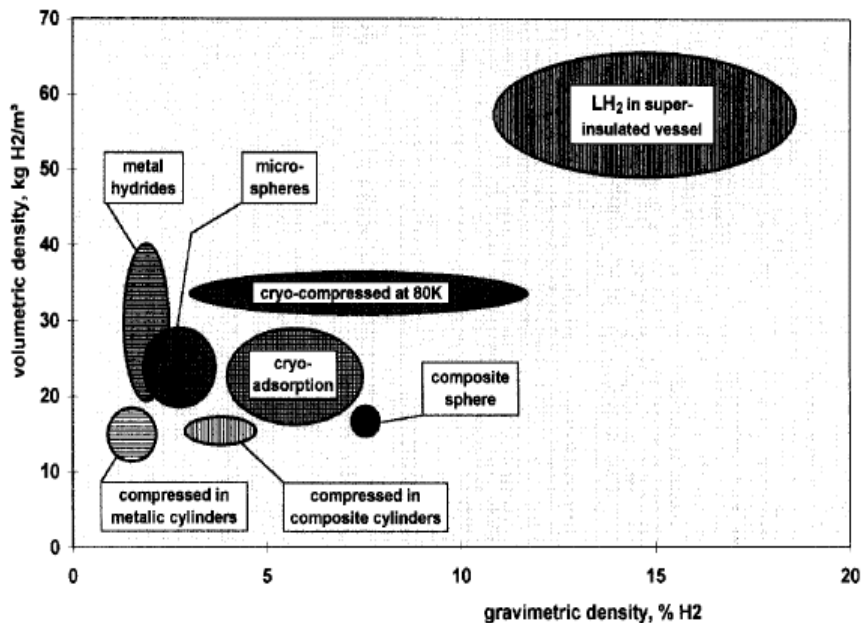


Fig. 4: Storage efficiency of hydrogen storage systems

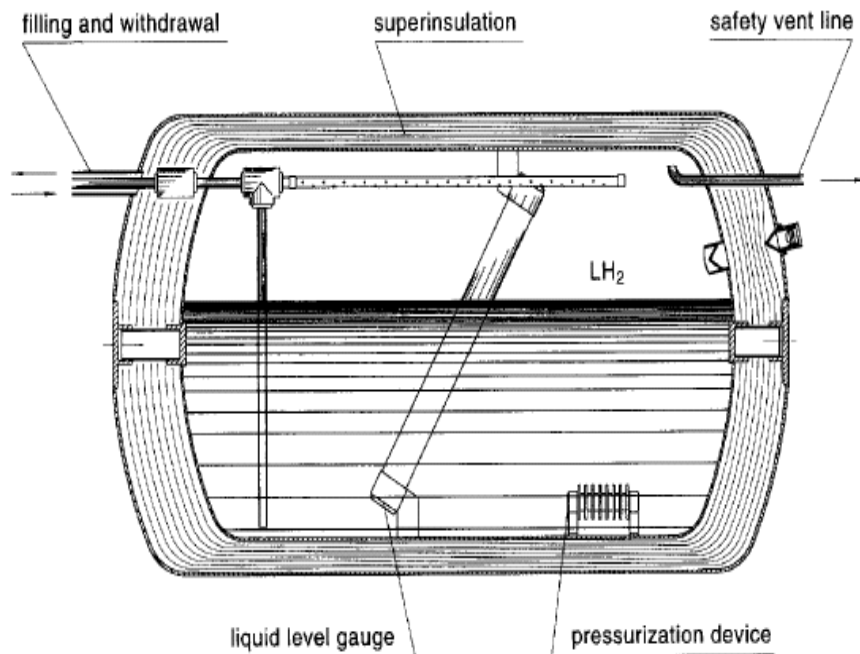


Fig. 5: Mobile liquid hydrogen storage tank.

with aluminium-lined, fiber-wrapped vessels to evaluate the damage caused by low temperature operation. All analyses and experiments to date indicate that no significant damage has resulted.

The pressure vessels need to be insulated with multilayer vacuum super insulation (MLVSI). MLVSI has a good thermal performance only under a high vacuum, at a pressure lower than 0.01 Pa (7.5 E-5 mm Hg). Therefore, the use of MLVSI requires that an outer jacket be built around the vessel. The design of the insulation is shown in Fig. 6. The insulation design includes access for instrumentation for pressure, temperature and level, as well as safety devices to avoid a catastrophic failure in case the hydrogen leaks into the vacuum space. Keeping a vacuum inside the insulation space requires a control of the outgassing of the materials that are in contact with the vacuum.

Insulated pressure vessels are being developed as an alternative technology for storage of hydrogen in light-duty vehicles. Insulated pressure vessels can be fueled with either  $\text{LH}_2$  or  $\text{CH}_2$ . This flexibility results in advantages compared to conventional hydrogen storage technologies. Insulated pressure vessels are lighter than hydrides, more compact than ambient-temperature pressure vessels, and require less energy for liquefaction and have less evaporative losses than  $\text{LH}_2$  tanks. The figure 6 shows a vacuum space for obtaining high thermal performance from the multilayer insulation

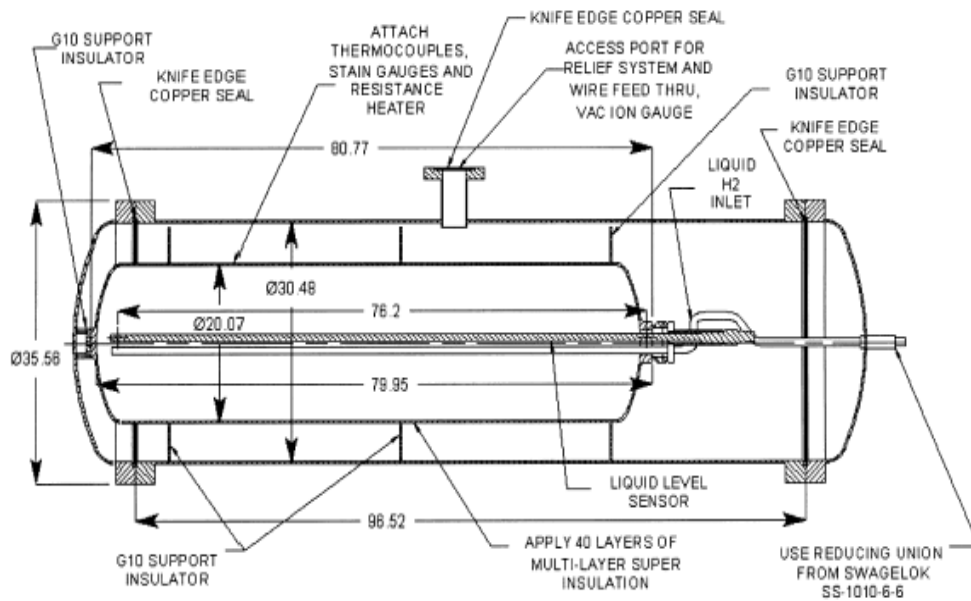
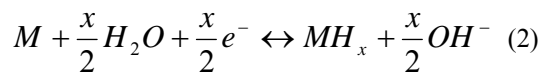


Fig. 6: Insulation design for pressure vessel

### 1.3 Metal-hydrides

The science and technology of reversible metal hydrides, in other words, the hydriding and dehydriding (H/D) of metals (M) by both direct dissociative chemisorption of  $H_2$  gas (1) and electrochemical (2) splitting of  $H_2O$  are very simple [25]:



For practical purposes metal-hydrides are intermetallic compounds (Fig. 7), which when exposed to hydrogen gas at certain temperatures and pressures, they absorb large quantities of hydrogen gas forming hydride compounds [26]. The formed hydrides can then, under certain temperatures and pressures, desorb the stored hydrogen. Hydrogen is absorbed interstitially in the metal lattice expanding the parent compound in the atomic and macroscopic level. Such metal-hydrides can expand as much as 30% causing the decrepitation of the original ingots into fine powders. Metal-hydrides represent an exciting method of storing hydrogen. They are inherently safer than compressed gas or liquid hydrogen and have a higher volumetric hydrogen storage capacity. Some hydrides can actually store hydrogen in densities twice as much of that of the liquid hydrogen ( $0.07g/cm^3$ ).



*Fig. 7: Metal-hydride based intermetallic alloys are melted into ingots, which are then crushed or decrepitated with hydrogen into powders*

### 1.3.1 Properties of hydrides

#### 1.3.1.1 Pressure–Composition–Temperature (PCT) properties

The most common expression of PCT properties is the familiar isothermal P–C hysteresis loop, shown in generalized [25] form in Fig. 8 and in real form in Figure 9 for the alloy with the composition  $\text{LaNi}_{4.7}\text{Al}_{0.3}$  [26]. Most practical hydriding metals do not show perfectly flat plateaux or zero hysteresis. Fig. 8 shows clearly the mathematical and numerical definitions of hysteresis, plateau slope and H-capacity which are generally used.

There are several ways to show H-capacity. The reversible capacity,  $\Delta(\text{H}/\text{M})_r$ , is conservatively defined as the plateau width, which can be considerably less than the maximum capacity,  $(\text{H}/\text{M})_{\text{max}}$ . In practice, depending on available pressure and temperature ranges, engineering capacity is usually somewhere between  $\Delta(\text{H}/\text{M})$  and  $(\text{H}/\text{M})_{\text{max}}$ . Capacity can be listed in either atomic H/M ratio or weight percent, both of which are used in some of the tables below. In calculating wt%, both H and M (i.e., not only M) are included in the denominator. In addition, it is sometimes useful to express capacity in volumetric terms, e.g., number of H atoms per unit volume (such as  $\text{crystal cm}^3$ ). This measure is listed in some of the tables below as  $\Delta N_{\text{H}}/V$ , where  $\Delta N_{\text{H}}$  represents the reversible capacity as defined in Fig. 8.

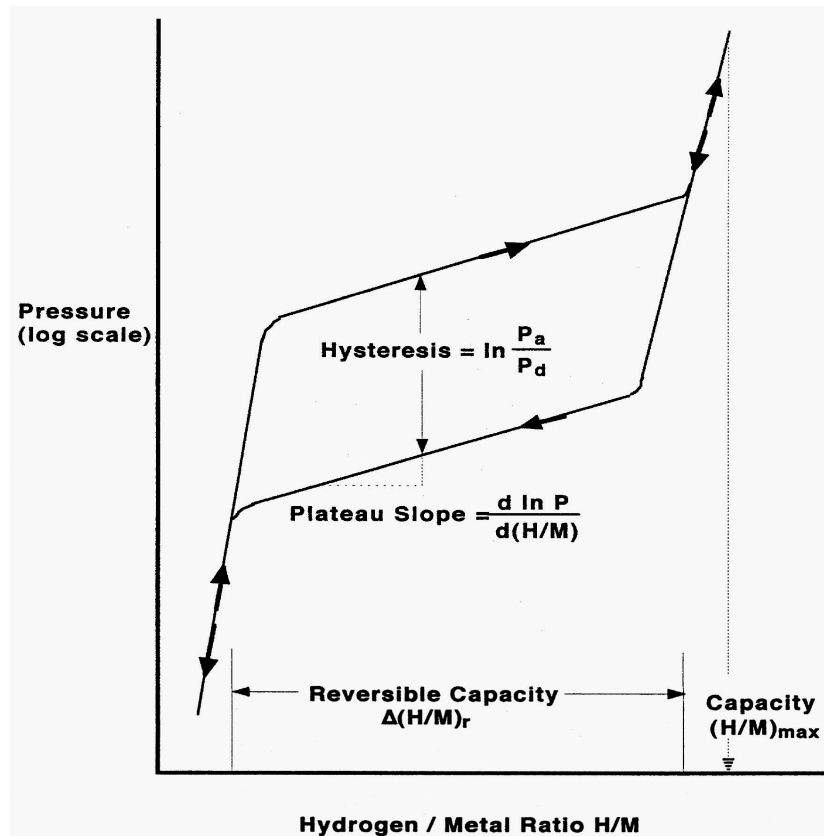


Fig. 8: Schematic Isothermal Pressure Composition (PCT) hysteresis loop [25]

Note that, this measure represents the volumetric density in crystal terms and does not include the void volumes inherent in engineering containers. In general, the mid-desorption plateau pressure,  $P_d$ , will be used in the graphs and tables below. Of course thermodynamics dictate the plateau pressures  $P$  must increase with temperature, usually close enough to the van't Hoff equation for engineering and comparison purposes,

$$\ln P = \frac{\Delta H}{RT} - \frac{\Delta S}{R} \quad (3)$$

where,  $\Delta H$  and  $\Delta S$  are the enthalpy and entropy changes of the hydriding reaction (1),  $T$  is absolute temperature and  $R$  is the gas constant.

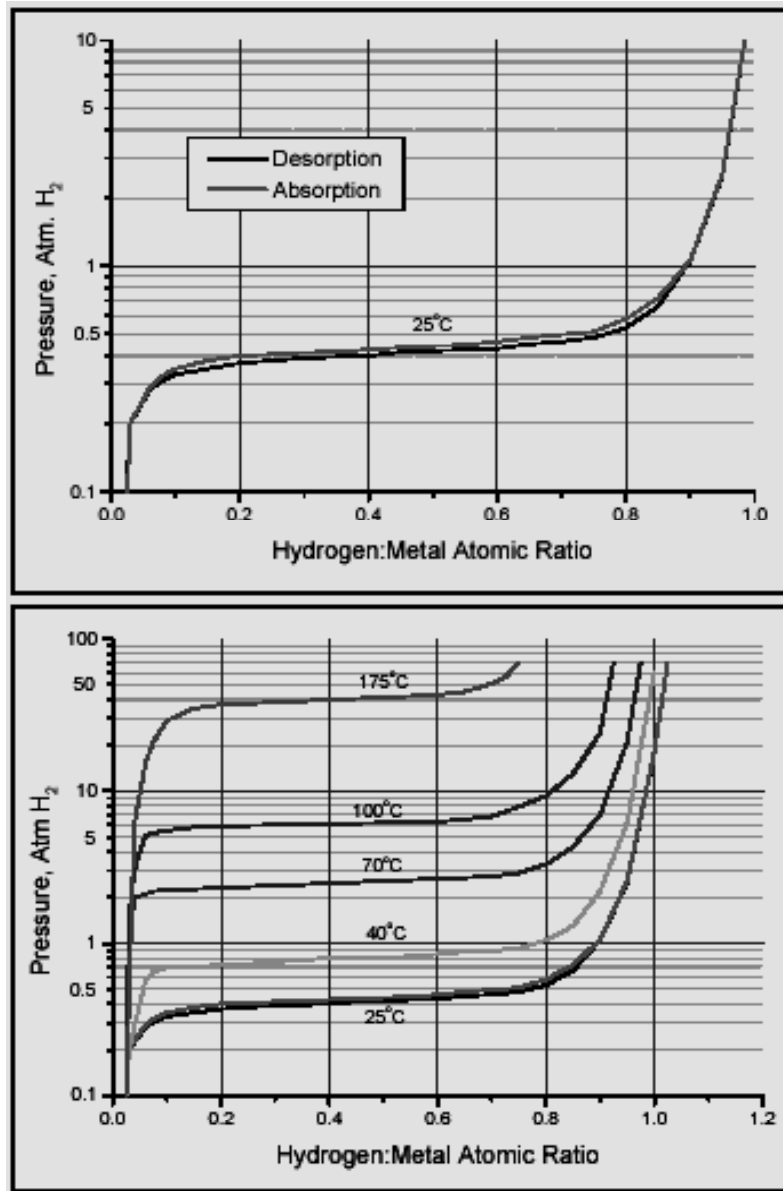


Fig. 9: Real PCT at different temperatures (25, 40, 70, 100 and 175°C) of  $\text{LaNi}_{4.7}\text{Al}_{0.3}$  [26]

For all of the hydrides to be discussed,  $\Delta H$  and  $\Delta S$  are negative, i.e., the hydriding (absorption) reaction is exothermic and the dehydriding (desorption) reaction is endothermic. The knowledge of  $\Delta H$  especially is important to the heat management required for practical engineering devices and is a fundamental measure of the M–H bond strength.

The van't Hoff plot ( $\ln P$  vs.  $1/T$ ), based on equation (3), is a convenient graphical

way to compare hydrides of varying thermal stability and will be used extensively below. In general, this report will focus mostly on alloys that will release hydrogen at or near ambient conditions, specifically 1–10 bar (absolute) and 0–100°C.

### 1.3.1.2 Other important properties

There are a number of important hydride properties [27-32] that must be considered in addition to the primary PCT properties. Some of the more important ones are listed below.

*Activation* is the procedure needed to hydride a metal the first time and bring it up to maximum H-capacity and hydriding/dehydriding kinetics. The ease of initial H<sub>2</sub> penetration depends on surface structures and barriers, such as the dissociation catalytic species and the oxide films. A second stage of activation involves internal cracking of metal particles to increase reaction specific surface. Decrepitation means the self-pulverization of large metal ingots and large particles into powder (mostly single grain fine particles). This phenomenon results from a combination of hydriding volume change and the brittle nature of hydriding alloys. The morphology of the decrepitated powder affects heat transfer and also the tendency of powder migration into undesirable places in the hydrogen storage tank, like valve seats, assisting pipes. Unfortunately, most hydride powders have poor heat transfer coefficients and require engineering means for thermal enhancement (e.g., Al foam, internal fins, etc.). The morphology of the powder can affect packing, which in turn can lead to internal gas impedance and container deformation.

*Kinetics* of hydriding and dehydriding can vary markedly from alloy to alloy. Fortunately, many room temperature hydrides have excellent intrinsic kinetics, so that the cycling of storage containers tends to be limited by heat transfer designs or accidental surface contamination. However, there are some materials that are kinetics limited, especially at low temperature.

*Gaseous impurity resistance* is a very important property, especially when the application is “open-ended” and uses new H<sub>2</sub> for each Hydriding/Dehydriding cycle, that H<sub>2</sub> often being impure. Depending on the alloy impurity combination, there can be several types of damage [33]:

- a) *Poisoning*, where capacity is quickly lost without a concurrent decrease of initial kinetics
- b) *Retardation*, where kinetics are quickly lost without loss of ultimate capacity
- c) *Reaction*, where the alloy is slowly corroded
- d) *Innocuous*, where there is no surface damage but there can be pseudo-kinetic decreases due to inert gas blanketing, an interparticle gas diffusion problem.

Usually, damages from poisoning and retardation are usually recoverable, but reaction damage is usually not.

*Cyclic stability* is important and widely variable from alloy to alloy. Alloys and intermetallic compounds are usually metastable relative to disproportionation, the

tendency to break up metallurgically (phase transformation) to form stable, not easily reversed hydrides. Even if very pure H<sub>2</sub> is used, disproportionation can occur with a resultant loss of reversible capacity.

*Safety* usually centers around pyrophoricity, the tendency for a hydride powder to burn when suddenly exposed to air, e.g., an accidental tank rupture. But the term can also include toxicity resulting from accidental ingestion or inhalation.

*Alloy cost* is influenced by several factors, including *raw materials cost, melting and annealing costs, metallurgical complexities, profit* and the degree of *PCT precision* needed for the particular application. It is important to point-out that the above factors in addition to raw materials cost can easily raise true alloy cost by more than 100%.

### 1.3.2 Hydride applications

It is useful to briefly list the main hydride applications, proposed and commercial, in terms of the properties required. More detail can be found elsewhere [34, 35].

#### 1.3.2.1 H-Storage

*Stationary storage* usually implies bulk storage and large amounts of alloy to be used. Therefore, in such a case, low alloy cost tends to be an important factor. On the other hand *vehicular storage* tends to require high hydrogen weight percent. In fact, most existing hydrides fall far short of what is desired in this property, as it shall be described below. Both kinds of storage desire easy activation to minimize container pressure and temperature requirements for the one-time activation. In both cases, good resistance to gaseous impurities is desirable in case impure H<sub>2</sub> is used or the inevitable accidental introduction of air occurs. In both cases, PCT properties should be roughly in the ambient temperature and pressure area so that waste heat from the environment or vehicle engine (or fuel cell) can be used for endothermic H<sub>2</sub> desorption. Kinetics are somewhat less important because of the relatively slow cycling of storage tanks.

#### 1.3.2.2 Compression

The compression of gaseous H<sub>2</sub> using thermal swings of hydride beds is an “open-ended” process and generally requires the alloy to have good impurity resistance and cyclic stability (high temperatures involved). Hydriding/Dehydriding cycling is relatively fast, so good kinetics and heat transfer are desired. If rapid cycling can be achieved, then relatively small inventories of alloy are needed and alloy cost becomes secondary to other factors. Good H-capacity is desired so that parasitic heat losses associated with thermal swings are minimized. PCT properties must be tunable to the input and output pressures desired and the input and heat sink temperatures available.

The relationship between temperature and pressure that must be taken into consideration when designing storage vessels provides powerful tool for hydrogen compression [36]. Referring back to Figure 9, an alloy that absorbs hydrogen at 1



bar pressure at 40°C will release hydrogen at 3 bar, when heated to 70°C, which represents a 300% pressure rise every 30°C. Figure 10 illustrates the hydride compression process.

By employing successively higher pressure hydride alloy stages in series, high pressure ratios can be generated. For example, using 85°C hot water as the energy source, a 5-stage hydride compressor will compress a 1.4 bar (21 psia) inlet pressure to 347 bar (5100 psia) resulting in a compression ratio of 242 (refer to Fig. 9).

Continuous high pressure hydrogen flow is produced by providing two identical hydride heat exchanger “Beds”, and utilizing simple and reliable one-way hydrogen check valves between each hydride stage. When one of the hydride beds is heated and the other bed is cooled, hydrogen absorption and compression occurs simultaneously. After hydrogen transfer is completed (in about 15 seconds), the hot and cold water flow is reversed, and hydrogen absorption and compression again occur simultaneously. The use of one-way hydrogen check valves prevents the hydrogen from back flowing, thus simply and passively allowing the hydrogen to flow into the next higher pressure hydride stage whenever a small pressure differential of about 0.1 bar (1.5 psi) is present.

Examples of hot water powered and electrically powered hydride compressors appear in Figures 11, 12 and 13, along with operating information in Table 1.

For hydrogen fuel vehicles, hydrogen will be stored at pressures of 250 to 700 bar. Hydride hydrogen compressors have demonstrated operation over 400 bar and operation over 500 bar is possible. A high pressure compressor and associated performance information appear in Figure 14 and 15.

### 1.3.2.3 Closed thermodynamic systems

This class of hydride applications includes the following:

- a) *Heat engines*, where heat is converted to mechanical energy in an expansion engine
- b) *Heat storage*, for example solar heat
- c) *Heat pumps*, where low-temperature heat is “upgraded” to higher temperature
- d) *Refrigerators*, where heat is converted to refrigeration

Included in heat engines are *actuators* and *temperature sensors*. All of these devices are “closed systems”, where H<sub>2</sub> is a contained “working fluid inventory”, so generally impurity resistance is relatively unimportant (assuming the systems are built very cleanly to start). Most (except (b)) are expected to cycle rapidly and involve relatively high temperatures, so good kinetics and cyclic stability are important. Like compressors, good capacity is desirable and PCT must be carefully tuned to the application. In the special case of heat pumps and refrigerators, where two or more different hydrides must be carefully matched to each other, achieving the exact desired PCT properties can be difficult or expensive. To work properly, or at least to maximize overall efficiency, most closed thermodynamic systems demand low hysteresis and low plateau slope.

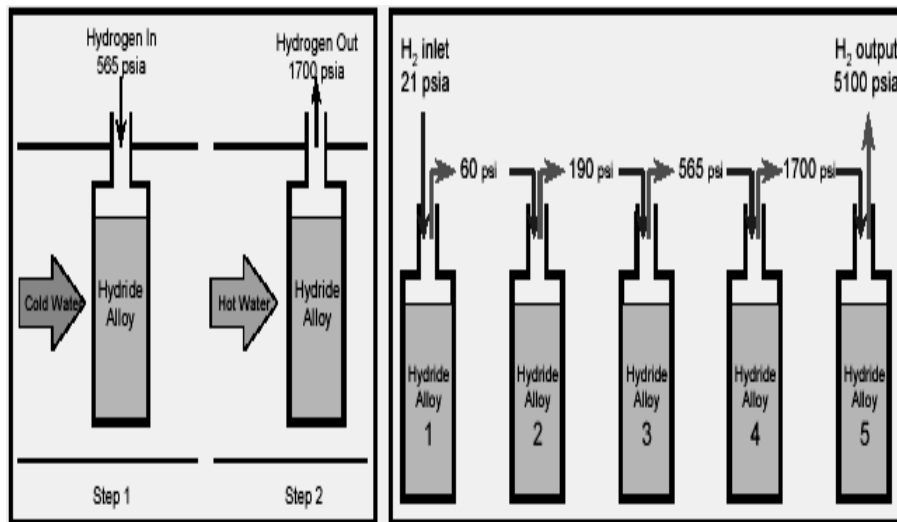
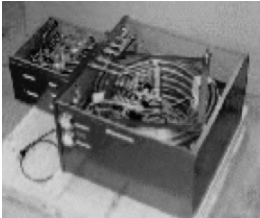

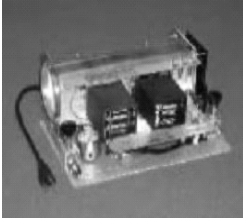


Fig. 10: Two-stage and multi-stage thermal hydrogen compression

		
<p>Fig. 11: 12 Nm<sup>3</sup>/h Compressor</p>	<p>Fig. 12: 21 MPa Compressor</p>	<p>Fig. 13: Electric Micro-Compressor</p>
<p>310 kPa</p>	<p>103 kPa</p>	<p>1.7 MPa</p>
<p>7 MPa</p>	<p>21 MPa</p>	<p>17 MPa</p>
<p>12 Nm<sup>3</sup>/h</p>	<p>425 liters/h</p>	<p>11 liters/h</p>
<p>40°C hot water</p>	<p>85°C hot water</p>	<p>75W electrical heater</p>

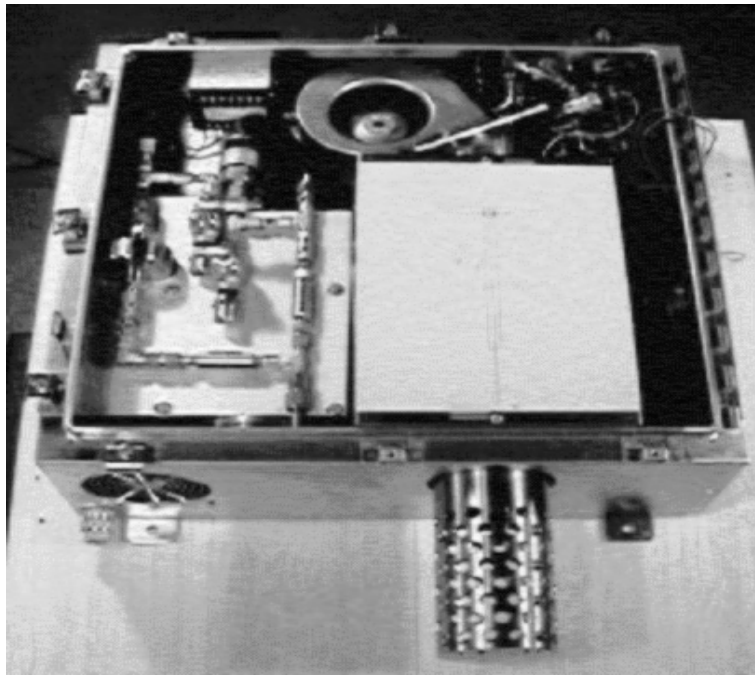


Fig. 14: A 408 bar (6000 psig) single-stage electric compressor

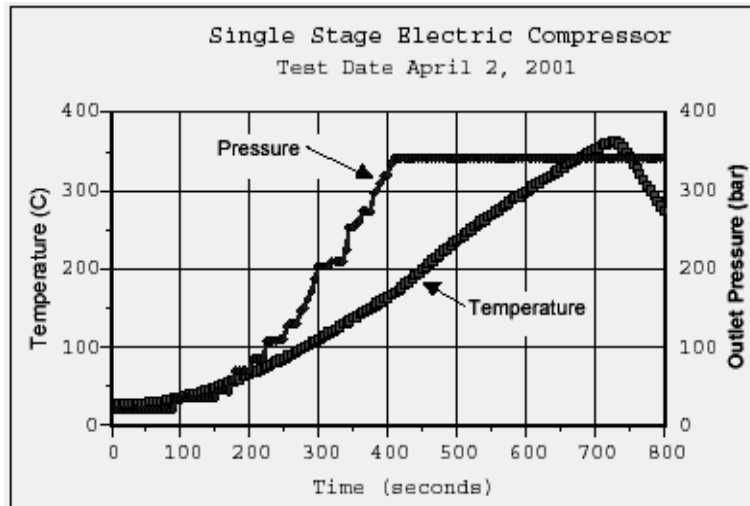


Fig. 15: Performance of a single-stage electric compressor

Hydride alloy heats of formation can be used as the basis for heat pump and air conditioning systems. Desorption of hydrogen from a metal-hydride is endothermic (requires heat). A hydride heat exchanger cools rapidly and dramatically if it takes the needed heat from ambient air. When emptied of hydrogen, the alloy can be recharged using hot air, either from a waste heat source or burner.

The cooling potential of hydride alloys is extraordinary. One gram of alloy delivers 158 Joules (38 calories) per cycle. If the cycle time is 15 seconds, 600 grams of alloy (0.2 liters) provides 3513 watts of cooling. A hydride air conditioner uses 50% less energy than traditional fluorocarbon cycles.

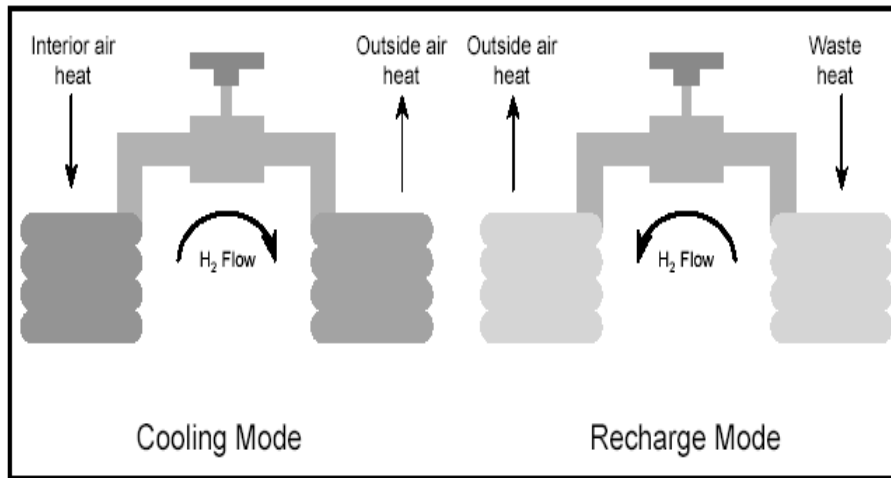
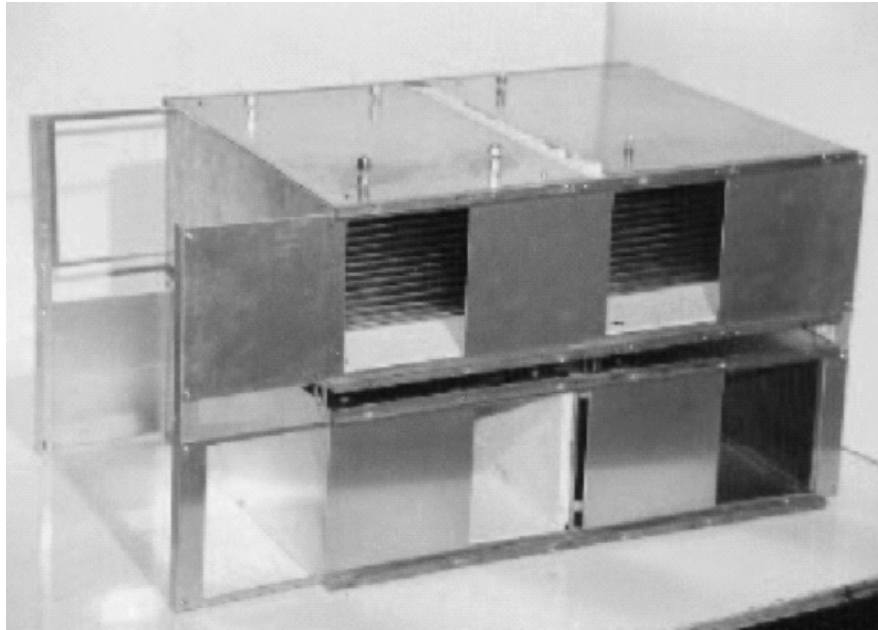


Fig. 16: Metal-hydride air conditioning system

In its simplest form, a hydride air conditioner consists of two interconnected hydride beds which operate in a reciprocating fashion, as illustrated in Figure 16. An automobile air conditioner proof of principal prototype was constructed and bench tested (Fig. 17). It consists of upper and lower hydride heat exchanger beds (two beds total). Each bed contains 500 individual, hermetically sealed hydride tubes that are 3.175 mm diameter by 610 mm long (1/8 inches diameter by 24 inches long).

Each tube is essentially a miniature air conditioner, with one half containing a high pressure (cooling) alloy and the other half containing a low pressure (regenerating) alloy. When one of the beds is cooling passenger compartment air, the other is being regenerated by hot exhaust gas. Ambient air provides the heat rejection function. Sliding gate valves direct air flows to the appropriate hydride sections. The decision to use individual, hermetically sealed tubes relate to safety in the event of a severe accident. Each tube contains 1/1000 of the hydrogen inventory. Even if a number of tubes are ruptured in an accident, only a fraction of the hydrogen inventory would be lost, minimizing flammability concerns. The specifications of this Ergenic's hydride automobile air conditioning prototype are listed in Table 2.



*Fig. 17: Metal-hydride automobile air conditioner proof-of-principal prototype*

*Table 2: Ergenic's hydride automobile air conditioning prototype specifications*

Nominal Cooling	9,000 Btu/h at 45°F, using a hot source gas temperature of 400°F, and an ambient air temperature of 100°F
Maximum Cooling	18,000 Btu/h at 45°F, using a hot source gas temperature of 500°F, and an ambient air temperature of 100°F
COP Thermal Efficiency	3 Btu of heat per 1 Btu of cooling
Mass (without fans)	30 kg (75 lbs)
Dimensions	635 mm L, 457mm W, 406mm H (25 by 18 by 16 in.)
Mass of Hydride used	14 kg (31 lbs)
Future Improvements	New heat exchanger design will reduce weight and size by 50%.

#### 1.3.2.4 Separation

Separation can be divided into two classes:

- a)  $H_2$  separation from other gases
- b)  $H$ -isotope separation

The first class can be further divided into gross separation, purification and gettering. All three subclasses require impurity tolerance, tailored PCT properties and other properties, that are specific applications. In the case of getters, to remove trace amounts of  $H_2$  from vacuum systems or other gases, very low room-temperature plateau pressures are required (e.g.,  $10^{-6}$  to  $10^{-10}$  bar).

H-isotope separation requires special properties involved with kinetic and PCT property differences among protium (H), deuterium (D) and tritium (T).

#### 1.3.2.5 Other applications

There are a number of lesser-known hydride applications: *liquid  $H_2$  control and boiloff capture, cryocooling, chemical catalysis, ammonia synthesis, methane synthesis, diamond synthesis* [37], *permanent magnet production* and others too numerous to detail in this report. The biggest commercial application is the *nickel metal hydride (NiMH) battery*, which is not the focus of the present report, although many aspects of it concern these applications as well.

### 1.3.3 Review of hydriding metals and alloys

Hydrogen is a highly reactive element and has been shown to form hydrides and solid solutions with many of metals and alloys. A hydride “family tree” of the elements, alloys and complexes is shown in Fig. 18. This report will concentrate on the alloy side of the tree, where H is usually bound in interstitial sites in a metallic state with usually minor distortions of the generally stable H-free alloy structures. However, the report will also briefly discuss the complexes and carbon-based materials which show very significant potential for future development.

#### 1.3.3.1 Elements

Most of the natural elements will hydride under appropriate conditions. Unfortunately, as shown by the van't Hoff lines of Fig. 19, the PCT properties are not very convenient relative to the 1–10 bar and 0–100°C range of utility chosen for practical applications (small box on the right of the diagram). Only vanadium (V) is in the range and there is past and present interest in solid solutions of V and other metals (to be discussed later). Nb is similar to V. Pd has been used for more than 100 years for H-storage, but it is very expensive, doesn't hold much H and requires heating well above 100°C to liberate that hydrogen.

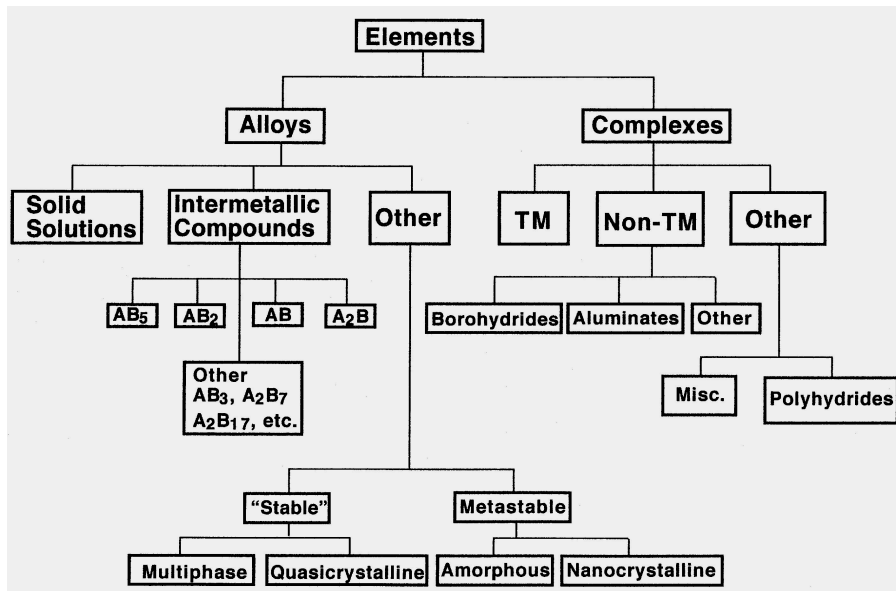


Fig. 18: Family tree of hydriding alloys and complexes (TM=Transition Metals)[25]

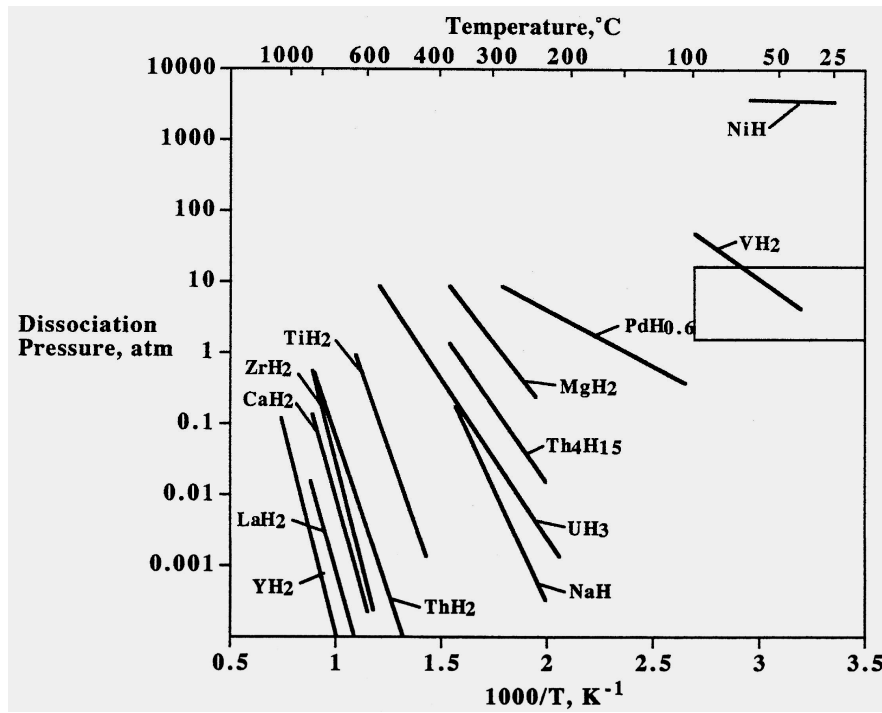


Fig. 19: Van't Hoff lines (desorption) for elemental hydrides. The box indicates 1-10 bar, 0-100°C

### 1.3.3.2 Metal alloys

In order to capitalize on practical applications of reversible hydrides, it is required to combine strong hydride forming elements A with weak hydriding elements B to form alloys (especially intermetallic compounds) that have the desired intermediate thermodynamic affinities for hydrogen. A classic and well-known example is the combination of La (forming  $\text{LaH}_2$  with  $25^\circ\text{C}$ ,  $P_d \approx 3 \times 10^{-29}$  bar and  $\Delta H_f = -208$  kJ/mol  $\text{H}_2$ ) with Ni ( $\text{NiH}$ ,  $25^\circ\text{C}$ ,  $P_d = 3400$  bar,  $\Delta H_f = -8.8$  kJ/mol  $\text{H}_2$ ) to form the intermetallic compound  $\text{LaNi}_5$  ( $\text{LaNi}_5\text{H}_6$ ,  $25^\circ\text{C}$ ,  $P_d = 1.6$  bar,  $\Delta H_f = -30.9$  kJ/mol  $\text{H}_2$ ). This extraordinary ability to “interpolate” between the extremes of elemental hydriding behavior has led to the modern world of reversible hydrides and the applications associate with this.

#### 1.3.3.2.1 $\text{AB}_5$ intermetallic compounds

The  $\text{AB}_5$ -type intermetallics [25] generally have a hexagonal crystal structure (Hauke phase, prototype  $\text{CaCu}_5$ , Strukturbericht  $\text{D2}_b$ , Pearson  $\text{hP6}$ , space group  $P6/mmm$ ). The near-ambient PCT properties of the hydrides were discovered accidentally at Philips Eindhoven about 1969 while studying the magnet alloy  $\text{SmCo}_5$ . The family has an extraordinary versatility because many different elemental species can be substituted (at least partially) into the A and B lattice sites. A-elements tend to be one or more of the lanthanides (at. no. 57–71), Ca or other elements such as Y, Zr, etc. The B-elements are based on Ni with many other possible substitutional elements such as Co, Al, Mn, Fe, Cu, Sn, Si, Ti, etc. Modern commercial  $\text{AB}_5$  hydrogen storage alloys are mostly based on the use of the lanthanide mixture Mischmetal ( $\text{Mm} = \text{Ce} + \text{La} + \text{Nd} + \text{Pr}$ ) for the A side and  $\text{Ni} + \text{Al} + \text{Mn} + \text{Co} + \dots$  on the B-side. The highly substituted Mm-based alloys were initially developed in the 1970s by Gary Sandrock in the USA and Osumi et al. in Japan and later optimized by Sakai et al. for NiMH battery applications [38]. Various versions of  $\text{Mm}(\text{Ni}, \text{Co}, \text{Mn}, \text{Al})_5$  form the basis of most of today’s commercial NiMH battery anodes.

The PCT and other properties of various representative  $\text{AB}_5$ -type of alloys are shown in Fig. 20 and Table 3. The broad range of PCT versatility and tunability is evident, with the  $25^\circ\text{C}$  plateau pressure variable over at least three orders of magnitude depending on the composition. With the exception of  $\text{MmNi}_5$  itself, hysteresis is generally quite low for the  $\text{AB}_5$ s. By annealing out the as-cast metallurgical composition fluctuations, rather flat plateaux are possible, even with multi-component alloys. H-capacity is on the uncomfortably low side, not exceeding 1.3 wt% on the plateau basis we are using for definition of the reversible component. Alloy raw material cost is a little high, at least in comparison to other systems ( $\text{AB}_2$  and  $\text{AB}$ ) to be shown later.  $\text{CaNi}_5$  has a good potential for both lower cost and higher H-content than the Mm- or La-based alloys, but unfortunately it has three plateaux and only the main (middle) plateaux is counted in Table 1. Even though that plateau has low  $\Delta(H/M)_r$ , the low density of  $\text{CaNi}_5$  results in competitive wt% and cost to the other  $\text{AB}_5$ s.



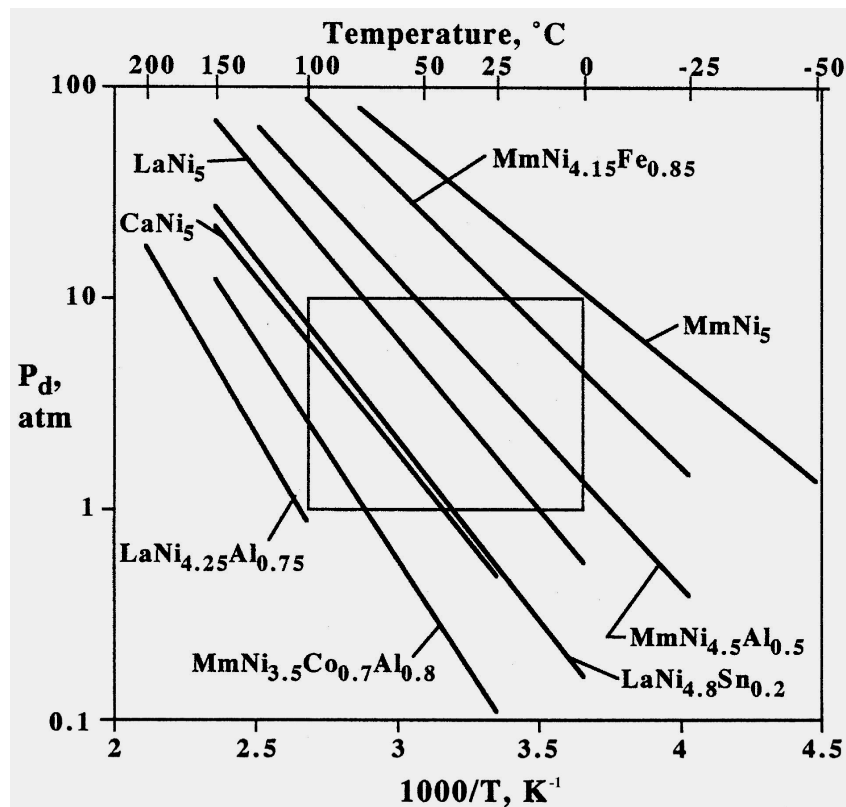


Fig. 20: Van't Hoff plots for several  $AB_5$  [25]

The  $AB_5$  alloys are easy to activate, seldom requiring any heating. They decrepitate on the first H/D cycle to fine powder which is mildly pyrophoric if suddenly exposed to air, a well-known factor that must be included in safety considerations. Figure 21 shows the morphology of the  $LaNi_5$  powders produced by hydrogen decrepitation. Both easy activation and pyrophoricity means the  $AB_5$  alloys do not form protective oxide layers. This property is a distinct advantage that gives  $AB_5$ s unusually good tolerance to small amounts of  $O_2$  and  $H_2O$  in the  $H_2$  [33]. These impurities do not poison the  $AB_5$ s but act as reactants that only slowly reduce capacity. CO is a strong poison, but regeneration can be accomplished by mild heating (e.g.,  $100^\circ C$ ) and flushing with clean  $H_2$ . Intrinsic kinetics of the  $AB_5$  alloys is very good, almost always better than practical engineering heat transfer (at least in good purity, CO-free  $H_2$ ).  $AB_5$  metallurgy is rather well understood and virtually single phase alloy can be relatively easily melted in large commercial quantities by vacuum induction melting.  $CaNi_5$ , and to lesser extents  $LaNi_5$  and  $MmNi_5$ , are subject to disproportionation. The partial substitution of Al or Sn on the B-side greatly reduces the disproportionation problem in  $LaNi_5$  and  $MmNi_5$ -based alloys, thus making the alloys more stable.

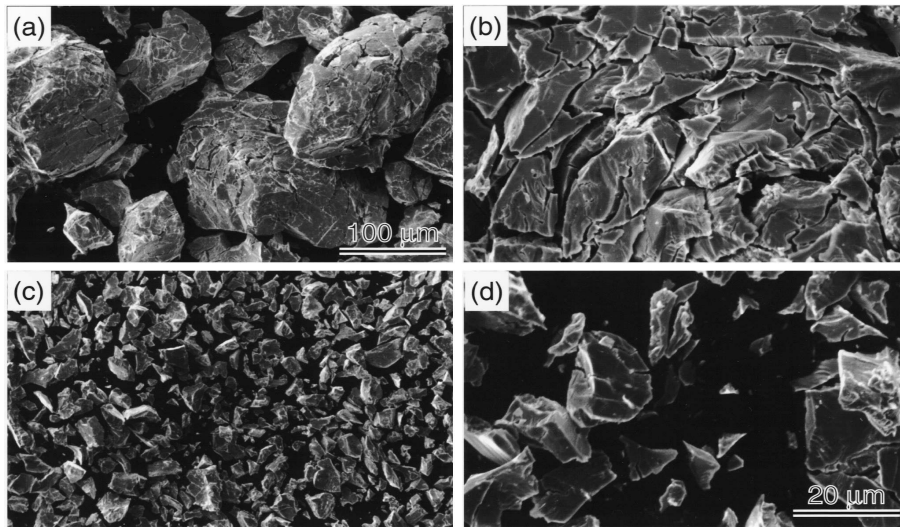
Table 3: PCT and cost properties of AB<sub>5</sub> hydrides

Composition	$\Delta H$ kJ mol <sup>-1</sup>	$\Delta S$ kJ mol <sup>-1</sup> K <sup>-1</sup>	25°C $P_d$ atm	$T$ for 1 atm $P_d$	Plateau	
					Hysteresis	Slope
MmNi <sub>5</sub>	21.1	0.097	23	-56	1.65	0.54
MmNi <sub>4.15</sub> Fe <sub>0.85</sub>	25.3	0.105	11.2	-32	0.17	0.36
MmNi <sub>4.5</sub> Al <sub>0.5</sub>	28.0	0.105	3.8	-6	0.11	0.36
LaNi <sub>5</sub>	30.8	0.108	1.8	12	0.13	0.13
LaNi <sub>4.8</sub> Sn <sub>0.2</sub>	32.8	0.105	0.5	39	0.19	0.22
CaNi <sub>5</sub> (M)	31.9	0.101	0.5	43	0.16	0.19
MmNi <sub>3.5</sub> Co <sub>0.7</sub> Al <sub>0.8</sub>	39.8	0.115	0.11	73	0.2 est.	1.2
LaNi <sub>4.25</sub> Al <sub>0.75</sub>	44.1	0.117	0.024	104	0.23	2.7

Composition	Density g cm <sup>-3</sup>	(H-Capacity) <sub>max</sub>		(H-Capacity) <sub>r</sub>		Alloy RMC <sup>c</sup>	
		H/M	wt.%	$\Delta H/M$	$\Delta wt.\%$	$\Delta N_H/V^b$	$\$ kg^{-1} H$
MmNi <sub>5</sub>	8.6	1.06	1.46	0.90	1.24	5.2	7.94
MmNi <sub>4.15</sub> Fe <sub>0.85</sub>	8.1	0.82	1.14	0.65	0.90	3.8	7.12
MmNi <sub>4.5</sub> Al <sub>0.5</sub>	8.1	0.85	1.2	0.58	0.83	3.5	7.17
LaNi <sub>5</sub>	8.3	1.08	1.49	0.93	1.28	5.2	9.87
LaNi <sub>4.8</sub> Sn <sub>0.2</sub>	8.4	1.06	1.4	0.92	1.24	5.1	9.69
CaNi <sub>5</sub> (M)	6.6	1.05	1.87	0.55	0.99	3.4	7.56
MmNi <sub>3.5</sub> Co <sub>0.7</sub> Al <sub>0.8</sub>	7.6	0.85	1.24	0.36	0.53	2.2	13.25
LaNi <sub>4.25</sub> Al <sub>0.75</sub>	7.6	0.77	1.13	0.53	0.78	3.1	9.68

<sup>a</sup> (M)=middle plateau for CaNi<sub>5</sub>.  
<sup>c</sup> RMC=Raw Materials Cost; \$ g<sup>-1</sup> H based on (H-Capacity)<sub>r</sub>.  
<sup>b</sup> Reversible volumetric capacities are approximate and in units of 10<sup>22</sup> H-atoms/crystal cm<sup>3</sup>.

Fig. 21: SEM images of LaNi<sub>5</sub> deprecitated after (a), (b) one cycle and (c), (d) five cycles [39]

### 1.3.3.2.2 AB<sub>2</sub> intermetallic compounds

Like the AB<sub>5</sub>s, the AB<sub>2</sub> intermetallics represent a large and versatile group of hydriding materials with PCT properties of value for the ambient temperature applications. The Internet database presently includes nearly 500 AB<sub>2</sub> entries, including multiple data on certain binary and multi-component compounds by various investigators [40]. The A-elements are often from the IVA group (Ti, Zr, Hf) and/or rare earth series (at. no. 57–71) or Th. The B-elements can be a variety of transition or non-transition metals with something of a preference for atomic numbers 23–26 (V, Cr, Mn, Fe). A very wide variety of substitutions are possible for both A- and B-elements, thus providing a high degree of fine tuning of PCT properties. The AB<sub>2</sub>s are largely based on two related Laves phase crystal structures:

- a) Hexagonal (prototype MgZn<sub>2</sub>, Strukturbericht C14, Pearson hP12, space group  $P6_3/mmc$ )
- b) Cubic (prototype MgCu<sub>2</sub>, Strukturbericht C15, Pearson cF24, space group  $Fd\bar{3}m$ ).

The first reported Laves phase hydrides were reported in the 1950s and 1960s by principal USA authors Trzeciak, Pebler and Beck. Practical AB<sub>2</sub> hydrides were identified in the 1970s by groups led by Shaltiel (Israel), Gamo (Japan), Buschow (Netherlands), Wallace (USA), Reilly (USA), Burnasheva (USSR) and others. These groups continued into the 1980s and were joined by efforts led by Kierstead (USA), Bernauer (Germany) and Ivey (Canada), among others. R&D on AB<sub>2</sub> has continued to this day in many laboratories around the world. Many others in addition to those listed above deserve credit. A much more complete list of references can be found in the AB<sub>2</sub> on-line database [40]. The PCT and other properties of various representative AB<sub>2</sub> alloys are shown in Fig. 22 and Table 4. PCT properties can be adjusted over ranges of temperature and pressure that cover our 1–10 bar, 0–100°C preference. H-capacities of AB<sub>2</sub> alloys are comparable to AB<sub>5</sub>s on a reversible (principal plateau) basis but generally higher on a (H-capacity)<sub>max</sub> basis. The AB<sub>2</sub>s often suffer from less distinct, narrower plateaux and a residual, essentially nonreversible “heel” compared to AB<sub>5</sub>s. When larger ranges of temperature and pressure are available from the application, AB<sub>2</sub>s tend to show higher capacities than AB<sub>5</sub>s. The AB<sub>2</sub> alloys do offer significant advantages over the AB<sub>5</sub>s in cost, at least if the A-element is mostly Ti and not Zr. As shown in Table 2, TiMn<sub>1.5</sub> and the widely used GfE commercial alloy Ti<sub>0.98</sub>Zr<sub>0.02</sub>V<sub>0.43</sub>Fe<sub>0.09</sub>Cr<sub>0.05</sub>Mn<sub>1.5</sub> have (H-capacity)<sub>r</sub>-normalized raw materials costs about half those of the best AB<sub>5</sub>s (Table 1). To make an important point on the use of V in AB<sub>2</sub> compositions, TiMn<sub>1.4</sub>V<sub>0.62</sub> should be compared to Ti<sub>0.98</sub>Zr<sub>0.02</sub>V<sub>0.43</sub>Fe<sub>0.09</sub>Cr<sub>0.05</sub>Mn<sub>1.5</sub>. Both alloys are similar in composition (including V-content) and have similar capacities, but TiMn<sub>1.4</sub>V<sub>0.62</sub> has six to seven times the raw materials cost. That is because pure V is very expensive compared to ferrovanadium, a low-cost product used by the steel industry. Therefore, V-containing alloys should also have some Fe present to allow the use of low-cost ferrovanadium.

AB<sub>2</sub> alloys are generally somewhat more difficult to activate than AB<sub>5</sub>s, although some will activate without heating, especially those higher in Zr or Mn (as opposed to Ti and Cr). Once activated, H/D kinetics are usually high. Although little good

quantitative data exist,  $AB_2$ s seem to be relatively sensitive to impurities in the  $H_2$  used; alloys high in Ti seem to passivate easily. When lanthanide elements are used in the A-side,  $AB_2$ s are very prone to disproportionation (even on the first cycle). The Ti or Zr-based alloys seem to have only minor disproportionation tendencies. Like the  $AB_5$ s,  $AB_2$ s decrepitate into fine powder. Alloys high in Zr and Mn are highly pyrophoric in the activated state, whereas those high in Ti and Cr seem not to be. The commercial production of  $AB_2$  compounds is more difficult than  $AB_5$  compounds and requires great metallurgical care. Because of the high melting points of the principal elements (Ti=1670°C, Zr=1855°C, Cr=1863°C), along with their high reactivity, it is often very difficult to use standard vacuum induction melting (VIM) in a conventional oxide crucible. More expensive cold-crucible vacuum arc melting is usually required. It is possible to induction-melt of  $ZrMn_2$  (melting temperature 1450°C) under argon in  $Al_2O_3$  crucibles but Mn has a high vapor pressure and corrections have to be made for its evaporation during melting.

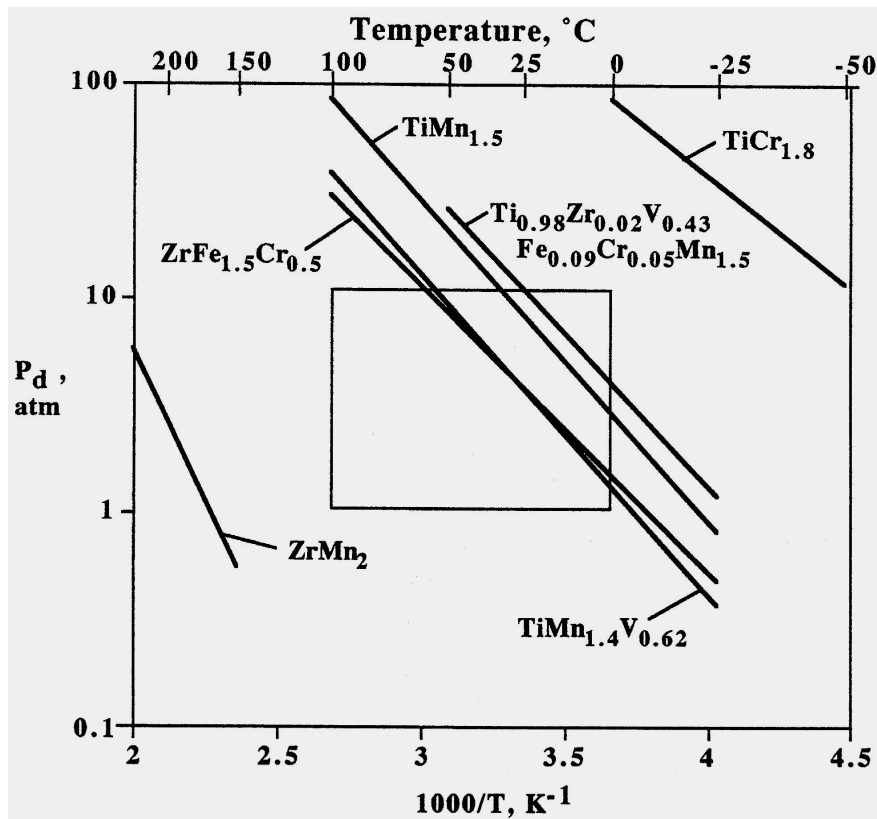


Fig. 22: Van't Hoff plots for various  $AB_2$  hydrides [25]

Table 4: PCT and cost properties of AB<sub>2</sub> hydrides

Composition	$\Delta H$ kJ mol <sup>-1</sup>	$\Delta S$ kJ mol <sup>-1</sup> K <sup>-1</sup>	25°C $P_d$ atm	$T$ for 1 atm $P_d$	Plateau	
					Hysteresis	Slope
TiCr <sub>1.8</sub>	20.2	0.111	182	-91	0.11	0.12
Ti <sub>0.98</sub> Zr <sub>0.02</sub> V <sub>0.45</sub> Fe <sub>0.09</sub> Cr <sub>0.05</sub> Mn <sub>1.3</sub>	27.4	0.112	11	-28	-	1.1
TiMn <sub>1.5</sub>	28.7	0.114	8.4	-21	0.93	0.57
ZrFe <sub>1.3</sub> Cr <sub>0.5</sub>	25.6	0.097	4.0	-10	0.34	1.26
TiMn <sub>1.4</sub> V <sub>0.02</sub>	28.6	0.107	3.6	-5	-	1.4
ZrMn <sub>2</sub>	53.2	0.121	0.001	167	0.99	0.74

Composition	Density g cm <sup>-3</sup>	(H-Capacity) <sub>max</sub>		(H-Capacity) <sub>r</sub>		Alloy RMC <sup>b</sup>		
		H/M	wt.%	$\Delta H/M$	$\Delta wt.\%$	$\Delta N_H/V^a$	$\$ kg^{-1}$	$\$ g^{-1} H$
TiCr <sub>1.8</sub>	6.0	1.25	2.43	0.45	0.85	2.7	8.64	1.02
Ti <sub>0.98</sub> Zr <sub>0.02</sub> V <sub>0.45</sub> Fe <sub>0.09</sub> Cr <sub>0.05</sub> Mn <sub>1.3</sub>	5.8	0.99	1.9	0.7	1.3	3.8	4.82	0.37
TiMn <sub>1.5</sub>	6.4	0.99	1.86	0.65	1.15	3.8	4.99	0.44
ZrFe <sub>1.3</sub> Cr <sub>0.5</sub>	7.6	1.03	1.5	0.62	0.9	3.3	10.90	1.21
TiMn <sub>1.4</sub> V <sub>0.02</sub>	5.8	1.14	2.15	0.56	1.1	3.1	29.40	2.67
ZrMn <sub>2</sub>	7.4	1.2	1.77	0.6	0.9	2.9	11.29	1.25

<sup>a</sup> RMC = Raw Materials Cost;  $\$ g^{-1} H$  based on (H-Capacity)<sub>r</sub>.  
<sup>b</sup> Reversible volumetric capacities are approximate and in units of 10<sup>22</sup> H-atoms/crystal cm<sup>3</sup>.

### 1.3.3.2.3 AB intermetallic compounds

The first demonstration of a reversible intermetallic hydride was demonstrated with the AB compound ZrNi by Libowitz in 1958. Unfortunately, ZrNiH<sub>3</sub> has a 1 bar desorption temperature of about 300°C, too high for practical applications. The first practical AB hydrides were demonstrated with TiFe around 1970 by Reilly and Wiswall at Brookhaven National Laboratory, USA. TiFe and its substitutional modifications remain the best of the AB alloys today. TiFe-based AB alloys are based on an ordered body-centered-cubic structure (prototype CsCl, Strukturbericht B2, Pearson cP2, space group  $Pm\bar{3}m$ ). They tend to have two plateaux (two distinct hydrides), both with reasonable pressures at room temperature (Fig. 23). PCT properties can be modified by partial substitution for Ti and Fe, e.g., Mn or Ni for Fe as shown in Figure 24. Tabulation of PCT properties and costs of typical alloys are shown in Table 4. TiFe and TiFe<sub>0.85</sub>Mn<sub>0.15</sub> show good volumetric and gravimetric reversible H-capacities, competitive with the best of the AB<sub>5</sub>s and AB<sub>2</sub>s. However, TiFe<sub>0.8</sub>Ni<sub>0.2</sub> is not so useful because of its low capacity and low plateau pressure. The low capacity of TiFe<sub>0.8</sub>Ni<sub>0.2</sub> is due to the fact the upper plateau is absent in this alloy, i.e., is at too high pressure range to be useful. TiFe and TiFe<sub>0.85</sub>Mn<sub>0.15</sub> offer low price, lower on a per unit H<sub>2</sub> storage capacity than anything heretofore presented. Hysteresis tends to be on the high side.

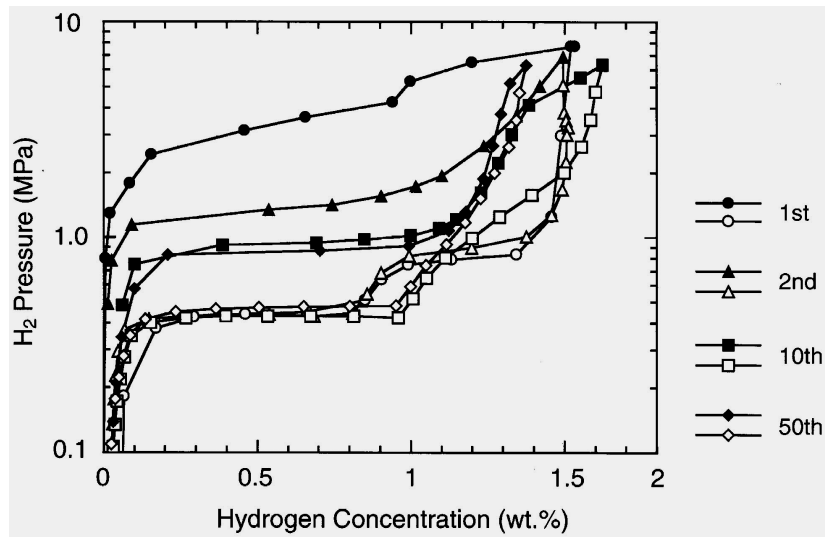


Fig. 23: PCT of TiFe with initial particle 150-300  $\mu\text{m}$  for the first, second, 10<sup>th</sup> and 50<sup>th</sup> cycles of hydrogen absorption/desorption [39]

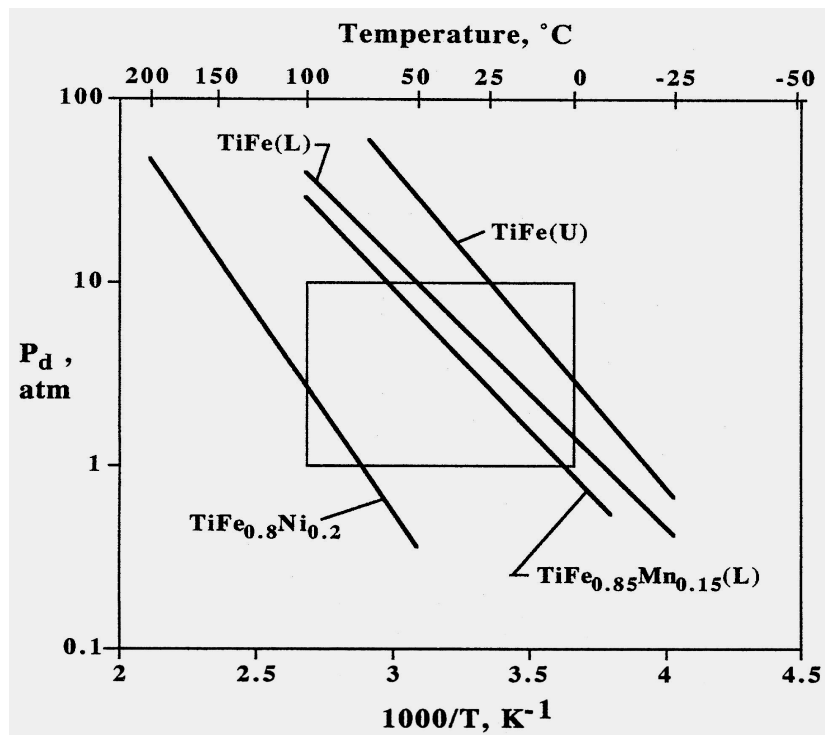


Fig. 24: Desorption Van't Hoff plots for TiFe-types of hydride. L indicates low plateau lines and U upper plateau lines.

Table 5: PCT and cost properties of TiFe-type hydrides (L=lower plateau)

Composition	$\Delta H$ kJ mol <sup>-1</sup>	$\Delta S$ kJ mol <sup>-1</sup> K <sup>-1</sup>	25°C $P_d$ atm	$T$ for 1 atm $P_d$	Plateau	
					Hysteresis	Slope
TiFe (L)	28.1	0.106	4.1	-8	0.64	0.0
TiFe <sub>0.83</sub> Mn <sub>0.15</sub> (L)	29.5	0.107	2.6	3	0.62	0.92
TiFe <sub>0.8</sub> Ni <sub>0.2</sub> (L)	41.2	0.119	0.1	73	0.05	0.36

Composition	Density g cm <sup>-3</sup>	(H-Capacity) <sub>max</sub>		(H-Capacity) <sub>r</sub>			Alloy RMC <sup>b</sup>	
		H/M	wt.%	$\Delta H/M$	$\Delta \text{wt.}\%$	$\Delta N_H/V^a$	$\$ \text{ kg}^{-1}$	$\$ \text{ g}^{-1} \text{ H}$
TiFe	6.5	0.975	1.86	0.79	1.5	5.0	4.68	0.31
TiFe <sub>0.83</sub> Mn <sub>0.15</sub>	6.5	1.0	1.9	0.80	1.5	5.0	4.83	0.32
TiFe <sub>0.8</sub> Ni <sub>0.2</sub>	6.5	0.7	1.3	0.42	0.8	2.9	5.5	0.68

<sup>b</sup> RMC=Raw Materials Cost;  $\$ \text{ g}^{-1} \text{ H}$  based on (H-Capacity)<sub>r</sub>.  
<sup>a</sup> Reversible volumetric capacities are approximate and in units of 10<sup>22</sup> H-atoms/crystal cm<sup>3</sup>.

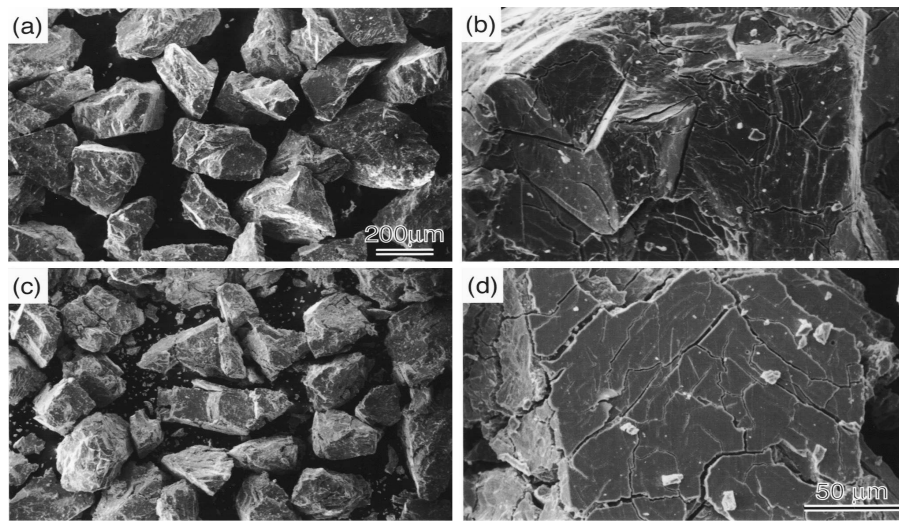


Fig. 25: SEM images of TiFe samples after (a), (b) one cycle, and (c), (d) 50 cycles

Activation is relatively slow and difficult for the TiFe-based Abs [41]. Binary TiFe needs to be heated to disrupt the natural oxide surface layer. Mn-modified TiFe will usually slowly activate at room temperature. In any event, it may take a day or more and high pressures (more than 50 bar) for complete activation. As might be expected, the passive oxide films that can easily form on TiFe (and its derivatives) result in a high degree of sensitivity to gaseous impurities in the H<sub>2</sub> used. On the positive side, and because of the tendency to form passive Ti-oxides, these materials seem to have little or no tendency for pyrophoricity. Cyclic stability of the lower plateau is excellent, but the upper plateau tends to drift higher and higher with H/D cycling, ultimately rendering it unusable. TiFe alloys deprecipitate more difficult than

the AB5 alloys. Figure 25 shows the morphology of the TiFe alloy decrepitated after several cycles.

The melting of TiFe-based ABs requires care. The metallurgy is made complex by the tendency of the alloys to pick up oxygen, which in turn tends to lower reversible capacity. Conventional oxide melting crucibles are not stable enough. Expensive arc melting will work. In summary, TiFe-based AB alloys have good PCT properties, good H-capacities and low raw materials costs, but the problems associated with activation, gaseous impurities and upper plateau instabilities have largely prevented their large scale commercial use in H<sub>2</sub> gas storage applications.

#### 1.3.3.2.4 A<sub>2</sub>B intermetallic compounds

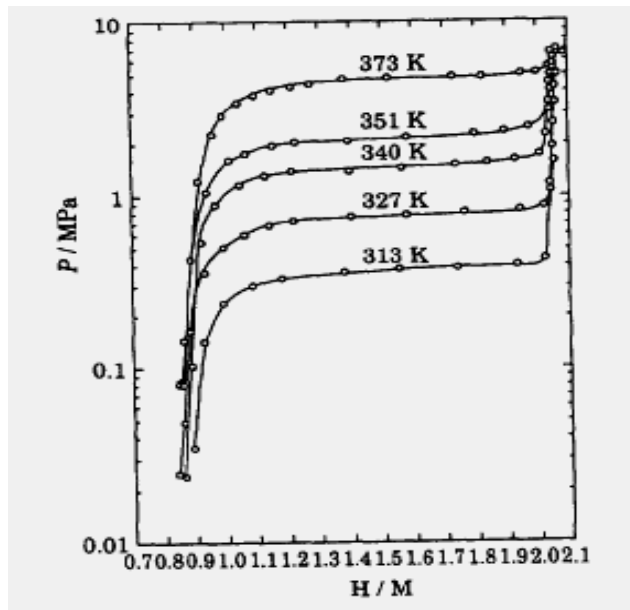
The A<sub>2</sub>B family of compounds represents an area of historical activity. Various crystal structures are possible. In one subfamily, A is typically of the Group IVA elements Ti, Zr or Hf and B is a transition metal, typically Ni. Another family is based on Mg<sub>2</sub>Ni, discovered in the late 1960s by Reilly and Wiswall (USA). Unfortunately, the A<sub>2</sub>Bs offer little in the 0–100°C, 1–10 bar range, at least with the present state of the art. They are invariably more stable. There has been extensive work on Mg<sub>2</sub>Ni for nearly three decades, both from fundamental and applications points of view. Actually, Mg<sub>2</sub>NiH<sub>4</sub> is a transition metal complex, not a metallic hydride.

As shown in Table 6, H-capacity and cost properties of Mg<sub>2</sub>Ni are attractive, but desorption temperatures are too high for most applications. Mg<sub>2</sub>Ni is not very amenable to modification of PCT properties by ternary and higher-order substitutions. Numerous attempts to significantly decrease desorption temperatures have not been particularly successful. There have been several successful attempts to increase absorption and desorption kinetics by surface treated or nanocrystalline and amorphous versions of Mg<sub>2</sub>Ni-related alloys (sometimes including catalysts), but the basic hydride thermodynamics have not been improved much.

Table 6: PCT and cost properties of Mg<sub>2</sub>NiH<sub>4</sub>

$\Delta H = -64.5 \text{ kJ mol}^{-1} \text{ H}_2$
$\Delta S = -0.122 \text{ kJ mol}^{-1} \text{ K}^{-1}$
25°C $P_d = 10^{-5} \text{ atm}$ (extrapolated)
$T$ for 1 atm $P_d = 255^\circ\text{C}$
$(\text{H}/\text{M})_{\text{max}} = 1.33$
$(\text{wt.}\%)_{\text{max}} = 3.6$
$(\Delta\text{H}/\text{M})_r = 1.23$
$(\Delta\text{wt.}\%)_r = 3.3$
$(\Delta\text{H}/\text{V})_r = 5.2 \times 10^{22} \text{ H-atoms/cm}^3$
Alloy Raw Materials Cost = \$6.26 kg <sup>-1</sup>
Alloy Raw Materials Cost = \$0.19 g <sup>-1</sup> H stored



Fig. 26: PCT diagrams of VH-VH<sub>2</sub> system [45]

$\Delta H = -43.2 \text{ kJ mol}^{-1} \text{ H}_2$
$\Delta S = -0.140 \text{ kJ mol}^{-1} \text{ K}^{-1}$
$25^\circ\text{C } P_a = 0.5 \text{ atm}$
$T \text{ for } 1 \text{ atm } P_a = 36^\circ\text{C}$
Hysteresis = 0.80
Plateau Slope = 0.45
$(\text{H}/\text{M})_{\text{max}} = 1.95$
$(\text{wt.}\%)_{\text{max}} = 3.7$
$(\Delta\text{H}/\text{M})_r = 0.95$
$(\Delta\text{wt.}\%)_r = 1.8$
$(\Delta\text{H}/\text{V})_r = 4.9 \times 10^{22} \text{ H-atoms/cm}^3$
Alloy Raw Materials Cost = \$10.63 kg <sup>-1</sup>
Alloy Raw Materials Cost = \$0.59 g <sup>-1</sup> H stored

Table 7: PCT and cost properties of  $(\text{V}_{0.9}\text{Ti}_{0.1})_{0.95}\text{Fe}_{0.05}$ 

### 12.3.3.2.5 Other intermetallic compounds

In addition to the AB<sub>5</sub>, AB<sub>2</sub>, AB and A<sub>2</sub>B intermetallic compounds discussed above, several other families of intermetallics have been shown capable of reversible hydriding/dehydriding reactions [40, 42-43]. Examples include AB<sub>3</sub>, A<sub>2</sub>B<sub>7</sub>, A<sub>6</sub>B<sub>23</sub>, A<sub>2</sub>B<sub>17</sub>, A<sub>3</sub>B and others. Most structures involve long-period AB<sub>5</sub> and AB<sub>2</sub> stacking

sequences and are thus crystallographically related to these two classic families. Although none of these have attained commercial levels of interest, at least the  $AB_3$  and  $A_2B_7$  phases do have PCT properties, which are in the range of our interest. Most either have narrow plateaux with long sloping upper legs (e.g.,  $GdFe_3$ ) or multiple plateaux (e.g.,  $NdCo_3$  or  $Pr_2Ni_7$ ).  $La_2Mg_{17}$  was once reported to have 6 wt% H-capacity, recoverable at room temperature [44], but that claim has never been independently confirmed.

### 1.3.3.2.6 Solid solution alloys

Metallurgically speaking, the term “solid solution alloy” designates a primary element (solvent) into which one or more minor elements (solutes) are dissolved. Unlike the intermetallic compound, the solute need not be present at an integer or near-integer stoichiometric relationship to the solvent and is present in a random (disordered) substitutional or interstitial distribution within the basic crystal structure. Several solid solution alloys form reversible hydrides, in particular those based on the solvents Pd, Ti, Zr, Nb and V. Perhaps the largest family of solid solution hydrides consists of the face-centered-cubic (A1) Pd-based alloys [40]. Although the PCT properties of many of the Pd solid solution hydrides are useful, they are of generally low gravimetric and volumetric H-capacity, e.g., seldom exceeding 1.0 wt%  $H_2$ . In addition they are prohibitively expensive. Ti- and Zr-based solid solution alloys form hydrides that are too stable, even when highly alloyed.

Vanadium has di-hydride properties (shown in Figure 26, [45]) compatible with useful ambient temperature H-storage (Fig. 19), so it is logical that binary and higher component solid solution's based on V offer further opportunities [46]. These alloys are all based on the simple body-centered-cubic (A2) crystal structure and their di-hydrides generally form a face-centered cubic structure (Strukturbericht C1, prototype  $CF_2$ , Pearson  $cF12$  and space group  $Fm\bar{3}m$ ). The first extensive hydride work on V solid solutions was done by the Reilly BNL (USA) group in the early 1970s, followed by the Libowitz Allied Chemical (USA) group in the 1980s. At present, there is strong activity by the Akiba group (Japan) [47]. There are many reported V solid solution hydriding alloys, but V–Ti–Fe seems to be one with good promise. For example, by varying  $x$  from 0 to 0.075 in  $(V_{0.9}Ti_{0.1-x})Fe_x$ , the di-hydride plateau pressure can be varied over more than an order of magnitude without affecting capacity [48]. The PCT and cost properties of one alloy in this V–Ti–Fe family,  $(V_{0.9}Ti_{0.1})_{0.95}Fe_{0.05}$ , are shown in Table 7. PCT properties are attractive for room-temperature applications with good  $(\Delta wt\%)_r$ . Even using low-cost ferrotitanium for the source of the Fe, the alloy raw materials price is on the high side. As mentioned earlier, pure V is very expensive and it is important that any V-based solid solution alloy must contain Fe so that commercial ferrovanadium can be used in its manufacture. Fortunately, ferrovanadium has been used successfully in the production of V–Ti–Fe hydriding alloys, although the major impurities Al and Si do seem to change the PTC properties significantly [49].

A new family of “Laves phase related BCC solid solution alloys” based on V–Ti–Mn has recently been reported [47]. Alloys contain a nanoscale lamellar structure,

possibly resulting from partial spinodal decomposition, and offer good room temperature capacity and reversibility. There is relatively little literature on the non-PCT properties of V solid solution hydrides, e.g., gaseous impurity effects. The high melting temperatures and high reactivity of V alloys probably restrict the available melting techniques to “cold crucible” methods such as vacuum arc or electron beam melting. No large-scale commercial batches of such alloys have been produced and hydrided. There has been no long-term cycling of V alloy hydrides, so it is uncertain if disproportionation or other metallurgical instabilities occur.

### 1.3.3.2.7 Summary of hydriding alloys

A qualitative summary of PCT and non-PCT properties of the alloy families discussed above is given in Table 8. Such a summary is mainly based on experience. The AB<sub>5</sub>, AB<sub>2</sub> and AB intermetallics offer the best collections of near room-temperature PCT properties, with the best combinations of good H-capacity and lowest raw materials cost. V solid solutions offer good capacity, but cost is questionable, secondary properties are not known well. The important point to be made is that there are no ideal hydriding alloys. There are many gaps to be filled and particular areas of R&D to follow within the framework of AB<sub>5</sub>, AB<sub>2</sub>, AB, A<sub>2</sub>B and V solid solution alloys, to be sure [42]. However, it must be argued that we are reaching a point of diminishing returns involving limits to the inherent thermodynamics and metallurgy of these conventional families of hydriding alloys. New and different approaches need to be explored in the future.

Table 8: Qualitative overview of the hydride types

Attribute	AB <sub>5</sub>	AB <sub>2</sub>	AB	A <sub>2</sub> B	V-SS
Versatility	+	+	+	-/0	0
H-Capacity	0	0/+	0/+	+	+
PCT	+	+	+	-	+
Activation	+	0	-/0	0	0
Impurity effects	+	0	-	0	-/?
Cyclic stability	-/0/+	-/0/?	-/0	0/?	?
Ease of manufacture	+	0	+	0	?
Pyrophoricity	0	-	+	+	+/0
Cost	0	+	+	+	-/0

\* Attribute key: - = problem; 0 = neutral; + = good; ? = uncertain.

### 1.3.3.3 Other approaches

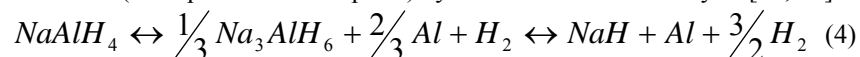
New directions for hydriding materials include amorphous and nanocrystalline alloys, quasi-crystalline alloys, transition and non-transition metal complexes and carbon. In the area of amorphous nanocrystalline alloys, usually made by sputtering or ball milling, there has been good progress made in increasing the A/D kinetics. It seems that, the desorption thermodynamics can be permanently changed, i.e., there seems to be little or no evidence the desorption temperatures of Mg-based alloys can be permanently decreased or the H-capacities significantly increased. Amorphous alloys do not have a plateau, which can limit practical applications. They are

inherently metastable in nature and will tend toward the equilibrium crystalline forms or larger grain sizes. In the relatively new area of quasi-crystalline alloys, there are only a limited number of available alloys. Those that have been hydrided are high in Ti, resulting in impracticably high desorption temperatures.

### 1.3.3.3.1 Hydride complexes

Complex hydrides are well known. One category comprises the transition metal complexes. When certain transition metals are combined with a Group IA or IIA element in the presence of hydrogen, a low valence complex of the transition metal and multiple H atoms will form. Such complexes are stabilized by the donation of electrons from the more electropositive IA or IIA elements. A well used example of this is  $Mg_2NiH_4$ , where Mg donates electrons to stabilize the  $[NiH_4]^{-4}$  complex. In effect, four hydrogen atoms bond with a single Ni atom and the two Mg atoms donate two electrons each to stabilize that high-H transition metal complex. There are a number of such transition metal complex hydrides that have been discovered around the world and are at least four groups that have contributed much of the historical activity in this area: (1) the Yvon group at the University of Geneva, (2) the Noréus group at Stockholm University, (3) the Bronger group at the Technische Hochschule Aachen and (4) the Moyer group at Trinity College (USA).  $Mg_2NiH_4$  is an exception to the general situation of TM complex hydrides in that it has a corresponding  $Mg_2Ni$  intermetallic. It is very significant that transition metal complex hydrides can be synthesized from combinations of electropositive elements and transition metals that do not form intermetallic compounds. For example, it is well known that Mg and Fe do not alloy at all in the H-free solid metallic state. Yet, when Mg and Fe powders are sintered in  $H_2$ , the high-H complex hydride  $Mg_2FeH_6$  forms. Because the formation and decomposition of transition metal complex hydrides usually require some metal atom diffusion, the kinetics tend to be rather slow compared to the traditional interstitial hydrides and high temperatures are needed for  $H_2$  desorption. However the high hydrogen contents possible (e.g.  $Mg_2FeH_6$  5.5 wt%  $H_2$ ) give potential to these materials as hydrogen storage materials. It is needed to find out how to make the TM complex hydrides more reversible, especially in the low temperature  $H_2$  desorption mode. This area is reviewed in this volume by Yvon [50].

Another major area of complex hydrides comprises the non-transition metal complexes. Examples include aluminates and borohydrides such as  $LiAlH_4$  [51] and  $NaBH_4$  ( $[AlH_4]^-$  and  $[BH_4]^-$  complexes), among many others. Although long used to generate  $H_2$  gas by reaction with  $H_2O$ , these hydrides have never been known to be very reversible from the gas phase point of view. Recently, Bogdanovic has importantly discovered that the two-step gas reaction for  $NaAlH_4$  can be made reversible (absorption and desorption) by the addition of Ti-catalysts [52, 53]:



The H-capacity for equation (4) is about 5.6 wt%; under cyclic conditions about 4 wt% reversible capacity can be achieved below 150°C as shown in Figure 27. Catalyzed complex hydrides offer a whole new area for low temperature, high capacity reversible hydrides. Recent developments with Ti- and Zr-catalyzed  $NaAlH_4$  are reported by Zidan et al. [54]

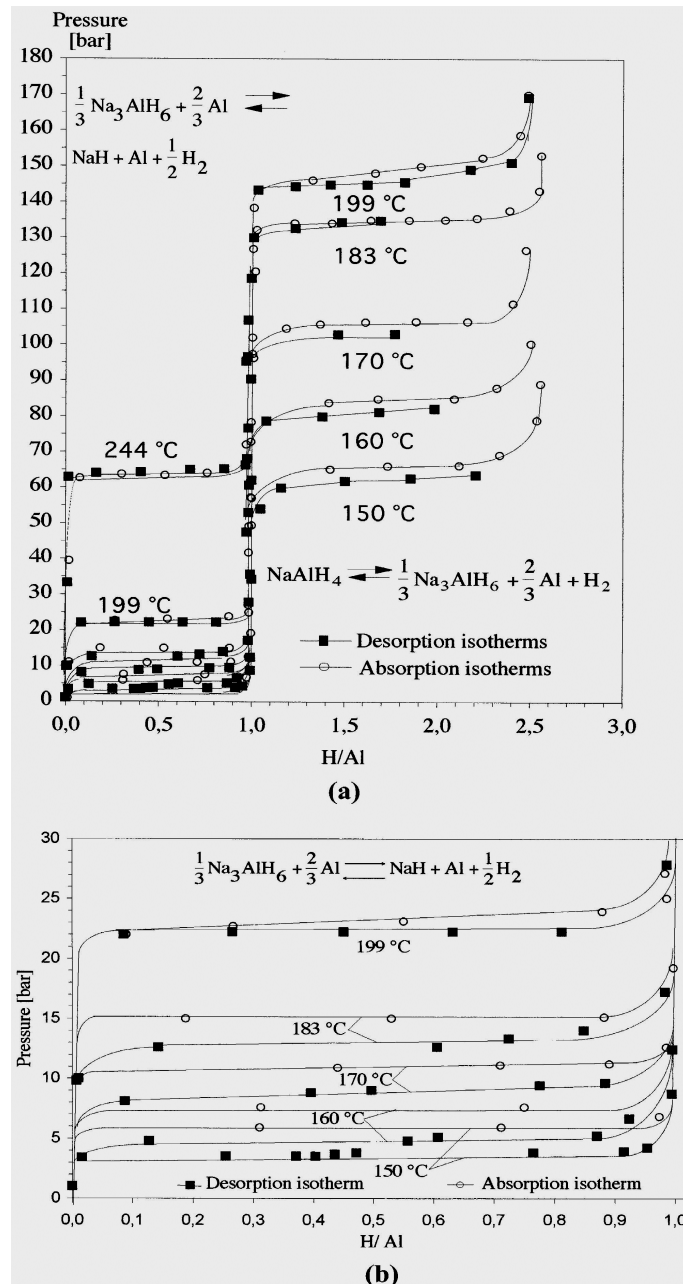


Fig. 27: PCT diagrams of Ti-doped NaAlH<sub>4</sub> at different temperatures (a), at higher resolution (b) [53]

### 1.3.3.3.2 Chemical hydrides

Chemical Hydride (LiH, NaH, CaH<sub>2</sub>) Slurries (in light mineral oil) are used as

hydrogen carriers and storage media [55]. The slurry protects the Hydride from an anticipated contact with moisture in the air and makes the Hydride pumpable. Hydrogen gas is produced by a chemical Hydride/water reaction. The main advantage [56] of the method is high hydrogen storage capacity (up to 25 wt% in LiH). The main disadvantage is that the system is not refillable, and it is difficult to extract the hydrogen.

### 1.3.3.3 Carbon

Study of storing H<sub>2</sub> on or in various forms of carbon has been very active lately. It has long been known that high surface area activated carbon will physisorb molecular H<sub>2</sub> and serve as a storage medium for the gas. However, because adsorption is by relatively weak Van der Waals interactions, significant storage of H<sub>2</sub> on C occurs only when the C is cold (below 150 K) and high pressures are applied. On the other extreme, H can be chemically bonded to the C<sub>60</sub> and C<sub>70</sub> fullerenes. H-contents as high as C<sub>60</sub>H<sub>48</sub> (6.3 wt% H) have been achieved. Unlike the purely physisorption process with activated carbon, C<sub>60</sub> carbon atoms form relatively strong covalent bonds with H atoms, with  $\Delta H$  on the order of -285 kJ/mol H<sub>2</sub>. This means that temperatures on the order of 400°C are needed for the breaking of that bond and the desired desorption of H<sub>2</sub> gas. The question is can the chemistry of the fullerene hydrides be controlled to lower stability, much like what has been successfully achieved with the metallic hydrides reported above

A clear potential has been demonstrated for room-temperature storage of H<sub>2</sub> molecules in single wall carbon nanotubes (a tubular form of the normally spherical fullerenes) by a group led by Heben (USA) [57]. SWNTs have internal dimensions on the order of 1–2 nm, about what is needed for the capillary “condensation” of H<sub>2</sub> near room-temperature. Predictions of room-temperature reversible 5–10 wt% H<sub>2</sub> have been made. If confirmed, such H-contents would surpass what is known for any reversible metal-hydride and open a new technology for “solid” hydrogen storage.

One final form of carbon proposed for near ambient temperature H-storage applications are “graphite nanofibers”, developed by Rodriguez and Baker of Northeastern University (USA). The new form of graphite is made by reacting hydrocarbons and CO on Ni- and Fe-based catalysts. By a mechanism not fully understood by the developers, this form of carbon is said to be capable of “condensing” extraordinary amounts of molecular H<sub>2</sub> within the graphite layers, up to 67 wt% [58]. Because H-contents of strongly bonded C–H chemical compounds do not exceed methane CH<sub>4</sub> (25 wt% H), as well as no obvious a priori physical process that could account for such high levels of H-intercalation, the reported measurements have been met with considerable scepticism. At this moment, the measurements of Rodriguez and Baker have apparently not been independently substantiated to date. If even partially confirmed, this new form of graphite would obviously be of great interest for H-storage. As always in science, time will be the great resolver of this interesting controversy.

### 1.3.4 Prospects on hydrogen absorbing materials

The development of reversible metal hydrides has had along, interesting and successful history. There are numerous alloys and intermetallic compounds that have properties of real commercial interest and value for applications. However, those hydrides that will readily release their H<sub>2</sub> at room-temperature have reversible gravimetric H-densities no more that about 2 wt%. This is not quite sufficient for fuel cell vehicles, perhaps the most active new area of hydrogen application. It could though be sufficient in some mobile applications and certainly for stationary applications offering a high volumetric hydrogen density. From a gas reaction point of view, the conventional alloys and intermetallic compounds seem to be reaching their thermodynamic limits relative to PCT and H-capacity. More research is needed concentrated more on the development of new high H-capacity alloys. Greater promise for the future lies in catalyzed hydride complexes although many difficulties need to be overcome. In the non-metal area, carbon has offers some renewed potential.

## 1.4 Other methods of hydrogen storage

### 1.4.1 Carbon-based materials

Low-temperature adsorption of hydrogen (at 150 K) on activated carbon has shown storage capacity of about 4 wt% [59-65]. The storage capacity seems to be related to the porosity and surface properties of the carbon bed. While the potential for gravimetric density is high the volumetric density is very low. Low adsorption temperatures dictate the use of insulated containers, and the boil-off calls for pressurized containers. These are significant drawbacks [64].

Fullerenes and nanotubes are single or multiple atomic layers of graphite wrapped together into very stable ball or tube molecules respectively. Fullerenes or mixed Fullerenes (MF) and some related organic hydrides can absorb up to 7 wt% of hydrogen and release it under suitable conditions [64]. For example, there is 7.7 wt% of hydrogen stored in C<sub>60</sub>H<sub>60</sub>. Experimental results by using liquid phase hydrogenation have already indicated a 6 wt% hydrogen storage feasibility in Fullerenes (corresponding to C<sub>60</sub>H<sub>48</sub>) at 180 °C under 2.4-2.7 MPa. There is no significant dehydrogenation at this temperature suggesting that the dehydrogenation temperature is higher than that for hydrogenation. In the presence of an Ir-base complex catalyst the dehydrogenation temperature is below 225 °C.

The Carbon Single-Wall Nanotubes (SWNTs) are elongated micropores of molecular dimensions (diameter approximately 1.2 nm). It has been shown [67-70] that hydrogen could be adsorbed at temperatures above 12 °C on arc-generated soot containing nanotubes. Materials that are composed predominantly of SWNTs may prove to be the ideal adsorbent for ambient temperature storage of hydrogen. However, experiments and simulations with pure SWNT ropes indicate that the pure material requires low temperature (80 K) and high pressure (40-120 bar) to stabilize a significant amount of hydrogen.

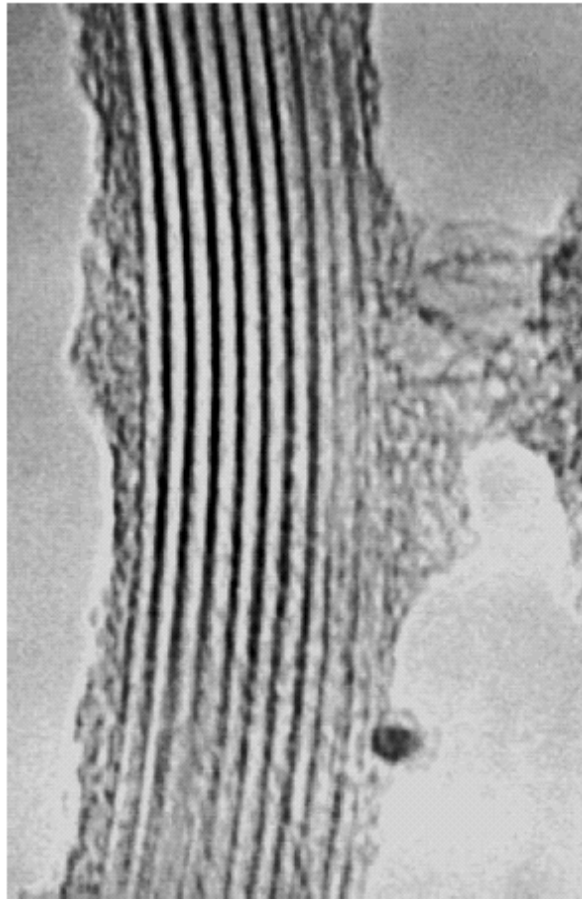
Carbon is well known as one of the better adsorbents for gases. This property is due

to (i) the ability of this material to exist in a very fine powdered form with highly porous structure and (ii) the existence of particular interactions between carbon atoms and gas molecules. During recent decades, many improvements have been accomplished to obtain microporous and ultra microporous carbonaceous materials having very high adsorbing properties for the most current gases. Indeed, hydrogen adsorption has already been investigated in activated carbon developing highly specific areas that would permit the gas adsorption in micropores whereas, the mesopores and the macropores do not influence the adsorption amount as they are only concerned with the gas compression [71-73].

One can imagine that the carbon nanotubes, the new microporous carbon macromolecules discovered by Iijima [74] 10 years ago, have been examined with a particular attention at the level of their potentiality to adsorb hydrogen in their regular nanometric microstructure. A number of publications are devoted to the experimental and theoretical study of gas adsorption on different adsorbent structures. In 1997, Dillon et al. [75] measured the hydrogen adsorption in carbon nanotubes by Temperature Programmed Desorption (TPD) method, in order to evaluate the hydrogen adsorption amount delivered during the gas desorption. They concluded that their results would lead to promising developments for hydrogen storage. Maddox and Gubbins [76, 77] evaluated the adsorption of gases in materials with cylindrical pores like tubes by Monte-Carlo simulations in a Grand Canonical Ensemble. Darkrim and Levesque [78, 79] were the first to compute hydrogen adsorption in opened carbon nanotubes in a wide range of pressure and temperature. They evaluated the optimizing adsorbent structures that would enable high adsorptive property by modifying both the tube diameters and the inter-tube spacing for different thermodynamic conditions. These relatively promising results lead to the development of many works on adsorption of hydrogen in carbon nanotubes at once by molecular simulations and by experiments. It must be recognized that theoretical approaches have given more coherent results than experiments whose data are relatively scattered and even contradictory [80, 81]. One of the main explanations is that the basic material is different in the two cases. The nanotubes considered in the molecular simulations are open tubes, well structured, without amorphous carbon and impurities, having well determined and chosen diameters and geometrical location in the bundles. On the contrary, because of difficulties of elaboration and purification, the nanotubes samples used, up to date, in experimental investigations are not of high purity, containing amorphous carbon and several impurities (generally catalytic residues resulting from their synthesis). Moreover, nanotubes themselves were not opened, or were partially opened, and only available in small quantities which are required for adsorption measurement methods carried out on very sensitive devices inevitably less accurate than conventional apparatuses.

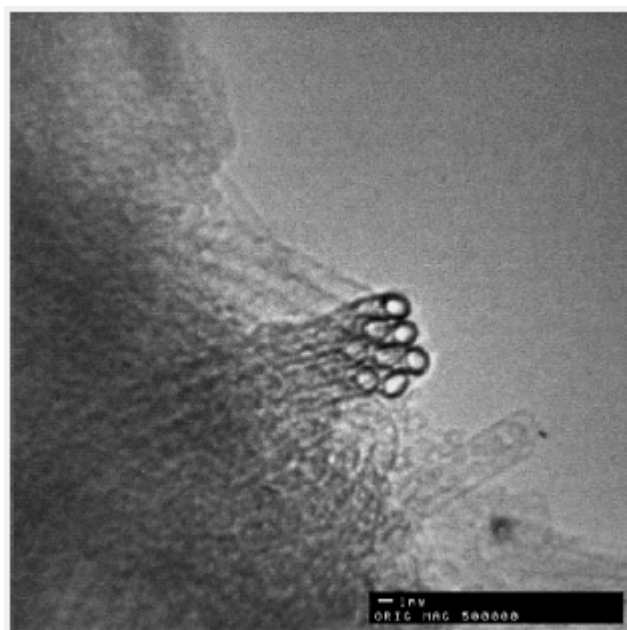
Since their discovery, (Carbon nanotubes) these new carbon tubular macromolecules have been predicted to have many interesting properties capable of numerous applications in mechanical, electronical and many other domains and thereby several synthesis methods have been developed. Nanotubes were thus obtained in two different main species characterized by the structure of their wall: the single-walled nanotubes (SWNT) and the multi-walled nanotubes (MWNT) (Fig. 28).





*Fig. 28: Multi-walled carbon nanotube microstructure. The different walls constituting the material appear in a longitudinal view. (Source <http://cnst.rice.edu/images>)*

SWNT consist of a graphene sheet rolled up into a cylinder of a few nanometers diameter and several microns length (Fig. 29). Most of them are aligned and packed together to form ropes of 10–100 parallel tubes. Their synthesis in significant quantities is yet a challenge to take up especially to obtain a pure material. The most recent way to obtain SWNT is the arc discharge method in the presence of catalyst (Ni–Y mixture) but the nanotubes so obtained coexist with various forms of carbon and metallic particles. To remove these impurities several techniques have been proposed: nitric acid treatment, dispersion by sonication in a surfactant, filtration and high-temperature heating under neutral or lightly oxidizing conditions [82, 83]. A MWNT is an arrangement of coaxial tubes of graphite sheets ranging in number from two up to about fifty. On each tube the carbon atoms are arranged in an helical fashion along the tube axis. The diameters of these MWNT range from a few to a few tens of nanometers and their length is of the order of 1  $\mu\text{m}$ . These nanotubes can be also synthesized from arc discharge technique [74–83] but were often obtained from catalytic pyrolysis of hydrocarbides [85].



*Fig. 29: Transmission electronic microscopy of a row of carbon nanotubes. A transversal view of the material is given. Source <http://cnst.rice.edu/images>*

The adsorption of hydrogen in carbonaceous materials corresponds to the amount of hydrogen adsorption which takes place near the carbon surface solid only due to the physical forces -Van der Waals interactions- that carbon atoms exert on hydrogen molecules. This is the reason why the phenomenon is called physisorption. The amount of gas adsorbed is excessive, it represents the additive amount of gas which can be introduced in a given volume with respect to the amount of gas occupying an equivalent volume at the same temperature and pressure in the absence of adsorption [86–88]. At a given temperature, the amount of gas adsorbed is only a function of the pressure and is released (desorbed) when pressure decreases: the phenomenon is reversible with pressure. So defined, the adsorption measures the additional storage gas capacity compared to the one of compressed gas in the same volume and under identical temperature and pressure conditions. The adsorption is expressed as a unit of quantity of gas with respect to a unit of quantity of adsorbent, the correspondent units are: mole per gram ( $\text{mole g}^{-1}$ ) or gram per gram ( $\text{g g}^{-1}$ ) or, now the most used, weight % (wt%), rarely, it is expressed in atom/atom, i.e. atom of hydrogen per atom of carbon.

There is a lot of research currently going on which is devoted to experimental and computational studies of carbon nanotube adsorption property. These materials, if one considers some articles published in the literature, seem to be good candidates for the hydrogen storage process. However, some questions persist!! In the future, some explanations are still needed for all scientists who are interested in the hydrogen storage by adsorption in carbon nanomaterials. In particular, as concerns the surface properties of these adsorbent materials: the chemical treatment during or after the carbon nanotubes synthesis; the mechanical treatment made on the tubes in

order to open their extremities and enable the gas adsorption inside the tubes; the amount of reactive nanotubes (attributed to their low purity rate after their synthesis) taken into account in the gas adsorption calculations; the presence or not of heteroatoms at their surface which can contribute to modify the electronic density at the nanotube surface and then the reactivity of the material can be reinforced (for instance it is possible to intercalate alkaline atoms between consecutive tubes); the accuracy of the volumetric and the gravimetric measurement methods should be mentioned; the definition of the hydrogen 'uptake' used by the authors in their works (excess of adsorption or total amount of the gas). Once these respective main influencing factors on the hydrogen adsorption in carbon nanomaterials are well-determined, one will be able to determine, explain and validate the various adsorption amounts published in the literature and to control their own adsorption data which are unfortunately often obtained on their own characterized materials [89-101].

#### 1.4.2 Glass microspheres

Glass microspheres are small, hollow spheres 25-500 microns in diameter constructed of a glass that becomes permeable to hydrogen when heated to 200-400°C. Hydrogen gas enters the microspheres and becomes trapped when they are cooled to room temperature. The hydrogen can then be recovered by reheating the microspheres [102-105]. Beds of glass microspheres can store pressurized hydrogen at 14% mass fraction and 10 kg H<sub>2</sub>/m<sup>3</sup> storage densities when the spheres are pressurized to 24.82 MPa.

Storage through glass microspheres is a promising technology for small-scale storage of gaseous hydrogen for vehicular applications. In an automobile, hydrogen diffusion through the walls of the microsphere can be achieved by heating to a temperature level of 200-300°C in a high-pressure hydrogen environment. The diffusion coefficient gets reduced to a large extent because of the effects of cooling and thus hydrogen becomes effectively encapsulated within the microspheres. Thus each microsphere functionally behaves like a miniature high-pressure storage vessel. Microspheres among several other advantages, offer the potential for low material cost, as far as automotive application is concerned. However, there are some problems which must be addressed before any large-scale implementation is carried out. The microspheres require high levels of pressure compressors and charging vessels. Being essentially a high-pressure gaseous storage system, it also suffers from the intrinsic problem of poor volumetric storage density of gaseous hydrogen. On a comparative scale, it has been found that the class microspheres could at best store only a fraction of the hydrogen in a given volume that can be stored either in liquid hydrogen storage system or in hydrides. It has been observed that some times the class microspheres leak slowly even at room temperature. Therefore it is absolutely essential to evaluate and optimize the class composition to be used in microspheres to rule out any possible leakage for the sake of safety.

It has been found that the most advanced microspheres [106, 107] can exhibit a burst of pressure about 1000 MPa. In such a system, hydrogen is charged into the glass spheres at a relatively high-pressure and high temperature conditions. As far as the installation of such a microsphere to an automotive is concerned, some arrangements

must be made to ensure heating of the sphere to enable the desired rate of hydrogen release. Moreover, for recharging of the glass microsphere, it has to be removed from the vehicle to a high temperature and high-pressure vessel.

### 1.4.3 Underground storage

Depending on the geology of an area, underground storage of hydrogen gas may be possible [9]. Underground storage of natural gas is common and underground storage of helium, which diffuses faster than hydrogen, has been practiced successfully in Texas [8]. For underground storage of hydrogen, a large cavern or area of porous rock with an impermeable caprock above it is needed to contain the gas. A porous layer of rock saturated with water is an example of a good caprock layer. Other options include abandoned natural gas wells, solution mined salt caverns, and manmade caverns. As mentioned with compressed gas containers, one consideration is the cushion gas that occupies the underground storage volume at the end of the discharge cycle [8, 16]. This can be as much as 50% of the working volume, or several hundred thousand kilograms of gas. Some storage schemes pump brine into the area to displace the hydrogen, but this increases the operating and capital costs.




## 2. HYDROGEN STORAGE SYSTEMS (VESSELS) INVOLVING METAL-HYDRIDES - EXAMPLES

Metal-hydrides are used in the form of metal powders, which are contained within metal-walled vessels [26]. Materials of construction must not be subject to hydrogen embrittlement and are typically, Aluminium, copper and stainless-steel. The vessels include special provisions to accommodate metal-hydride powders. First, the alloy absorbs so much hydrogen that it physically expands up to 25% in volume. The vessel must accommodate this expansion to prevent plugging or rupture from the expanded alloy. For high hydrogen flow rates, the vessel must be designed for low pressure drop and to prevent the fine powdered alloy from being fluidized and transported out of the vessel causing contamination of the piping and the valves. The vessel must transfer heat at rates required by the alloy heats of hydride formation ( $\Delta H_f$ ), for example for  $\text{LaNi}_5$   $\Delta H_f=30.8$  kJ/mol  $\text{H}_2$ . For such an alloy, in order to store  $15\text{Nm}^3\text{H}_2$ , the vessel has to be designed to transfer 20.625 MJ of heat away from 105 kg of  $\text{LaNi}_5$  powder (assuming a reversible H-capacity of 1.28 wt%).

Containment vessels can assume many sizes and shapes. For applications that require hydrogen delivered at a low rate over many hours, large diameter cylinders can be used. In order to support the heat transfer required for rapid hydrogen delivery or refill, alloys are contained within small diameter tubing that have a high surface area to volume ratio.

A number of interrelated factors must be considered when designing metal-hydride storage vessels. Hydrogen capacity delivery flow rate and pressure are the obvious primary factors. To supply a 250 Watt PEM fuel cell for one hour, the vessel must often contain up to 500 Whr hydrogen capacity ( $\approx 168$  liters) to accommodate the 50% operating efficiency of the fuel cell. A hydrogen flow rate of 2.8 liters per minute will sustain operation at 250 Watt.

Examples [26] of metal-hydride storage vessels made by Ergenics' Inc., (USA), are shown and listed in Figure 30, 31 and 32. Relevant data that illustrate the range of operating characteristics appear in Table 7

		
Fig. 30: ST-1-AL Vessel	Fig. 31: 25 kWh Storage Unit	Fig. 32: Load Leveling Storage Unit
60 minutes	15 minutes	1 minute
70 liters	7600 liters	1100 liters
0.75 l/min	570 l/min	666 l/min
50mmDx165mmH	290mmx290mmx780mm	300mmDx350mmL
0.86 kg	93 kg	10 kg
Aluminum	Aluminum	Stainless Steel

Because alloy plateau pressure is a function of temperature, the operating temperature range of the application becomes a primary factor for the design of the hydrogen storage system. Normally, an alloy is selected that will deliver the minimum acceptable pressure at the lowest ambient temperature. The system must retain the elevated pressure that will occur at the highest ambient temperature. For example, if a PEM fuel cell needs to operate in temperatures ranging from  $-20^{\circ}\text{C}$  to  $60^{\circ}\text{C}$ , an alloy is selected which will deliver hydrogen at just above atmospheric pressure (1.1 bar), at  $-20^{\circ}\text{C}$ . The hydrogen containment system must be designed to handle the higher pressure that will occur at  $60^{\circ}\text{C}$ , in this case, about 10 bar. For these reasons, pressure regulators are often used. Occasionally, applications will have a waste heat source that can be used to maintain the temperature of the storage system, allowing pressure to remain constant.

Different designs of metal-hydride storage vessels made in Japan Automobile Institute by Uchida et al. [108], are shown in Figures 33 and 34. The PCT for one of

the alloys used for these designs is shown in Figure 35. The performance of each design is shown in Figures 36 and 37.

Japan Steel Works Ltd (JSW) has developed different models of metal-hydride storage vessels for low and high capacity storage. These together with their specifications are shown in Figures 38, 39 and 40, for small, medium and large size tanks, respectively.

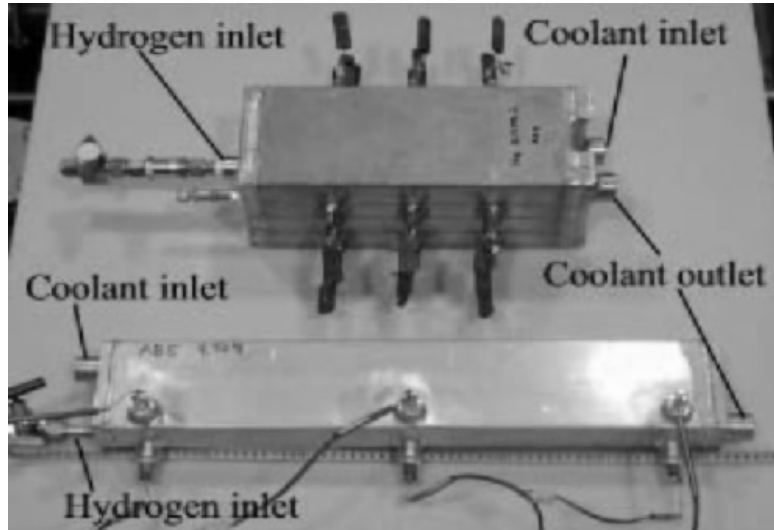


Fig. 33: Two types of small size Metal-hydride tanks (Upper: Plate-fin type, Lower: Divided-chamber type)

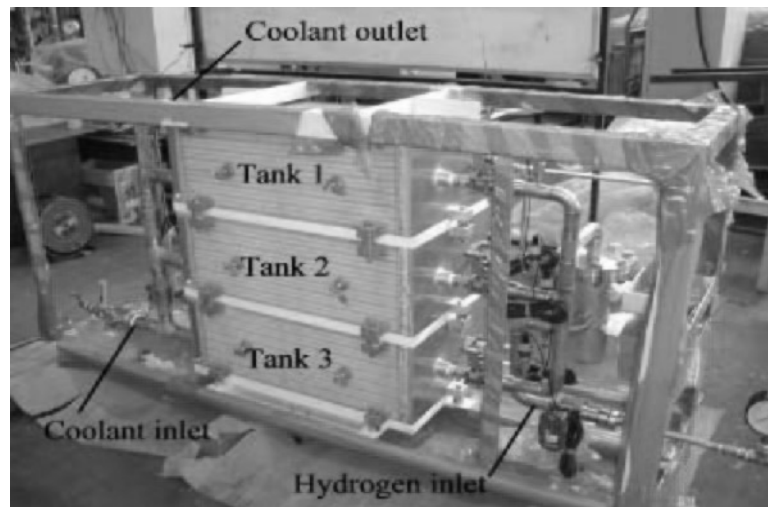


Fig. 34: Metal-hydride tank of Plate-fin type with a capacity of  $31.25\text{Nm}^3\text{H}_2$ , using 264 kg of Metal-hydride

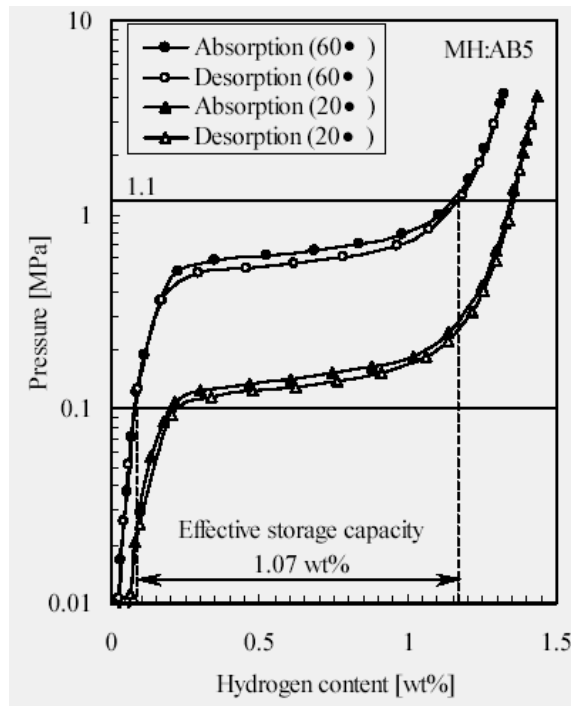


Fig. 35: PCT diagram of AB<sub>5</sub> metal-hydride alloy

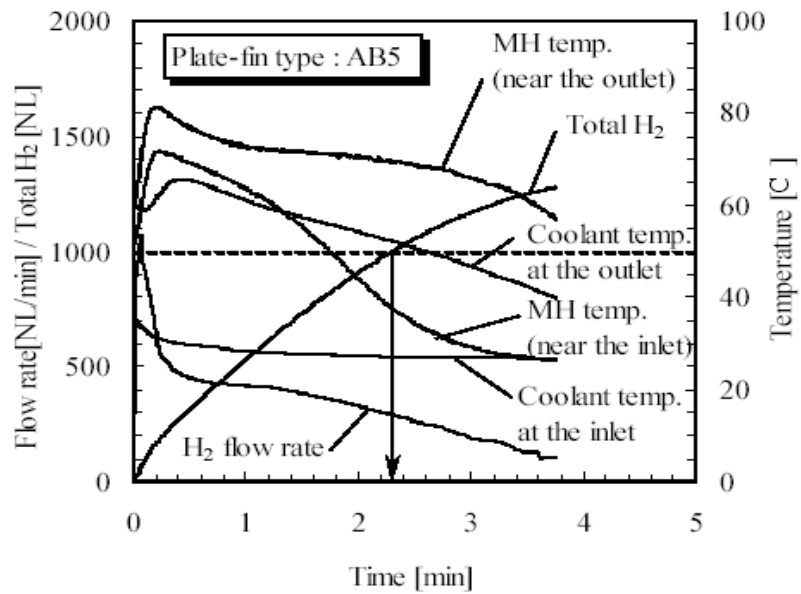


Fig. 36: Charging characteristics of plate-fin type tank

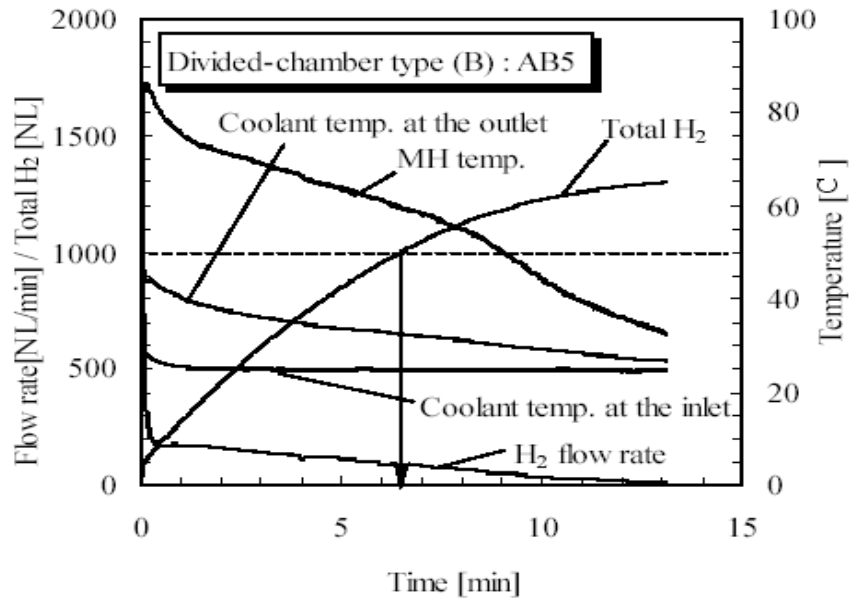
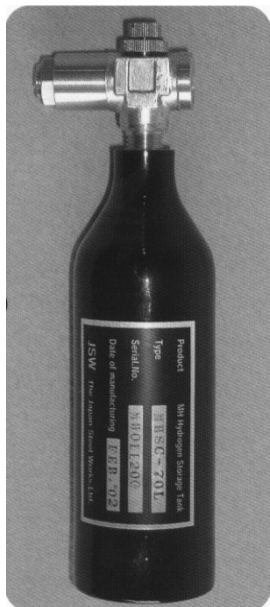


Fig. 37: Charging characteristics of divided-chamber type tank



Small Cylinder Type MH Tank (MHSC-70L)

### Specification of small MH tank

Model	MHSC-50L	MHSC-70L
Hydrogen Capacity	50 L	70 L
Tank Structure	Aluminum Alloy Vessel	
Utility requirement	Inlet Pressure	1.0 MPa
	Hydrogen Charging Rate	About 0.5 hr (in water bath at 20°C)
	Outlet Pressure	0.17 MPa
	Hydrogen Discharging Rate	0.12 L/min.
	Environment Temperature	About 25°C
Dimension	φ 50 x H135 mm	φ 50 x H170 mm
MH Weight	0.33 kg	0.49 kg
Total Weight	0.7 kg	0.9 kg
Overpressure Protection	Relief Valve	

Other hydrogen capacities (up to 200 L) is also available.

Fig. 38: JSW small (50, 70 liters H<sub>2</sub>) Metal-Hydride tank



## Medium Size MH Tanks Water Cooling Type

Model			MHPF-1M	MHPF-3M	MHPF-10M	
Hydrogen Capacity		Nm <sup>3</sup>	1	3	10	
Storage Density	Weight	Nm <sup>3</sup> /kg	0.052	0.059	0.065	
	Volume	Nm <sup>3</sup> /m <sup>3</sup>	156	175	188	
Utility requirement	Inlet Pressure		MPa			
	Cooling Water Temp.		°C			
	Flow Rate	L/min		4~8	12~24	40~80
		MPa		0.1		
	Heating Water Temp.		°C			
	Flow Rate	L/min		4~8	12~24	40~80
Dimension		mm	152W x 297D x 142H	305W x 327D x 173H	495W x 627D x 173H	
weight		kg	19	51	154	
Alloy Weight		kg	8	24	78	

Fig. 39: JSW medium (1, 3, 10 Nm<sup>3</sup>H<sub>2</sub>) Metal-Hydride tanks with water cooling

## Large Scale Storage System

This system is for a hydrogen refueling station and capable of both storing and compressing hydrogen.



### Specifications

Hydrogen Absorbing Conditions	Hydrogen Desorbing Conditions
Inlet Pressure : 0.05MPa	Outlet Pressure : 0.8MPa
Filling Rate : 20Nm <sup>3</sup> /h	Supply Rate : 20Nm <sup>3</sup> /h
Hydrogen Capacity : 75Nm <sup>3</sup>	
Utility Requirement	
Cooling Water : 20°C, 8m <sup>3</sup> /h	
Heating Water : 90°C, 11,900kJ/h	
Dimension : 1,100W x 1,800D x 1,230H[mm]	

Fig. 40: JSW large (75 Nm<sup>3</sup>H<sub>2</sub>) Metal-Hydride tank with water cooling

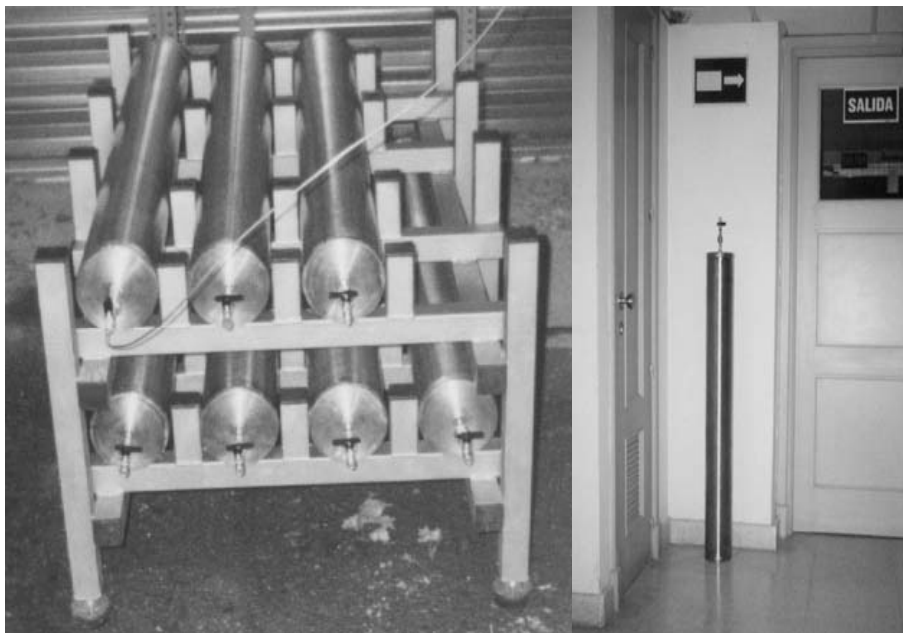
Labtech Int. Ltd [109] stationed in Bulgaria developed its own Metal-Hydride storage systems, a few of which are shown in Figures 41 and 42. Figure 41 shows a small MH tank containing 1.2 Nm<sup>3</sup> H<sub>2</sub>. The H-storage is light (11kg), easy to be charged and it is supposed to be charged in about 30 minutes.

Figure 42 shows a Labtech 80 Nm<sup>3</sup> Hydrogen Storage System installed in the Instituto de Catalisis y Petroleoquimica, CSIC, Madrid, Spain. This Storage releases very pure hydrogen with outgoing pressure from 1.5 bar to 15 bar in the temperature range from 0° to 40°C. Maximum necessary charging pressure is 20 bar at 40°C. The

storage consist of eight single SS units each with capacity of  $10 \text{ Nm}^3$ . This amount is equal to hydrogen stored in one "RED"  $\text{H}_2$  bottle at 220 Bar. The weight of this single unit is 75 kg. Figure 43 shows the PCT diagrams of some of the  $\text{AB}_5$  alloys used by Labtech for Metal-Hydride Storage



*Fig. 41: A Labtech  $1.2 \text{ Nm}^3 \text{ H}_2$  Metal-Hydride storage tank*



*Fig. 42: A Labtech  $80 \text{ Nm}^3$  Hydrogen Storage System installed in the Instituto de Catalisis y Petroleoquimica, CSIC, Madrid, Spain.*

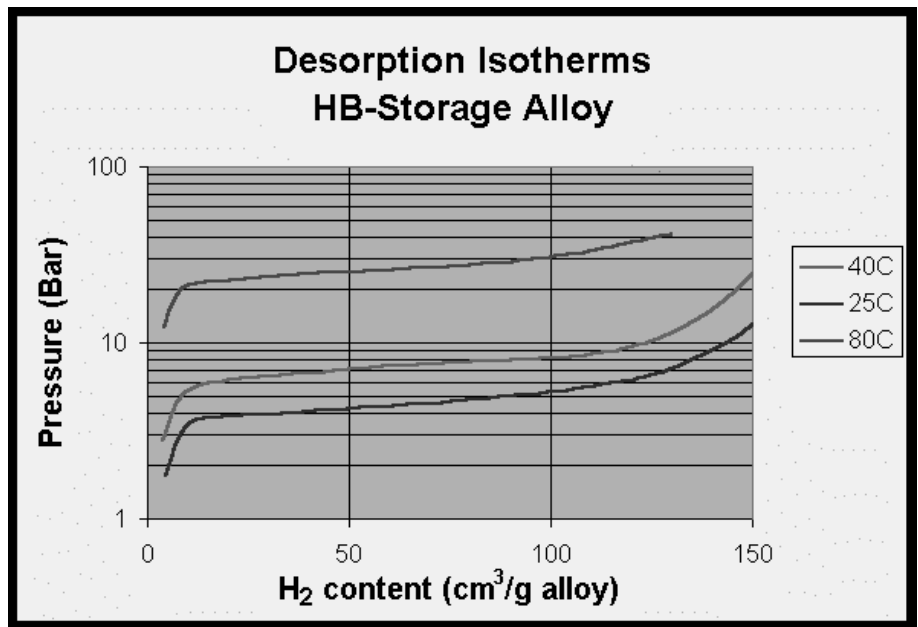
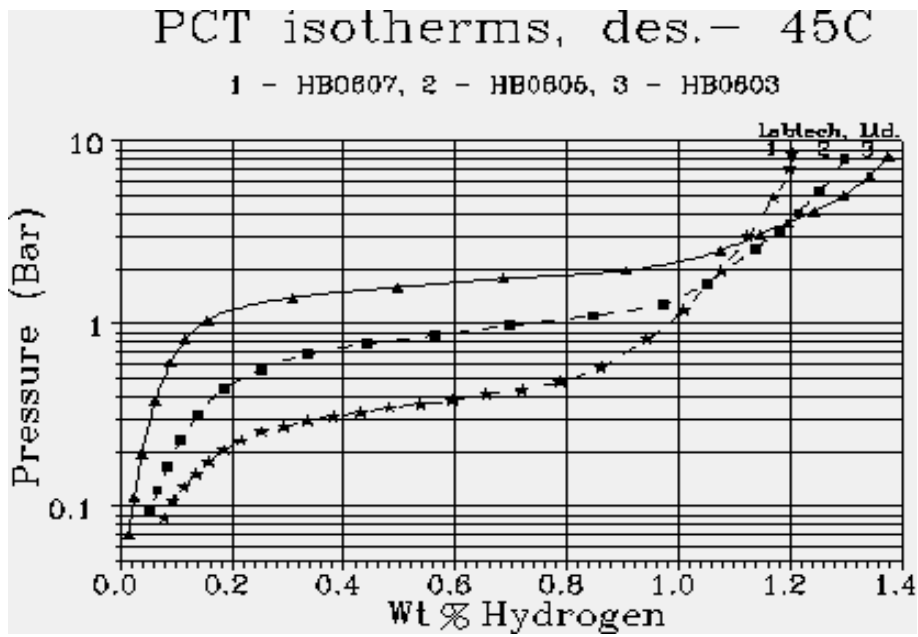


Fig. 43: PCT diagrams of some of the AB<sub>5</sub> alloys used by Labtech for Metal-Hydride Storage

### 3. CASE STUDIES OF INTEGRATED HYDROGEN SYSTEMS – FOCUS ON HYDROGEN STORAGE SYSTEMS

In this section, case studies of integrated hydrogen systems focusing on the hydrogen storage systems used will be briefly described [110]

#### 3.1 Solar-Wasserstoff-Bayern hydrogen demonstration project at Neunburg Vorm Wald, Germany

Major system components were installed on an industrial scale at a demonstration facility located in Neunburg vorm Wald, Germany for a potential future energy supply based on hydrogen generated by utilizing (solar) energy unaccompanied by release of carbon dioxide. Initial technical aspects of the stepwise transition from our present-day energy supply primarily aligned for fossil fuels were considered. Most of the plant subsystems are prototypes of innovative technologies. Among others, the facility includes photovoltaic solar generators, water electrolyzers, catalytic and advanced conventional heating boilers, a catalytically heated absorption-type refrigeration unit, fuel cell plants for stationary and mobile application, an automated liquid hydrogen (LH<sub>2</sub>) filling station for test vehicles, and a gaseous hydrogen (GH<sub>2</sub>) filling station (Figures 44, 45). Focal points of the investigations were performance of the plant subsystems and their interaction under practical operating conditions. Analysis of the work yielded a reliable database for updated assessment of the prospects and challenges of solar hydrogen technology.

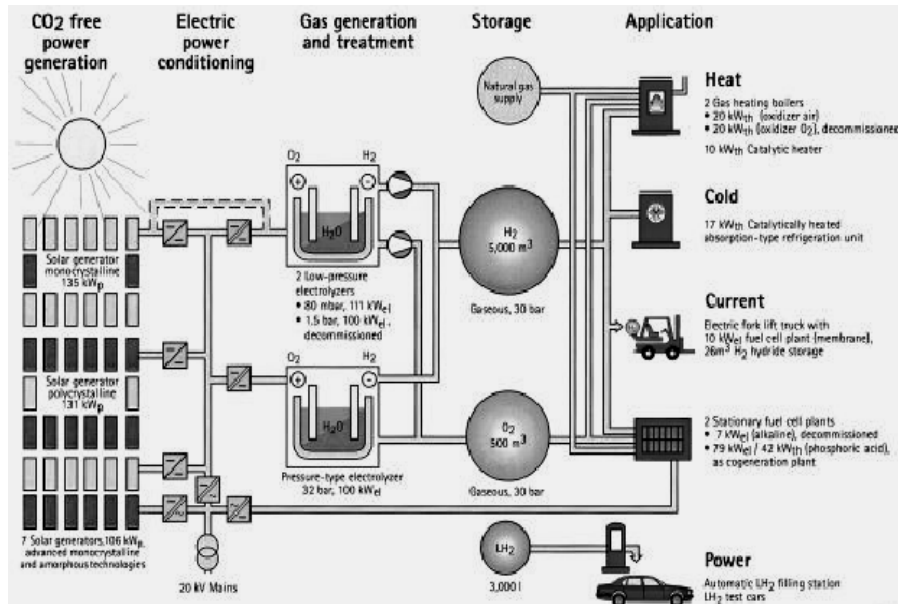
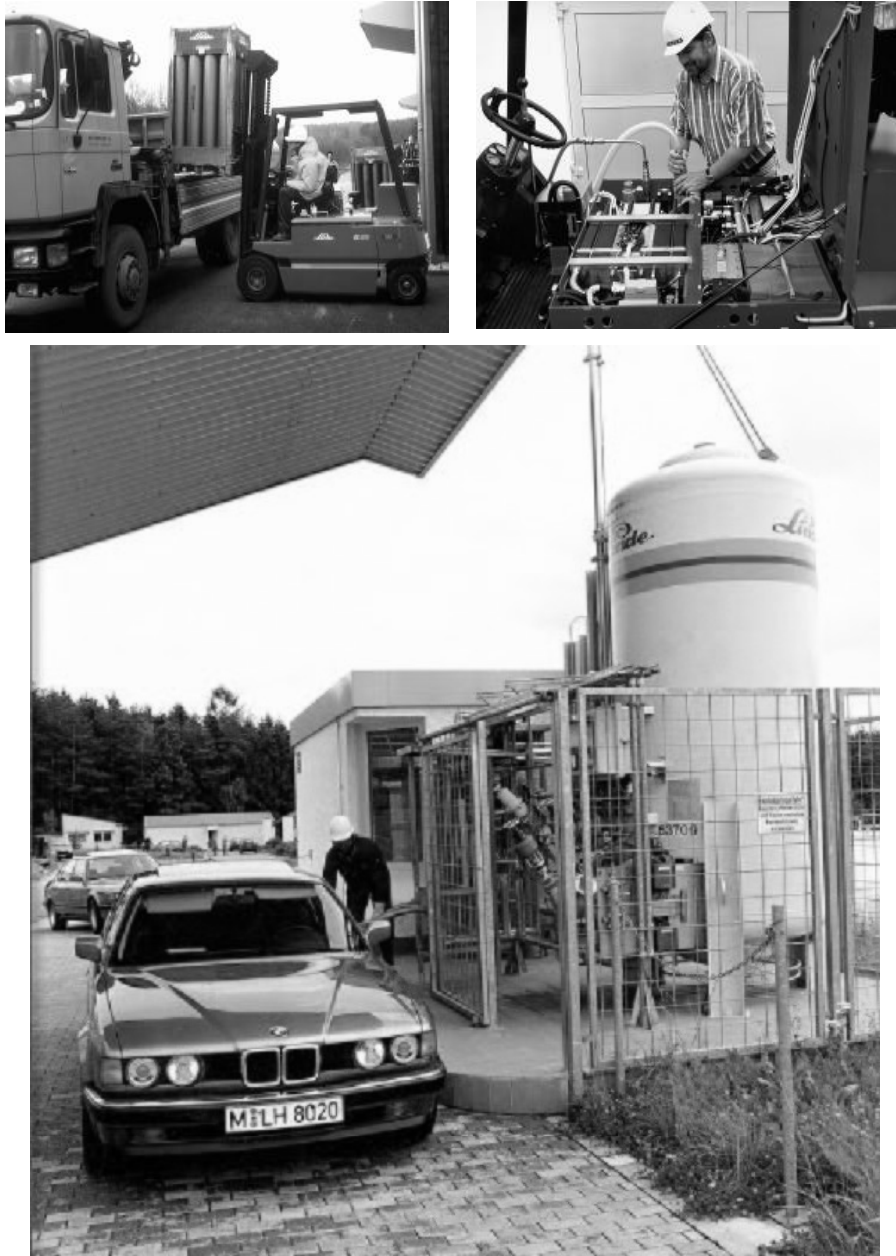


Fig. 44: Simplified system diagram with hydrogen storage as GH<sub>2</sub> and LH<sub>2</sub>

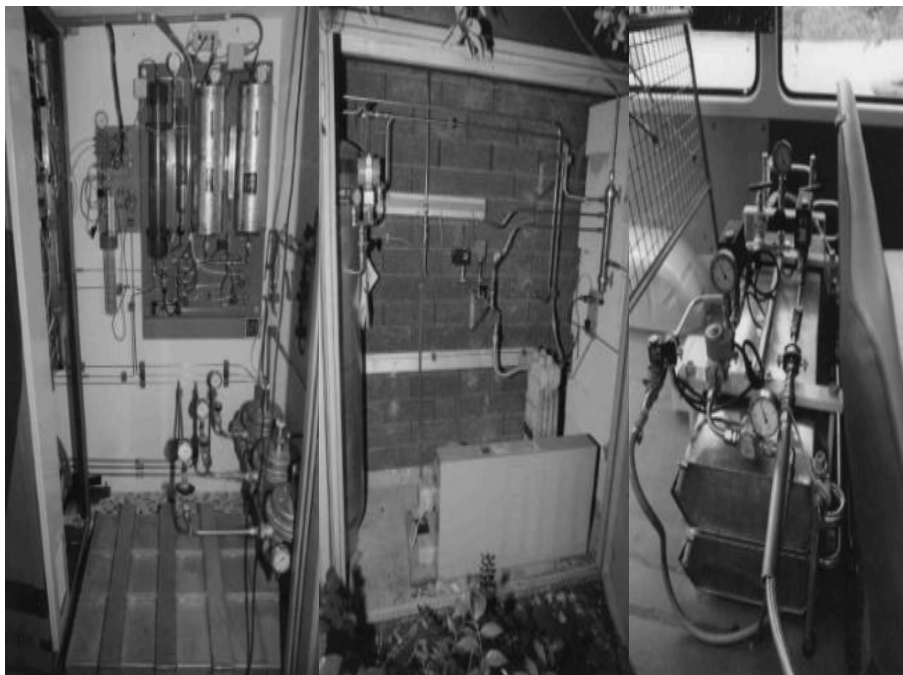


*Fig. 45: Pictures of the electric fork-lift (top) operating with a fuel cell running on hydrogen stored in metal-hydrides and the liquid hydrogen filling station (bottom)*

### **3.2 Solar hydrogen plant on the Markus Friedli residential house**

Solar radiation is transformed by PV panels into electric current which passes a control unit and a DC-DC converter before being transformed by an electrolyzer into

chemical energy (hydrogen) or stored in batteries and/or injected into the grid. A small part of auxiliary energy is supplied by the electric grid for operation of the control unit, electrolyzer regulation, purification unit and hydrogen compressor. However, the electrolyzer can, in principle, also be operated from the public grid via an AC-DC converter. Water is needed as a feed, for cooling the electrolyzer, and for removing electrolyte from the hydrogen gas. Some hydrogen is consumed in the purification step, where any oxygen in the hydrogen stream is catalytically reacted with hydrogen. Hydrogen is transferred into an intermediate storage tank and then compressed for seasonal storage into a metal hydride storage tank (Figure 46). The latter is connected to house appliances such as a stove and a laundry machine (no longer in operation), and a second metal hydride storage tank is located in a minivan (which can alternatively also be fueled with gasoline). The household is exclusively powered by the battery stack via a DC-AC converter and is completely separated from the public grid. The schematic diagram of the system is shown in Figure 47



*Fig. 46: Metal-hydride storage tank (left picture on the bottom), compressor with compressed gas storage vessel (centered picture), and M-H storage tank for the minivan*

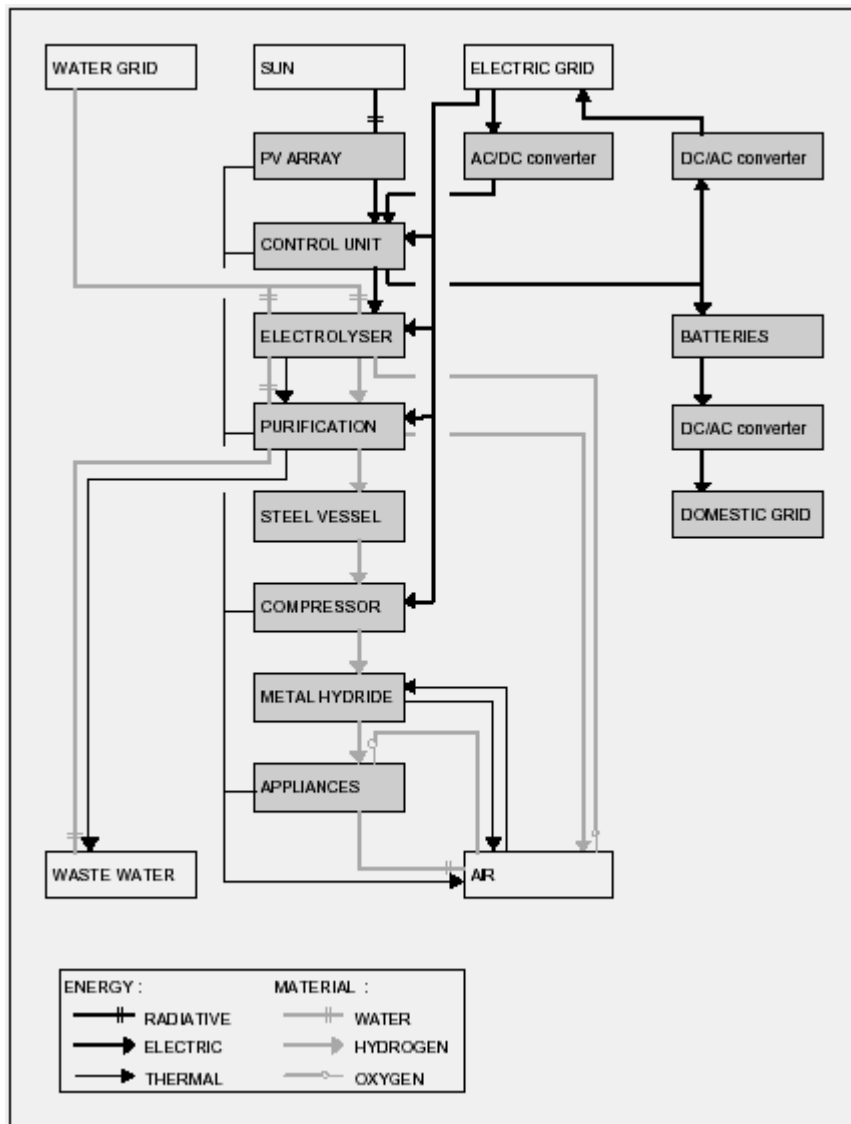
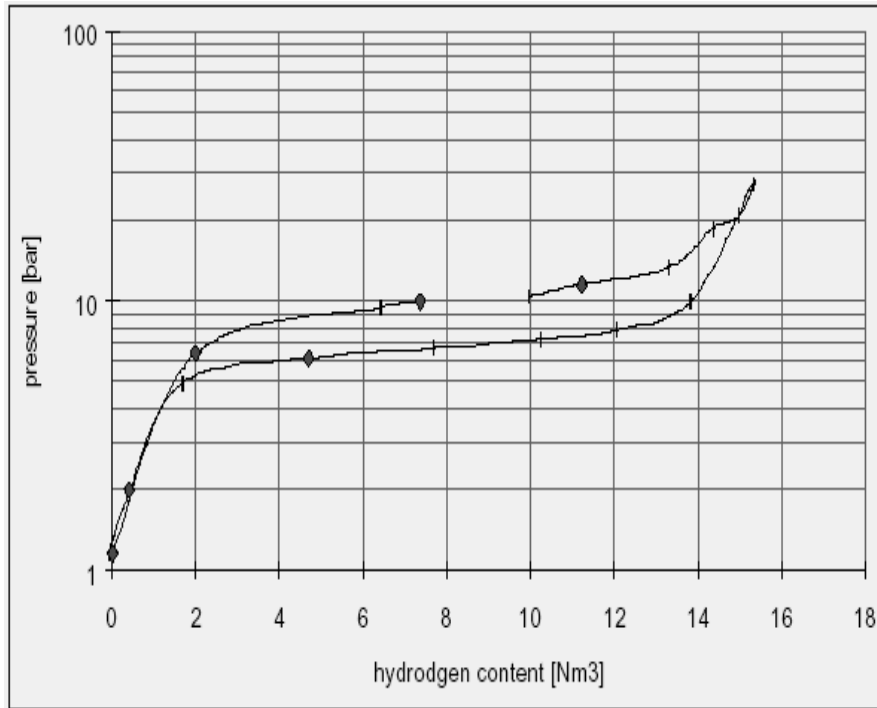


Fig. 47: Schematic diagram of the system and energy / materials flow



Supplier	Japan Metals & Chemicals
Pressure range	1.2 - 29 bar
Capacity	19 Nm <sup>3</sup> (nominal at 20°C, 30 bar)
Volume	15.2 Nm <sup>3</sup> (measured at 5.3°C, between 1.2 and 27 bar)
	91 l (total), 15 l (metal hydride)
Weight	235 kg
Alloy composition	Ti <sub>0.98</sub> Zr <sub>0.02</sub> V <sub>0.43</sub> Fe <sub>0.09</sub> Cr <sub>0.05</sub> Mn <sub>1.5</sub>
Storage efficiency	1.8 wt% (alloy, total), 1.3 wt% (alloy, reversible)
	0.54 wt% (tank, reversible)
Heat of absorption/desorption	14.4 MJ for 14 Nm <sup>3</sup>

Fig. 48: PCT (at 5.3°C) (top graph) and specifications (bottom) of the metal-hydride tank used for hydrogen storage

### 3.3 Alexander t. Stuart renewable energy test site

The A.T. Stuart Renewable Energy Test Site (RETS) located at Stuart Energy Systems (SES) Inc. in Toronto has been operating since May 1991. Located on the roof of the SES factory, the system was built to demonstrate a simple low cost



renewable hydrogen system (Figure 49). In its current configuration, a 2.45 kW (peak) PV flat panel array provides 12 VDC (nominal) to an electrolyzer consisting of a cell bank of six “meteorological” type electrolysis cells. The oxygen produced by the electrolysis process is vented and the hydrogen gas fills a gas holder, which supplies a small single stage air-cooled compressor. The hydrogen is compressed to 7 bar and stored in a small tank. A separate PV array charges batteries, which provide power to the control system and the compressor motor.



*Fig. 49: The Alexander T. Stuart renewable energy test site*

### **3.4 Phoebus Jülich demonstration plant**

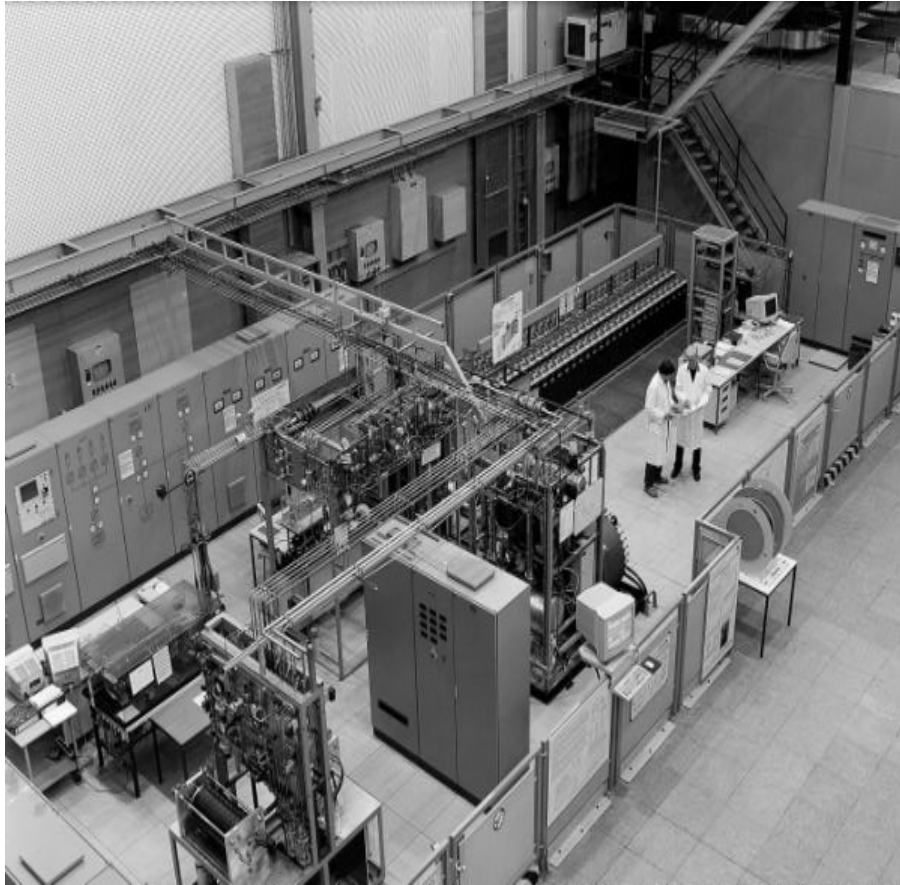
The PHOEBUS demonstration plant (Figure 50) has been designed to provide an autonomous solar electricity supply to the central library building of the Research Centre Jülich with an installed capacity of 38 kWel. The major components of the plant in its first phase of operation are:

1. A photovoltaic field with four facade and rooftop integrated generators consisting of monocrystalline modules with an active area of 312 m<sup>2</sup>, peak power output of 43 kWp, and an electrical energy output of 29 MWh/yr;
2. A pair of DC/DC-converters (5 kW each) for each photovoltaic field, adjusting the voltage to the level given by the DC-grid which has the actual

- voltage level of the battery system;
3. A system of 110 lead batteries of the OPzS OCSM type with electrolyte recirculation, designed for a DC-grid voltage of 220 V (200-260 V), and a capacity of 304 kWh, 1380 Ah over 10 hours;
  4. A bipolar 21 cell electrolyzer with an active cell area of 2500 cm<sup>2</sup>, a current of 750 A, a current density of 3 kA/m<sup>2</sup>, with 30% KOH solution, 80°C operating temperature, an operating pressure of 0.7 MPa and 90% efficiency in design load operation at a design power rating of 26 kW; maximum hydrogen production is 6.5 Nm<sup>3</sup>/h and maximum oxygen production is 3.25 Nm<sup>3</sup>/h;
  5. A storage system for the product gases, hydrogen (6.5 Nm<sup>3</sup>/h) and oxygen (3.25 Nm<sup>3</sup>/h), leaving the electrolyzer at 0.7 MPa. The hydrogen is compressed to 12 MPa and stored in 18 pressure bottles of 1.4 m<sup>3</sup> each with a total geometrical volume of 25m<sup>3</sup> for H<sub>2</sub> (3,000 Nm<sup>3</sup> H<sub>2</sub>). The oxygen is compressed to 7 MPa and stored in one high pressure storage unit of 20 m<sup>3</sup>, sufficient for the whole seasonal storage requirements;
  6. An alkaline fuel cell system consisting of KOH gas diffusion electrode fuel cell of the Siemens BZA 4-2 type with a design power output of 6.5 kW at 48 V and 135 A, with a system efficiency at design load of 63% (LHV of H<sub>2</sub>) and 70% at 30% partial load.

### 3.5 Schatz solar hydrogen project

The Schatz Solar Hydrogen Project began in the fall of 1989. It is a stand-alone photovoltaic energy system that uses hydrogen as the storage medium and a fuel cell as the regeneration technology. Its goal is to demonstrate that hydrogen is a practical storage medium for solar energy and that solar hydrogen is a reliable and abundant energy source for our society. A schematic for the system is shown in Figure 51. It is installed at the Humboldt State University Telonicher Marine Laboratory (124.15°W, 41.06°N) and the Lab's air compressor system, used to aerate aquaria, is the load. When PV power is available, it is used directly to supply the load. Any excess power is supplied to the electrolyzer to produce hydrogen gas. When the array cannot provide electricity, the stored hydrogen serves as fuel for the fuel cell, providing uninterrupted power. If the storage is depleted, the system returns to utility power supplied by the grid.



*Fig. 50: An overview of the experimental hall with fuel cell, alkaline electrolyzer, gas treatment unit, high pressure electrolyzer, battery system (from left to right) and all other subsystems (except the gas storage vessels)*

The objectives of the Schatz Project are:

1. to assess the storage efficiency of hydrogen when used as a medium to store solar electricity
2. to assess the use of a proton exchange membrane fuel cell as a means of regenerating electricity from stored hydrogen and oxygen
3. to design, test, and utilize a computer based control system which will allow for efficient component integration and provide for reliable, unattended operation
4. to monitor operating and environmental parameters to chronicle system performance and to allow development of a simulation model



*Fig. 51: The Schatz solar hydrogen project*

### 3.6 INTA solar hydrogen facility

The INTA program on hydrogen technologies had two main objectives, as defined in 1989:

- The use of hydrogen as a storage medium for solar electricity
- The use of integrated systems: PV, electrolysis, hydrogen storage, and fuel cells for manned space missions.

The space related activities were abandoned on 1993. Since 1994, hydrogen activities were concentrated on the utilization of hydrogen in fuel cells in a non-centralized electricity generation services sector as well as a clean fuel for transportation. The Solar Hydrogen Pilot Plant consisted of three phases. Figure 52 shows the general configuration of the facility. The pilot plant for solar hydrogen production (Phase I) was designed, constructed and evaluated during 1991-93. The storage system (Phase II) was defined and evaluated during 1993-95. Both systems were used during Phase III (1994-96) in conjunction with phosphoric acid (PAFC) and proton exchange membrane fuel cells (PEMFC).

The main characteristics of the pilot plant are:

- 8.5 kWp photovoltaic field
- 5.2 kW alkaline electrolyzer
- 24 m<sup>3</sup> metal hydride (TiMn<sub>2</sub>) storage
- Conventional pressurized gas installation for bottles of 8.8 m<sup>3</sup> at 200 bar

- PAFC of 10 kW
- Two PEMFC stacks of 2.5 and 5 kW (hydrogen/air).

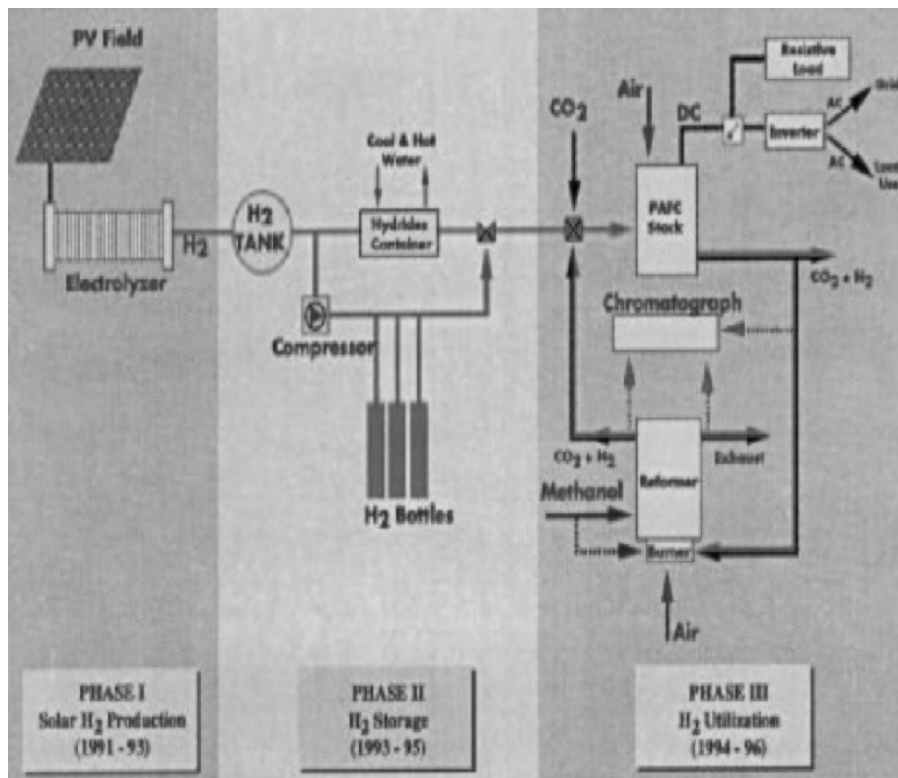


Fig. 52: INTA Solar Hydrogen Facility: General Configuration

The metal hydride storage system (Figure 53) consists of an intermediate buffer, a hydrogen purification unit, a metal hydride container and a cooling water supply system. Suitable instrumentation and sensors were prepared in order to control the system and acquire data for later evaluation. The intermediate buffer is connected to the electrolyzer hydrogen delivery valve. Once set point pressure is reached, hydrogen passes through the purification unit and fills up the hydride container. The hydride storage container consists of a pressurized tank filled with metal hydride powder, a cooling/heating shell, water supply and hydrogen supply provided with safety and shut-off valves. This hydride container was manufactured by GfE mbH, from Nürnberg, Germany. A solar thermal collector facility supplies hot water at 80°C. Cooling water at 15°C is available on site.

The pressurized gas storage system (Figure 53) uses the same intermediate buffer and the purification unit as the metal hydride storage system. When hydrogen is stored as a compressed gas, hydrogen passes from the intermediate buffer to a two-stage air driven gas booster compressor that increases the hydrogen pressure to 200 bar. Hydrogen is bottled in metallic cylinders with 8.8 Nm<sup>3</sup> of hydrogen capacity at

200 bars. The hydrogen purity is measured by a Teledyne analyzer. Additional sensors and manometers give information about the process. Nitrogen gas is available on site to proceed with shut-down and start-up under safe conditions.



*Fig. 53: Storage System: intermediate buffer (left), horizontal hydride container tank (middle), and 200-bar bottle and compressor (right).*

### **3.7 Clean air now: solar hydrogen fuelled trucks**

Started in August 1994, the CAN Solar Hydrogen Vehicle Project demonstrated a practical application of renewable hydrogen. The demonstration featured a solar energy hydrogen generating system, fuelling station, and a small fleet of Ford trucks with internal combustion engines (ICEs) converted to use hydrogen. CAN oversaw, directed and managed the overall project. Other team members included the Xerox Corporation; The Electrolyzer Corporation (currently Stuart Energy Systems Inc.); Praxair Incorporated; Solar Engineering Applications Corporation (currently Photovoltaics International, LLC); Kaiser Engineering; City of West Hollywood; W. Hoagland & Associates, Incorporated; Touchstone Technology; the University of California, Riverside, College of Engineering – Center for Environmental Research & Technology (CE-CERT); Matrix Construction and Engineering, Incorporated; and the Energy Technology Engineering Center (ETEC). The Xerox-CAN Solar Hydrogen Production Facility Scheme is shown in Figure 54. The hydrogen-powered utility vehicle fleet was operated by the Xerox Corporation in El Segundo

and by the City of West Hollywood. The project was funded by the White House Technology Reinvestment Project (contracted through the U.S. Department of Energy), CAN, SCAQMD, and the rest of the project team.

The goal of the CAN-Xerox project was to demonstrate the use of solar-generated hydrogen as an alternate clean fuel for utility transportation vehicles. This project utilized state of the art, “off-the-shelf” technology including photovoltaic (PV) electricity generation and water electrolysis production of hydrogen. The hydrogen-fuelled CAN Ford Ranger trucks represented a significant advancement in the development of ultra-low emission vehicles (ULEVs). By using hydrogen fuel, these trucks eliminated air pollutant emissions of CO, CO<sub>2</sub>, and unburned hydrocarbons, while significantly reducing emissions of nitrogen oxides (up to 90%). Hydrogen produced from electrolysis of water powered by PV electricity, is a clean, practically inexhaustible power source for automobiles.

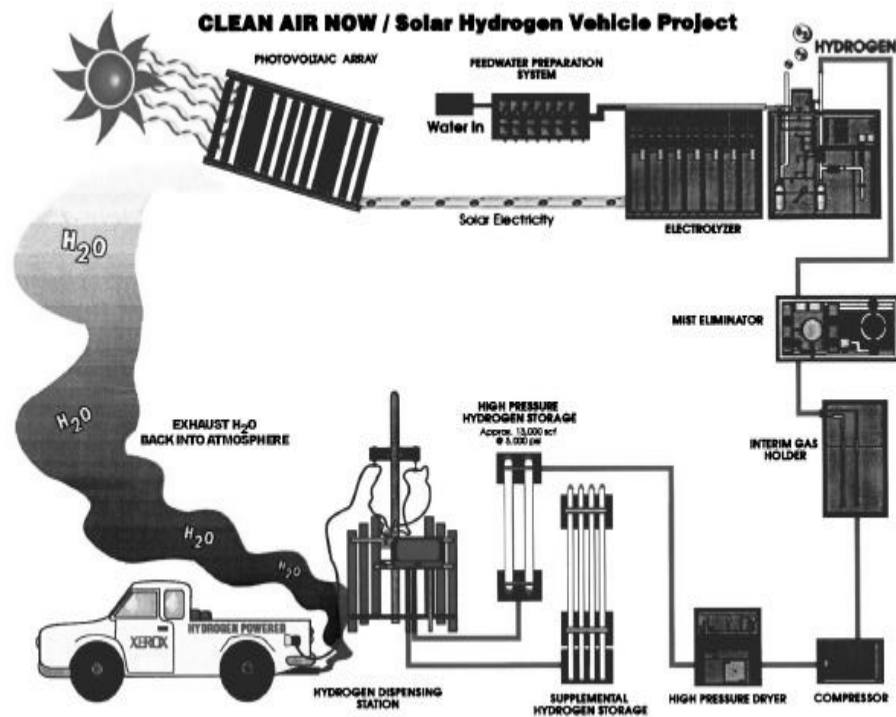


Fig. 54: The Xerox-CAN Solar Hydrogen Production Facility Scheme

The hydrogen storage system consisted of twenty-four 2200 psig, 22.5 cubic foot ASME storage vessels (holding ~74,000 scf of hydrogen at 2200 psig) and two 5000 psig, 26.6 cubic feet ASME storage vessels (holding ~14,000 scf of hydrogen at 5,000 psig). The two 5,000 psig vessels were the only vessels filled from the electrolysis system. The 2,200 psig vessels were filled by an external hydrogen supply source, and were only used when hydrogen was not available from the two high-pressure storage vessels. The two high-pressure vessels were protected with two safety relief valves, one valve on each vessel, with each relief valve set to

relieve at 4,600 psig.

The hydrogen dispensing system consisted of an Automotive Natural Gas Inc. (ANGI) fuelling post, piping, and valving. The ANGI fuelling post used a dual-hose rated for operation at 5,000 psig. The system was termed a “fuelling post” simply because there were no automatic dispensing or metering functions provided (Pictures 7.2 and 7.3). The piping and valving downstream of the high-pressure storage vessels were all designed to operate to at least 4,600 psig. The dual-hose unit features hose retractors, and the breakaway force was 25 pounds pull on a hose (approximately). These components were protected from overpressure conditions by means of two pressure relief devices installed on the two high-pressure storage vessels. To preclude the overpressurization of the utility vehicle hydrogen storage tanks, a relief valve set to relieve at 3,900 psig was installed on the nozzle side of the dispensing system, with a gas regulator set at 3,500 psig.



*Fig. 55: Refueling the Ballard Fuel Cell Bus at the CAN Solar Hydrogen Refueling Station (left), UCRI at Solar Hydrogen Refueling Facility (right)*

### **3.8 Palm desert renewable hydrogen transportation project**

This project was begun in January 1996 and is scheduled for completion in March 1999. Participants in the project include the U.S. Department of Energy (DOE), the Schatz Energy Research Center (SERC), the South Coast Air Quality Management District (SCAQMD), the City of Palm Desert, SunLine Transit Agency, W.L. Gore & Associates, ASE Americas, DuPont, and Teledyne Brown Engineering. The first phase of this project entailed the design and construction of the three PUVs. Each PUV consists of a standard E-Z-Go electric golf cart that was converted from pure



battery operation to operation with a proton exchange membrane (PEM) fuel cell with a very small battery to supply peak loads. This vehicle has a top speed of 13 mph and a range of 15 miles.



	PUVs	NEV
Membrane Material	DuPont Nafion™ 115	Gore PRIMEA™
Number of Cells	64	96
Fuel Cell Power @ 600 mV/cell	4.0 kW	9.0 kW
Active Area	300 cm <sup>2</sup>	300 cm <sup>2</sup>
Fuel Cell Operating Temperature	50 - 60°C (120 - 140 F)	50 - 65°C (120 - 150 F)
Body and Chassis	E-Z-Go Golf Cart	Kewet El-Jet 3
Traction Bus Voltage (nominal)	36 V	48 V
Electric Motor Size	1.5 kW (2.0 hp)	7.5 kW (10 hp)
Top Speed	13 mph (21 km/h)	35 mph (56 km/h)
Range	15 mi (24 km)	30 mi (48 km)
Hydrogen Tank Volume	14 liters	31.1 liters
Gas Storage Pressure	2,000 psig (138 bar)	3,000 psig (207 bar)

*Fig. 56: The two vehicles (PUV in left and NEV at right) together with their specifications*

The second phase involved the design and construction of an NEV. This vehicle consists of a Kewet (Danish) electric vehicle that was converted in a manner similar to the PUVs. It has a top speed of 35 mph and a range of 30 miles. All four of these vehicles are currently seeing daily use in Palm Desert. The final phase of the project consists of the design and construction of a solar hydrogen generation station and a

hydrogen refueling station. The design portion of this phase is complete while the actual construction awaits final funding from the DOE. In conjunction with the delivery of the first vehicle, it was necessary to construct a temporary refueling station so that they could be readily refueled prior to the construction of the solar hydrogen generation station and refueling station. This was done by designing a multi-tank cascade system that utilizes commercially available hydrogen cylinders. This system allows the vehicles to be refueled to approximately 2,000 psig in a matter of minutes. The permanent refueling station will enable us to fill the NEV tanks to 3,000 psig, its design pressure, while the PUVs will continue to be filled to 2,000 psig. The two vehicles together with their specifications are shown in Figure 56.

### **3.9 Other demonstration projects**

#### **3.9.1 HYSOLAR: 350 kW demonstration plant (KACST/DLR)**

The objectives of this task were the design, installation and safe experimental operation of a directly coupled 350 kW concentrated photovoltaic, advanced electrolysis system with compressed hydrogen storage. The plant was installed in the Kingdom of Saudi Arabia at the Solar Village of the King Abdulaziz City for Science and Technology (KACST) research site, about 50 km north of Riyadh. The plant was designed and installed between January 1991 and August 1993 by a joint German-Saudi Arabian team with the help of external subcontractors. After a safety inspection and release of an operation permit by the German TUEV Südwest, the plant started up on August 19, 1993.

#### **3.9.2 Self-sufficient solar house (Fraunhofer ISE, Freiburg)**

With the self-sufficient solar house, the Fraunhofer Institute for Solar Energy Systems has been demonstrating the ramifications of supplying the entire energy demand for a single-family home from solar energy incident on the roof and walls, even under Central European climatic conditions (Freiburg). The house, which had no electricity connection, no gas connection and no oil tank during the 5 year project period, is experimental in character (see Figure 57).

It incorporates a whole range of novel building and energy technologies, which have been tested and improved in detail under real living conditions. The house has been occupied by a family since October, 1992. In the first major planning step towards energy self-sufficiency, the energy demand of the house had to be minimized by combining proven energy-saving technology with highly efficient thermal collectors and PV modules. The need for space heating could be reduced to almost zero and, consequently, seasonal storage was not necessary. The demand for electricity was significantly reduced by using energy-efficient household appliances, for a total energy consumption of less than 10 kWh/m<sup>2</sup>.

In order to meet the remaining energy demand (during periods without sunshine and for cooking), the decision was made for a hydrogen/oxygen energy storage system. This system is essential to the autonomy of the energy supply, and it also provides the possibility for seasonal storage of solar generated electricity. In summer, PV-

generated electricity is used for the electrolysis of water to hydrogen and oxygen, which are stored in tanks (1500 kWh). Flameless combustion of the hydrogen is the source of heat for cooking, and it is also used to heat the inlet air in the ventilation system on particularly cold days. If additional electricity is required, it is produced from the reaction of hydrogen with oxygen in a fuel cell. As it is only operated during periods with little sunshine, the waste heat from the fuel cell at a temperature of about 70°C has been used to provide backup heat for the hot water heater via a heat exchanger.



*Fig. 57: Self-Sufficient Solar House in Freiburg, Germany utilizing hydrogen technology*

### **3.9.3 Solar hydrogen pilot plant (Helsinki University of Technology)**

Since 1989 solar hydrogen systems have been studied at Helsinki University of Technology. The work so far has comprised the construction of a small self-sufficient pilot plant for 1-2 kWh/day load, and the development of a numerical simulation program H2PHOTO for system sizing and optimization. In the study under way, special emphasis is placed on the seasonal storage subsystem (electrolyzer, hydrogen storage, and fuel cell), to improve its round-trip efficiency and reliability. This subsystem had been found to be critical for overall performance. The pilot plant includes the following components:

- 1.3 kWp a-Si PV-array

- 14 kWh lead acid battery as short-term buffer storage
- 800 W pressurized (max. 30 bar) alkaline electrolyzer
- 500 W phosphoric acid fuel cell
- 200 Nm<sup>3</sup> steel vessel storage
- 0-500 W resistive load.

It was designed and constructed during 1990-1993. The purpose of the pilot plant is to demonstrate the technical feasibility of components and the integrated system. During recent years, the hydrogen production and conversion components have been comprehensively studied and the operation experiences were collected from the whole system from several test runs. Based on thousands of operation hours, the system has generally operated smoothly, but further improvements in component reliability and durability are needed. The numerical simulation program H2PHOTO was primarily developed for system sizing and optimization to estimate the overall performance over extended periods of time. It has been verified against measurements performed in the pilot plant and used to improve the overall efficiency of the pilot plant by comparing alternative control strategies. In the next phase of the project, additional electrolyzers, hydrogen storage options and fuel cells were studied in a laboratory scale test bench, giving more emphasis to solid polymer technologies.

#### 4. CONCLUSIONS

Hydrogen is considered to be a secondary form of clean energy, which has the advantage that it can be stored. Electricity from Photovoltaics and Wind Generators can be used to electrolyse the water and produce oxygen and hydrogen, which can be stored. Efficient storage of hydrogen is an important parameter in order to promote hydrogen in the energy sector.

Hydrogen can be stored as pressurized gas in steel or special composite vessels, as liquid in special insulated vessels, as chemical hydrides, as adsorbed in carbon nanotubes and as absorbed in metal-hydrides. Each storage method has advantages and disadvantages related to the hydrogen gravimetric density, the hydrogen volumetric density and the cost per liter of hydrogen stored. For mobile applications the high hydrogen gravimetric density is quite important while for stationary applications high hydrogen volumetric density is more important.

For practical applications, pressurized gas storage and metal-hydride storage seems to be the most suitable. In the case of pressurized gas storage, there is a need of developing new high pressure vessels to withstand pressures up to 700 bar. In the case of metal-hydrides, there is a need of increasing their gravimetric density to more than 2 wt%. Presently, there are only a few companies offering hydrogen storage systems based on metal-hydrides with storage capacity between 1 liter and 75Nm<sup>3</sup>H<sub>2</sub>.

A major limitation of metal-hydride based systems is that, in high hydrogen capacity systems there is a great demand on cooling/heating the metal-hydride due to the exothermic/endothermic reaction during hydrogen absorption/desorption. Therefore,

new designs of high heat transfer systems with high hydrogen volumetric densities are needed.

Continuing research on materials and systems is needed in order to provide reliable, high capacity hydrogen storage systems for large scale applications. Such systems will contribute largely to the fast diffusion of hydrogen into the European energy sector, contributing to the less-dependence on fossil fuels and to a cleaner environment.

#### ACKNOWLEDGEMENTS

The present work has been funded by the European Union within the 5<sup>th</sup> Framework Programme under the contract number ENK-CT-2001-00536 (RES2H2) for the project entitled “Cluster Pilot Project for the Integration of Renewable Energy Sources into European Energy Sectors Using Hydrogen (H<sub>2</sub>)”.

#### REFERENCES

- [1] Wade A Amos, Cost of Storing and Transporting Hydrogen, November 1998, NREL/TP-570-25106
- [2] Multi-Fuel Reformers for Fuel Cells Used in Transportation, Assessment of Hydrogen Storage Technologies, DOE/CE/50343-3, May 1995
- [3] Bryan D. James, et. al, Making the case for direct Hydrogen storage in Fuel cell vehicles. The National Hydrogen Association’s 8<sup>th</sup> Annual U.S. Hydrogen meeting Proceedings, March 11-13-1197 Alexandria Virginia USA
- [4] Fred, Mitlitsky et. al., Vehicular Hydrogen storage Using Light Weight Tanks (Regenerative Fuel Cell Systems), Proceedings of the 1999 U.S. DOE Hydrogen Program review, NREL/CP-570-26938, May 4-6, 1999 Lakewood, Colorado USA.
- [5] Andrew Haland, High-Pressure Conformable Hydrogen Storage for Fuel Cell Vehicles, Proceedings of the 2000, U.S. DOE Hydrogen Program review, NREL/CP-570-28890, May 9-11, 2000, San Ramon California USA
- [6] Schwarz., J.A.; Amonkwah, K.A.G. (1993). *Hydrogen Storage Systems*. Washington, DC: U.S. Geological Survey.
- [7] Garret, D.E. (1989). *Chemical Engineering Economics*. New York: Von Nostrand Reinhold.
- [8] Hart, D. (1997). *Hydrogen Power: The Commercial Future of the Ultimate Fuel*. London, UK: Financial Times Energy Publishing.
- [9] Zittel, W.; Wurster, R. (1996). *Hydrogen in the Energy Sector*.
- [10] B.D. James, et. al., Comparison of Onboard Hydrogen Storage for Fuel Cell Vehicles., Task 4.2 Final Report under subcontract 47-2-R31148, prepared for Ford Motor Co. under DOE Prime Contract DE-AC02-94CE50389, Directed Technologies, Inc., 1996
- [11] D. Tiller et. al., Development of an all-composite tank for high pressure hydrogen storage. 14<sup>th</sup> World Hydrogen Energy Conference, June 9-13 2002 Canada
- [12] NASA Glenn Safety Manual, Chapter 6, Hydrogen Propellant, Revision Data, 10/96.
- [13] Walter, R.J. and W.T. Chandler, *Effect of High Pressure Hydrogen on Metals*, ASM Technical Report NI. D8-14.2, Presented at the 1968 Materials Engineering Exposition & Congress, 14-17 October 1968, Detroit, Michigan.
- [14] Timmerhaus, C.; Flynn, T.M. (1989) *Cryogenic Engineering*. New York:

- Plenum Press.
- [15] Huston, E.L., (1984), Liquid and Solid Storage of Hydrogen. @ Proceedings of the 5th World Hydrogen Energy Conference. Vol. 3; July 15-20, 1984, Toronto, Canada.
- [16] Taylor, J.B.; Alderson, J.E. A.; Kalyanam, K.M.; Lyle, A.B.; Phillips, L.A. (1986).
- [17] A Technical and Economic Assessment of Methods for the Storage of Large Quantities of Hydrogen. @ *International Journal of Hydrogen Energy*. (11:1); pp. 5-22. nanotubes. *Applied Physics Letters* 74 (16), 2307-2309. Kesten, M. and Meyer, G., Offence and geloste Probleme bei Wasserstofftransport and speicherung. Presentation at BAM, Berlin, 13 December 1995.
- [18] F. Michel, et. al., On Board Equipment For Liquid Hydrogen Vehicles. *Int. Journal of Hydrogen Energy*, Vol. 23, No. 3, pp. 191-199, 1998.
- [19] L. M. Das., On-Board Hydrogen Storage Systems for Automotive Application. *Int. Journal of Hydrogen Energy*, Vol. 21, No. 9, pp. 789-800, 1996.
- [20] S.M. Aceves et. al., Analytical and Experimental Evaluation of Insulated Pressure Vessels for Cryogenic Hydrogen Storage. *Int. Journal of Hydrogen Energy*, Vol. 25, pp. 1075-1085, 2000.
- [21] S.M. Aceves et. al., Insulated Pressure Vessels for Hydrogen Storage on Vehicles. *Int. Journal of Hydrogen Energy*, Vol. 23, No. 7, pp. 583-591, 1998.
- [22] S. A. Sherif et. al., Liquid Hydrogen: Potential, Problems, And A Proposed Research Program. *Int. Journal of Hydrogen Energy*, Vol. 22, No. 7, pp. 683-688, 1997.
- [23] A. Domasenko et. al., Production, Storage And Transportation of Liquid Hydrogen. Experience of Infrustructure Development And Operation. *Int. Journal of Hydrogen Energy*, Vol. 27, pp. 753-755, 2002.
- [24] Kaganer MG. Thermal insulation in cryogenic engineer-ing. Jerusalem, Israel: Israel Program for Scientific Translation, 1969.
- [25] G. Sandrock, "A panoramic overview of hydrogen storage alloys from a gas reaction point of view", *J. Alloys and Comp.*, 293-295, (1999) 877-888
- [26] D.H. DaCosta M. Golben and D.C. Tragna, "Metal Hydride Systems for the Hydrogen Planet", Proceedings of the 14<sup>th</sup> World Hydrogen Energy Conference, eds. R. D. Venter and T. K. Bose, Canada, June 9-13, 2002
- [27] F. J. Liu, G. Sandrock and S. Suda, *J. Alloys and Comp.*, 231 (1995) 392-396
- [28] F. J. Liu, G. Sandrock and S. Suda, *J. Alloys and Comp.*, 232 (1996) 232-237
- [29] J. Huot, G. Liang, S. Boily, A. van Neste and R. Schultz, *J. Alloys and Comp.*, 293-295 (1999) 495-500
- [30] H. Aoaki, K. Aoki and T. Masumoto, *J. Alloys and Comp.*, 231 (1995) 804-809
- [31] H. Sakakuchi, T. Tsujimoto and G. Adachi, *J. Alloys and Comp.*, 223 (1995) 122-126
- [32] K. Nishimura, K. Sato, Y. Nakamura, C. Inazumi, K. Oguro, I. Uehara, S. Fujitani, I. Yoneyzy, *J. Alloys and Comp.*, 268 (1998) 207-210
- [33] G.D. Sandrock, P.D. Goodell, *J. Less-Common Met.* 104 (1984) 159.
- [34] G. Sandrock, S. Suda, L. Schlapbach, in: L. Schlapbach (Ed.), *Topics in Applied Physics, Applications, Hydrogen in Intermetallic Compounds II*, Vol. vol. 67, Springer, Berlin, 1992, p. 197.
- [35] G. Sandrock, Applications of Hydrides, in: Y. Yurum (Ed.), *Hydrogen Energy System—Production and Utilization of Hydrogen and Future Aspects*, Kluwer Academic, Dordrecht, 1995, p. 2
- [36] M. Golben, D. H. DaCosta, "Advanced Thermal Hydrogen Compression" Proceedings of the 34<sup>th</sup> Intersociety Energy Conversion Engineering

- Conference, Warrendale, PA:SAE International, 1999
- [37] L. Schlapbach, A. Zuttel, O. Kuttel, P. Groning, P. Aebi, Hydrogen in materials science, this volume.
- [38] T. Sakai, I. Uehara, H. Ishikawa, R&D on MH electrode materials and Ni-MH batteries in Japan, this volume.
- [39] H. Inui, T. Yamamoto, M. Hirota and M. Yamaguchi, *J. Alloys and Comp.*, 330 (2002) 117-124
- [40] G. Sandrock, G. Thomas, IEA/DOE/SNL Hydride Databases, Internet URL <http://hydpark.ca.sandia.gov>.
- [41] H. Aoki, K. Aoki and T. Masumoto, *J. Alloys and Comp.*, 231 (1995) 804-809
- [42] G. Sandrock, State-of-the-Art Review of Hydrogen storage in Reversible Metal Hydrides for Military Fuel Cell Applications, Final Report for ONR Contract N00014-97-M-0001, NTIS Order No. AD-A328 073/2INZ.
- [43] G. Sandrock, Hydrogen-Metal Systems, in: Y. Yurum (Ed.), Hydrogen Energy System – Production and Utilization of Hydrogen and Future Aspects, Kluwer Academic, Dordrecht, 1995, p. 135.
- [44] K. Dutta, K. Srivastava, O. Srivastava, in: T.N. Veziroglu, P.K. Takahashi (Eds.), Hydrogen Energy Progress VIII, Vol. vol. 2, Pergamon, 1990, p. 1027.
- [45] J. J. Reilly and R. H. Wisall, *Inorganic Chemistry*, 9 (1970) 1678-1682
- [46] E. Akiba and H. Iba, *Intermetallics* 6 (1998) 461-470
- [47] E. Akiba, H. Iba, Hydrogen absorption by Laves phase related BCC solid solutions, this volume.
- [48] J.F. Lynch, A.J. Maeland, G.G. Libowitz, *Z. Phys. Chem. NF* 145 (1985) 51.
- [49] K. Nomura, E. Akiba, *J. Alloys Comp.* 231 (1995) 513.
- [50] K. Yvon, New metal hydrides, this volume.
- [51] J. Chen, T. Kiyobayashi, Q. Xu, H. T. Takeshita, H. Tanaka, T. Sakai and N. Kuriyama, "Hydrogen Storage Properties of Lithium Aluminum Hydrides", Proceedings of the 14<sup>th</sup> World Hydrogen Energy Conference, eds. R. D. Venter and T. K. Bose, Canada, June 9-13, 2002
- [52] B. Bogdanovic, M. Schwickardi, *J. Alloys Comp.* 253-254 (1997) 1.
- [53] B. Bogdanovic, R. A. Brand, A. Marjanivic, M. Schwickardi and J. Tolle, *J. Alloys and Comp.*, 302 (2000) 36-58
- [54] R.A. Zidan, S. Takara, A.G. Hee, C.M. Jensen, *J. Alloys Comp.* 285 (1999) 119.
- [55] Ronald W. Breault, et. at., Hydrogen Transmission/Storage with a metal Hydride/ Organic Slurry, Proceedings of the 1998, U.S. DOE Hydrogen Program review, NREL/CP-570-25315, Vol II April 28-30, 1998 Alexandria, Virginia USA.
- [56] Eugene Long, A Portable Power System Using PEM Fuel Cells, The National Hydrogen Association's 8<sup>th</sup> Annual U.S. Hydrogen meeting Proceedings, March 11-13-1997 Alexandria Virginia USA.
- [57] A.C. Dillon, K.M. Jones, T.A. Bekkedahl, C.H. Kiang, D.S. Bethune, M.J. Heben, *Nature* 386 (1997) 377.
- [58] A. Chambers, C. Park, R.T.K. Baker, N. Rodriguez, *J. Phys. Chem. B* 102 (1998) 4253.
- [59] Chrishna Sapru et. al., Develop Improved Metal Hydride Technology for the storage of Hydrogen, Final Report, December 4, 1998, DOE/GO/10145-T1
- [60] J.C. Wang, et. at., Hydrogen Storage in Fullerenes and in an Organic Hydride, Proceedings of the 1998, U.S. DOE Hydrogen Program review, NREL/CP-570-25315, Vol II April 28-30, 1998 Alexandria, Virginia USA.
- [61] Joakim Pettersson et. al., Hydrogen storage alternatives a technological and economic assessment KFBs DNR 1998-0047 Dec, 1999

- [62] A.C. Dillon., et. al., Carbon Nanotubes Materials for Hydrogen Storage, Proceedings of the 1996, U.S. DOE Hydrogen Program review, NREL/CP-430-20036, Vol II April 18-21, 1995 Coral Gables, Florida USA
- [63] A.C. Dillon., et. al., Carbon Nanotubes Materials for Hydrogen Storage, Proceedings of the 1996, U.S. DOE Hydrogen Program review, NREL/CP-430-21968, Vol II May 1-2 1996 Maiami, Florida USA.
- [64] J. C. Wang., et. al., Hydrogen Storage In Fullerenes and Liquid Organic Hydrides, Proceedings of the 1999 U.S. DOE Hydrogen Program review, NREL/CP-570-26938, May 4-6, 1999 Lakewood, Colorado USA.
- [65] A.C. Dillon., et. al., Carbon Nanotubes Materials for Hydrogen Storage, Proceedings of the 1999 U.S. DOE Hydrogen Program review, NREL/CP-570-26938, May 4-6, 1999 Lakewood, Colorado USA
- [66] Schwarz, J., 'Activated Carbon-Based Hydrogen Storage Systems', in the Proceedings of the 1994 DOE / NREL Hydrogen Program Review, pp 149-164, Livermore, CA, Apr 18-21, 1994
- [67] Dillon, A. C., Jones, K. M., and Heben, M. J. (1996) Carbon nanotube materials for hydrogen storage. *1996 Department of Energy/National Renewable Energy Laboratory (DOE/NREL) hydrogen program review*, Proceedings.
- [68] Ye, Y., et. al., (1999) Hydrogen adsorption and cohesive energy of single-walled carbon
- [69] Eugene Long, A Portable Power System Using PEM Fuel Cells, The National Hydrogen Association's 8<sup>th</sup> Annual U.S. Hydrogen meeting Proceedings, March 11-13-1197 Alexandria Virginia USA
- [70] F. Lamari Darkrim, et. al., Review of Hydrogen Storage by Adsorption in Carbon Nanotubes. *International Journal of Hydrogen Energy* 27 (2002) 193-202
- [71] Amankwah KA, Noh JS, Schwartz JA. *Int J Hydrogen Energy* 1989;14:437.
- [72] Zhou Y, Zhou L. *Ind Eng ChemRes* 1966;35:4166.
- [73] Zhou Y, Zhou L. *Science China* 1996;39:598.
- [74] Iijima S. *Nature* 1991;354:56.
- [75] Dillon AC, Jones KM, Bekkedahl TA, Kiang CH, Bethune DS, Heben MJ. *Nature* 1997;386:377.
- [76] Maddox MW, Gubbins KE. *Langmuir* 1995;11:2988.
- [77] Maddox MW, Sowers SL, Gubbins KE. *Adsorption*, 1996;2:23.
- [78] DarkrimFL, Levesque D. *J ChemPhys* 1998;109:4981.
- [79] DarkrimFL, Levesque D. *J Phys ChemB* 2000;104:6773.
- [80] Dresselhaus M, Williams K, Eklund P. *MRS Bull* 1999;1:45
- [81] Tibbetts G. Proceedings of the 10th Canadian Hydrogen Conference, Quebec, 28-31 May, Canadian Hydrogen Association, 2000. MS. *Science* 1999;286:1127.
- [82] Rinzler AG, Liu J, Dai H, Nikolaev P, Hu2man CB, Rodriguez-Macias FJ, Boul PJ, Lu AH, Heymann D, Colbert DT, Lee RS, Fisher JE, Rao AM, Eklund PC, Smalley RE. *Appl Phys A: Solids Surf* 1998;67:29.
- [83] Vaccarini L, Goze C, Aznar R, Micholet V, Journet C, Bernier P, Metenier K, Beghin F, Gavillet J, Loiseau A. *C R Acad Sci Paris* 1999;327(II b):935. MS, Herbst J. Proceedings of the 10th Canadian Hydrogen Conference, Quebec, Canadian Hydrogen Association, 2000.
- [84] Ebbesen TW, Ajayan PM. *Nature* 1992; 358:220.
- [85] Colbert DT, Zhang J, McClure SM, Nikolaev P, Chen Z, Hafner JH, Owens DW, Kotula PG, Carter CB, Weaver JH, Rinzler AG, Smalley RE. *Science* 1994; 266:1218.
- [86] Lauerhaas JM, Dai JY, Satlur A, Chang RPH. *J Mater Res* 1997;12:1536.
- [87] Chen P, Zhang HB, Lin GD, Hong Q, Tsai KR. *Carbon* 1997;35:1495. Ninth



- Canadian Hydrogen Conference “Hydrogen Power Now”, Vancouver, Canada, Published by Canadian Hydrogen Association, 1999.
- [88] IUPAC Pure Appl Chem 1985;57:603.
- [89] Gordon PA, Saeger RB. Ind Eng Chem Res 1999;38:4647.
- [90] International Clean Energy Network using Hydrogen Conversion (WE-NET), 1998 Annual Summary Report on Results NEDO-WE-NET-98, New Energy and Industrial Technology Development Organization (NEDO), March 1999.
- [91] International Clean Energy Network using Hydrogen Conversion (WE-NET), 2000 Annual Summary Report on Results NEDO-WE-NET-00, New Energy and Industrial Technology Development Organization (NEDO), March 2001.
- [92] Development of Hydrogen Absorbing Alloys for Small Scale Transportation and Storage System, Annual Report of WE-NET Task11, Foundation of Osaka Science and Technology Center, March 1999.
- [93] Development of Hydrogen Absorbing Alloys for Small Scale Transportation and Storage System, Annual Report of WE-NET Task11, Foundation of Osaka Science and Technology Center, March 2000.
- [94] Development of Hydrogen Absorbing Materials, Annual Report of WE-NET Task11, Foundation of Osaka Science and Technology Center, March 2001.
- [95] B. Bogdanovic and M. Schwickardi, International Symposium on Metal-Hydrogen Systems, August 25-30 (1996), Les Diablerets, Switzerland
- [96] A. Chambers, C. Park, R. T. K. Baker, N. M. Rodriguez, J. Phys. Chem B., 102, 4253 (1998)
- [97] M. Rzepka, P. Lamp, M. A. de la Casa-Lillo, J. Phys. Chem., 102, 10894 (1998)
- [98] Q. Wang, J. K. Johnson, J. Chem. Phys., 110, 577 (1999)
- [99] Q. Wang, et al. J. Phys. Chem. B., Vol. 103, No. 23, P. 4809 (1999)
- [100] Q. Wang, et al. J. Phys. Chem. B., Vol. 103, No. 2, P. 277 (1999)
- [101] Kenji Aihara On the Development of Hydrogen Absorbing Materials in WE-NET Project of Japan 2001
- [102] Wade A Amos Cost of Storing and Transporting Hydrogen, November 1998, NREL/TP-570-25106
- [103] Hart, D. (1997) *Hydrogen Power: The Commercial Future of the Ultimate Fuel*.
- [104] Schwarz, J., ‘Activated Carbon-Based Hydrogen Storage Systems’, in the Proceedings of the 1994 DOE / NREL Hydrogen Program Review, pp 149-164, Livermore, CA, Apr 18-21, 1994
- [105] Glenn D., Rambach, et. al., Hydrogen Transport and Storage in Engineer Glass Microspheres, Proceedings of the 1996, Vo. II, U.S. DOE Hydrogen Program Review, NREL/CP-430-21968, May 1-2, 1996, Miami, Florida USA.
- [106] L. M. Das., On-Board Hydrogen Storage Systems for Automotive Application. Int. Journal of Hydrogen Energy, Vol. 21, No. 9, pp. 789-800, 1996.
- [107] Glenn D., Rambach, Hydrogen Transport and Storage in Engineer Glass Microspheres, Proceedings of the 1995, Vo. II, U.S. DOE Hydrogen Program review, NREL/CP-430-20036, April 18-21, 1995, Coral Gables, Florida USA
- [108] H. Uchida, K. Oyakawa and S. Watanabe, “Development of Metal Hydride Tank for Quick Charge”, Proceedings of the 14<sup>th</sup> World Hydrogen Energy Conference, eds. R. D. Venter and T. K. Bose, Canada, June 9-13, 2002
- [109] Labtech Int. Ltd, <http://labtech.solo.bg>
- [110] “Case Studies of Integrated Hydrogen Systems”, International Energy Agency Hydrogen Implementing Agreement Final Report for Subtask A of Task 11 - Integrated Systems, Thomas Schucan, Paul Scherrer Institute, CH-5232 Villigen PSI Switzerland, 1999